An autonomous sea going Raman/SERS instrument for in situ detection of chemicals in sea water

vorgelegt von
Diplom - Ingenieur Chemietechnik
Anna Kolomijeca
Riga, Latvia

Von der Fakultät II – Mathematik und Naturwissenschaften
der Technischen Universität Berlin
zur Erlangung des akademischen Grades
Doktor - Ingenieur
Dr. Ing.

genehmigte Dissertation

Promotionsausschuss:

Vorsitzender:	Prof. Dr. Mario Dähne
Berichter:	Priv.-Doz. Dr. Heinz-Detlef Kronfeldt
Berichter:	Prof. Dr. Ulrike Woggon
Berichter:	Prof. Dr. Per Hall

Tag der wissenschaftlichen Aussprache: 3. September 2013

Berlin 2013
D 83

Dedicated to the loving memory of Vera Kolomijeca (Grandma)

Acknowledgements

I gratefully acknowledge Priv.-Doz. Dr. Heinz-Detlef Kronfeldt for his constant support and help during my stay in the laser spectroscopy group, as well as providing an opportunity and topic for my PhD work. I would like to thank Prof. Dr. Ulrike Woggon, Prof. Dr. Mario Dähne, Technical University Berlin and Prof. Dr. Per Hall, University of Gothenburg, Sweden, for organization of my PhD examination.

I also would like to thank all my colleagues from the SENSEnet project; an EU Framework 7 funded Marie Curie Initial Training Network, under contract number PITN-GA-2009-237868, with a special thanks to Dr. Douglas Connelly (co-coordinator) and Dr. Carla Sands (project manager) for the opportunity to conduct sea trials in the Arctic, their cooperation and funding.

Many thanks are expressed to the colleagues of Laser Spectroscopy Group, Institute of Optics and Atomic Physics, Technical University Berlin: Dr. Yong-Hyok Kwon (SENSEnet) for preparation of Ag, DMCX:MTEOS substrates, Hossam Ahmad for preparation of gold island substrates, Dr. Kay Sowoidnich for help and advices, Bernd Geisler for technical support as well as Halah Al Ebrahim and Maria Fernandez Lopez (SENSEnet). Furthermore, I would like to thank Priv.-Doz. Dr. Bernd Sumpf from Ferdinand-Braun-Institut, Leibniz-Institut für Höchstfrequenztechnik, for interesting lectures in laser physics which greatly increased my understanding of this topic. Thanks to Dr. Ralf Prien, Leibniz-Institute for Baltic Sea Research, Germany, for helpful and valuable advice.

Kind acknowledgements are expressed to the colleagues from IFREMER La Syene, France: Eng. Pierre Leon, Dr. Vincent Rigaud and Francois Roland for providing an opportunity to do my placement and for their constant help during my experiments. Many thanks to the technical team, especially Christophe Duchi for his help in final construction of the Sea Going Instrument, Eric Emery for help in the cruise and Dr. Chadi Gabriel.

I thank Dr. Sheri White and Senior Engineer Norm Farr for hosting me in Woods Hole Oceanographic Institution, MA, USA and providing valuable information for my studies, as well as Dr. Peter Brewer and Dr. Edward Peltzer for kind hospitality in Monterey Bay Aquarioum Research Institute, CA, USA and very valuable information. I thank Dr. Jules Jaffe for meeting me in SCRIPPS Institution of Oceanography, CA, USA. I acknowledge Prof. Geir Wing Gabrielsen for meeting in the Norwegian Polar Institute, Svalbard, and very helpful information about research and pollution in the Arctic area, which was a guide for my work.

Finally, I sincerely thank my love Alex Strange for great help, care, constant support and assistance in construction of the sea going instrument as well as my family: mom - Svetlana Kolomijeca and brother - Pavels Kolomijecs for encouragement of my research.

Abstract

The continuous monitoring of dangerous pollutants at very low concentrations (nM range) in the sea is of global importance to ensure environmental protection. To realize a technological basis for this purpose, an autonomous in situ sea going instrument for SERS (surface enhanced Raman spectroscopy) detection of selected chemicals was developed and tested.

The selectivity and sensitivity of the applied technique was verified by extensive laboratory investigations, with more than 100 water and sediment samples collected at chosen locations from three continents: Europe, America, and Asia. For the first time, such a worldwide comparison of specimens was carried out applying a combination of SERS with SERDS (shifted excitation Raman difference spectroscopy), by means of a microsystem diode laser with two slightly shifted emission wavelengths (671.0 nm and 671.6 nm). Here, polycyclic aromatic hydrocarbons (PAHs) as fluoranthene, acenaphtylene, and pyrene as well as biphenyl could be identified as main pollutants – usually as a mixture of several chemicals, very rarely (< 5 %) as a single component.

Based on the laboratory experiments, portable Raman equipment was developed. Further studies were carried out in the Arctic area onboard a research vessel, in order to prove the ability of the system to work under harsh field conditions. Various SERS surfaces were successfully tested for its suitability for pollutant detection and stability during short (hours) and long term (days) measurements in surface seawater, which was continuously pumped on board through a pipe. The highest stability of the substrates could be achieved when immersed in fresh water, with an overall intensity decrease of only 5 % after 7 days of exposure. In contact with seawater, the overall intensity is reduced by 2 % within the first 10 h and by 20 % after 7 days. Spiking tests with selected PAHs dissolved in seawater showed lower in situ measured limits of detection compared to the calculated values for the laboratory experiments, e.g. 0.3 nM for anthracene (laboratory: 1 nM) and 1 nM for fluoranthene (laboratory: 1.2 nM).

Finally, for the first time an autonomous sea going instrument was constructed, including the SERS sensor with integrated microsystem diode laser, compact laser drivers, a

specially developed miniature spectrometer, all required electronic components, a microcomputer and a rechargeable battery. All parts of the system are contained in a pressure-resistant housing, enabling underwater experiments down to a depth of 100 m. The instrument was successfully tested in the Mediterranean Sea at IFREMER La Syene-Sur-Mer in the local harbor and during sea trials, detecting characteristic signals of fluoranthene and biphenyl. Even without SERS enhancement, Raman signals from the salt ions (SO_4^{2-}) in seawater could be detected with integrations times of 10 s.

The conducted experiments clearly demonstrate the applicability of innovative Raman, SERDS, and SERS/SERDS sensors for the in situ detection of hazardous environmental pollutions, in the nM-range, in seawater at any area of interest.

Zusammenfassung

Die kontinuierliche Überwachung von Schadstoffen im Meerwasser in sehr geringen Konzentrationen (nM-Bereich) ist von weltweitem Interesse, um einen wirkungsvollen Umweltschutz zu gewährleisten. Zur Realisierung einer technologischen Plattform für derartige Untersuchungen wurde ein autonomes, meerestaugliches In-situ-System für den Nachweis ausgewählter Chemikalien mit Hilfe der oberflächenverstärkten Ramanspektroskopie (SERS) entwickelt und getestet.

Die Selektivität und Empfindlichkeit der verwendeten Technik wurde anhand umfangreicher Laboruntersuchungen verifiziert. Dabei kamen mehr als 100 Wasser- und Sedimentproben ausgewählter Orte von 3 Kontinenten (Europa, Amerika und Asien) zum Einsatz. Unter Verwendung eines Mikrosystem-Diodenlasers mit zwei leicht gegeneinander verschobenen Anregungswellenlängen (671,0 nm und 671,6 nm) konnte so erstmalig ein weltweiter Vergleich der Proben mit einer Kombination von SERS und SERDS (shifted excitation Raman difference spectroscopy) durchgeführt werden. Als wesentliche Verschmutzungen ließen sich dabei polyzyklische aromatische Kohlenwasserstoffe (PAKs) wie beispielsweise Fluoranthen, Acenaphtylen oder Pyren sowie Biphenyl identifizieren. Diese Substanzen traten dabei häufig in einem Gemisch auf, in seltenen Fällen (< 5 %) jedoch auch als einzelne Komponenten.

Aufbauend auf den Laboruntersuchungen erfolgte die Entwicklung eines portablen Ramansystems. Weiterführende Untersuchungen an Bord eines Forschungsschiffes in der Arktis konnten die Einsatzfähigkeit des Systems unter rauen Umgebungsbedingungen verifizieren. Dabei wurden zahlreiche SERS-Oberflächen erfolgreich hinsichtlich ihrer Eignung zum Schadstoffnachweis sowie ihrer Stabilität analysiert. Die Stabilitätstests auf kurzen (Stunden) und langen (Tage) Zeitskalen erfolgten mit Hilfe von Oberflächenwasser, das über eine Rohrleitung kontinuierlich an Bord gepumpt wurde. Die Substrate zeigten bei einer Lagerung in Frischwasser mit einem Intensitätsabfall von nur 5 % nach 7 Tagen die besten Resultate. In Kontakt mit Meerwasser ergab sich eine Reduktion der Intensität von lediglich 2 % innerhalb der ersten 10 Stunden sowie von 20 % nach 7 Tagen. Die Zugabe

ausgewählter PAKs in das Meerwasser in verschiedenen Konzentrationen ergab im Vergleich zu den Laboruntersuchungen verbesserte Nachweisgrenzen von 0,3 nM für Anthracen (Labor: 1 nM) und 1 nM für Fluoranthen (Labor: 1,2 nM).

Abschließend wurde erstmals ein autonomes, meerestaugliches Messgerät konstruiert, das den SERS-Sensor mit integriertem Mikrosystem-Diodenlaser, kompakte Lasertreiber, ein speziell entwickeltes Miniaturspektrometer, alle erforderlichen elektronischen Bauteile, einen Mikrocomputer sowie einen wiederaufladbaren Akku enthält. Alle Komponenten des Systems befinden sich in einem druckfesten Gehäuse, das für den Unterwasser-Einsatz bis zu einer Tiefe von 100 m konzipiert ist. Das Messgerät wurde erfolgreich im Mittelmeer bei der IFREMER in La Syene-Sur-Mer im dortigen Hafen sowie bei Einsätzen auf See getestet, wobei sich charakteristische Ramansignale von Fluoranthen und Biphenyl nachweisen ließen. Auch ohne die Anwendung der SERS-Substrate konnten bei Integrationszeiten von 5–10 s Ramansignale von Salzionen (SO_4^{2-}) im Meerwasser detektiert werden.

Die durchgeführten Untersuchungen verdeutlichen die Einsetzbarkeit innovativer Raman-, SERDS- und SERS/SERDS-Sensoren zum In-situ-Nachweis gefährlicher Umweltschadstoffe im Meerwasser im nM-Bereich an beliebigen Untersuchungsorten.

List of publications

Parts of this thesis have already been published in the following papers:

1. A. Kolomijeca, F. Roland, P. Leon, H. D. Kronfeldt. Autonomous in-situ Raman sensor, suitable for surface enhanced Raman spectroscopy (SERS) for detection of chemicals in the sea. *Universal Journal of Applied Science*, in preparation, 2013.

2. A. Kolomijeca, H.D. Kronfeldt. Miniaturized on-board Raman system based on SERS (Surface Enhanced Raman scattering) applied for seawater and sediment investigations on an Arctic sea-trial. *Journal of Applied Spectroscopy*, in preparation, 2013.

3. R. Ossig, A. Kolomijeca, Y.-H. Kwon, F. Hubenthal, H.-D. Kronfeldt. SERS signal response and SERS/SERDS spectra of fluoranthene in water on naturally grown Ag nanoparticle ensembles. *Journal of Raman Spectroscopy*, 44(5): 717-722, 2013.

4. A. Kolomijeca, H.-D. Kronfeldt, Y.-H. Kwon. A Portable Surface Enhanced Raman (SERS) Sensor System Applied for Seawater and Sediment Investigations on an Arctic Sea-trial. *International Journal of Offshore and Polar Engineering (IJOPE)*, 23: 1-5, 2013.

5. A. Kolomijeca, Y.-H. Kwon, H.-D. Kronfeldt. A Portable Surface Enhanced Raman (SERS) Sensor System Applied for Seawater and Sediment Investigations on an Arctic Sea-trial, *Proceedings of the Twenty-second International Offshore and Polar Engineering Conference, Rhodes/Greece*, 1398 – 1402, 2012. **Awarded as "Best Student Paper".**

6. Y.-H. Kwon, A. Kolomijeca, R. Ossig, F. Hubenthal, H.-D. Kronfeldt. Naturally Grown Ag Nanoparticle SERS Substrate as Chemical Sensor in Water Body Applying a 488 nm Microsystem Diode Laser. *Proceedings of the Twenty-second International Offshore and Polar Engineering Conference, Rhodes/Greece*, 795 – 800, 2012.

7. A. Kolomijeca, Y.-H. Kwon, H.-D. Kronfeldt (T. Vo-Dinh, R.A. Lieberman, G. Gaulitz, eds). Surface-enhanced in-situ Raman-sensor applied in the arctic area for analyses of water and sediment. *Proceedings of SPIE 8366, Baltimore / USA*, 2012.

8. Y.-H. Kwon, R. Ossig, A. Kolomijeca, F. Hubenthal, H.-D. Kronfeldt (T. Vo-Dinh, R.A. Lieberman, G. Gaulitz, eds). Naturally grown silver nanoparticle ensembles

for 488 nm in-situ SERS/SERDS-detection of PAHs in water. *Proceedings of SPIE 8366, Baltimore / USA,* 2012.

9. A. Kolomijeca, Y.-H. Kwon, K. Sowoidnich, R. D. Prien, D. E. Schulz-Bull, H.-D. Kronfeldt. High Sensitive Raman Sensor for Continuous In-situ Detection of PAHs. *Proceedings of the Twenty-first International Offshore and Polar Engineering Conference, Hawaii / USA,* 859 – 862, 2011.

10. H. Ahmad, A. Kolomijeca, K. Sowoidnich, H.-D. Kronfeldt. Application of Shifted Excitation Raman Difference Spectroscopy (SERDS) for In-situ Investigations in the Deep Sea. *Proceedings of the Ninth ISOPE Ocean Mining Symposium, Hawaii / USA,* 78 – 82, 2011.

11.Y.-H. Kwon, A. Kolomijeca, K. Sowoidnich, H.-D. Kronfeldt. High Sensitivity Calixarene SERS Substrates for the continuous In-situ Detection of PHS in Sea-water. *Proceedings of SPIE 8024, Orlando/ USA,* 2011.

Contents

List of Tables

List of Figures

1. Introduction

1.1. Marine pollution and monitoring

Rapid technological progress vastly increased the quality of human life, changing living conditions in the world, which brought numerous advantages in communication, medicine, life comfort, travelling and many other aspects. But along with positive sides of technological progress comes one very serious problem: pollution in water, air and soil.

Incomplete combustion of oil products, applications of pesticides in agriculture, accidents in the nuclear power industry, oil spills and many others, can lead to catastrophes and create a serious danger to our planet and all human kind [EP, 2013].

70% of the earth is covered by water making our planet the "richest" of all in our solar system [Wotton, 2012]. All life forms including humans are dependent from it, making water an essential life source on our planet.

Some studies show that poor water quality causes the death of about 14,000 people daily [West, 2006] and is responsible for constant extinction of animal species. Therefore, it is extremely important to control, monitor, and reduce pollution in the water body. Pollution can have many forms, but the most dangerous are not detectible by the human eye or by simple filter systems, thus creating complex and challenging tasks for scientists.

Marine pollution is usually caused by human activities and has been defined by GESAMP [GESAMP, 2013] as being introduced by men directly or indirectly in the form of substance or energy into the marine environment, which results in causing harm to living resources and is hazardous to human health. It can be further classified as persistent, toxic, able to bio accumulate and can be in a form of heavy metals (for example: Cd, Hg, Pb),

petroleum hydrocarbons (PAHs, oil spills), persistent organic pollutants (PCB's, TBT), pesticides, dioxins, nutrients (nitrate, ammonia, phosphate) [Zielinski *et al.*, 2009].

Further classification involves marine toxins (naturally produced by marine microalgae [Zielinski *et al.*, 2009; Grovel *et al.*, 2003], harmful algal blooms (can occur naturally [Adams *et al.*, 2000] or due to human activities [Lam and Ho, 1989]), pathogenic agents as viruses, bacteria and protozoa [Zielinski *et al.*, 2009; Pepper *et al.*, 1996].

Most countries in the world have strict legislation regarding water pollution. There are international laws, European laws and UK legislation for water quality standards. Most of them can be found in [LE, 2011].

Various environmental monitoring programs (including seawater monitoring) have been created by EU projects such as: MEECE [MEECE, 2010], HERMIONE [HERMIONE, 2012], DS^3F [DS^3F] and many more (see reference [EU, 2007 - 2011]); USA projects: NOAA [NOAA, 2013], EPA [EPA, 2012a]; International projects: UNESCO [UNESCO, 1992], GOOS [GOOS, 2008], GEOHAB [GEOHAB, 2008], UNEP [UNEP, 2004].

Projects funded also by the European Union provide high efficiency for developing new monitoring methods and in situ sensors. One example is the SENSEnet project, in the seventh EU Framework, funded by Marie Curie Initial Training Network, which brings together leading scientists and researchers from across Europe with the aim of developing novel sensors for the marine environment [SENSEnet, 2013]. This project sponsors current research.

Numerous detection methods have been developed which are suitable for large, intermediate and small scales, depending on the pollution type.

Large scale pollution monitoring involves remote/radar systems and is applied from above via satellites or aircrafts, being able to cover large areas. Such systems are well suited for detection of oil spills [Zielinski *et al.*, 2006; Gruner *et al.*, 1991], chlorophyll and as consequence harmful blooms [Zielinski *et al.*, 2001; Browell, 1977]. However, radar systems are limited to the upper level of the water, therefore unable to detect heavy metals, marine toxins and pathogens.

Summary: (+) covering a large scale
(+) relatively fast and non-complicated monitoring (observation type)
(-) limited applications.

Intermediate scale control involves in situ platforms as **a**utonomously **o**perated **v**ehicles (AOVs), **r**emotely **o**perated **v**ehicles (ROVs) and moorings. These systems are immersed in the water making it possible to detect heavy metals (as lead [Bundy *et al.*, 1996], iron (II) and manganese (II) [Prien *et al.*, 2006]), radionuclides [Gostilo *et al.*, 2000], petroleum hydrocarbons [Zelinski and Brehm, 2007], some nutrients (as nitrate, bromide and bisulfite) [Jonson and Coletti, 2002], harmful blooms [Babin *et al.*, 2005], but rarely detects pathogens or marine toxins [Zielinski *et al.*, 2009].

Summary: (+) suitable for various applications
(+) covering significant areas
(+) can work in autonomous mode
(-) complicated in design.

Small scale or point measurements can be achieved either with sensors or taking water samples from particular areas and further analyzing them in the laboratory. This method can detect most water pollution types [Zielinski *et al.*, 2009] but is usually very costly, time consuming, often complex and covers very small areas. Additionally, sample quality may change during time due to temperature and pressure differences, the presence of light or due to the absorption to the container walls.

Summary: (+) detect most pollution types
(-) costly
(-) time consuming
(-) covering “point” areas only.

As we can see, large-scale monitoring systems are very useful but can only detect certain types of pollution, while small scale monitoring does not provide equilibrium between the economical factor (time and costs) and efficiency in terms of scale size/possible sample change. Therefore, an excellent compromise is to develop sea going instruments for

intermediate scale of seawater monitoring because they can be applicable to various monitoring needs (pollution, oxygen level and nutrient sensors etc.), cover significant areas and can be self-sustainable, e.g. work in autonomous regime.

1.2. Intermediate scale seawater monitoring systems and underwater networks.

Various groups all over the world developed and successfully adapted in situ sensors in different sea going instruments measuring, e.g. dissolved oxygen, nutrients, minerals, hydrothermal vents, methane hydrates, CH_4 and CO_2 in sea water, temperature, pressure, etc. These groups are Monterey Bay Aquarium Research Institute (USA) [MBARI, 2013; Brewer *et. al*, 2011], Woods Hole Oceanographic Institution (USA) [WHOI, 2013; White 2010, White 2008], SCRIPPS Institution of Oceanography (USA) [SCRIPPS, 2013], Institute Francais de Recherche pour l'exploitation de la mer (France) [IFREMER, 2013], National Oceanography Center (UK) [NOCS, 2013], Leibniz Institute for Baltic Sea Research (Germany) [IOW, 2013], Center of Marine Environmental Science (Germany) [MARUM, 2013] and others.

An amazing ROV network forms regional-scale underwater ocean observatory in the project of NEPTUN Canada [NEPTUN, 2013], hosted by University of Victoria, Canada. 800 km of power transmission and fiber optic communication cables are connected over the northern part of the Juan de Fuca tectonic plate, off the west coast of Vancouver Island in British Columbia. It is plugged directly to the internet and covers various research themes; for example fluid flow in the seabed, earthquakes and plate tectonics, marine processes and climate change, however it does not detect any pollution directly [Best, 2012]. "Sister" projects of NEPUN are VENUS, operated by University of Victoria, Canada and MARS - deployed by MBARI, USA. VENUS is a cabled sea floor observatory with a network of about 50 km and maximum 300 m depth , which study coastal oceans in two sites near Victoria and Vancouver, British Columbia. Sensors deployed in this network provide

real time information and measurements of salinity, temperature and pressure 24 hours a day [VENUS, 2013]. MARS underwater network is 52 km of undersea cable that carries data and power to a "science node" 891 meters below the surface of Monterey Bay. Various sensors are connected to it: “eye of the sea” – low-light camera; “FORCE experiment” - study the effects of increased carbon dioxide concentrations in seawater on marine animals; “Benthic rover” - measures oxygen consumption by seafloor animals; “Seafloor seismometer” – detects earth quakes; “DEIMOS echo sounder”-detects marine life; “Deep sea environmental sensor processor” – automated DNA laboratory; “ALOHA mooring” - measure tides and current changes [MARS, 2013]. As we can see, all those networks unfortunately do not provide direct measurements of pollution.

Complex ROVs have been created by many groups, for example ROVs “Ventana”, and “Doc Ricketts” by MBARI [MBARI, 2013], “Jason/Media” by WHOI [WHOI, 2013], “Victor 6000”, “Sysif”, “Nautile” by IFREMER [IFREMER, 2013], “Cherokee”, “Quest” by MARUM [MARUM, 2013] and others. Usual ROV systems include sample collection, video monitoring, pressure/temperature sensors.

In situ identification of toxins is also possible using the same method but very few groups use it. For example, surface plasmon resonance (SPR) technique can be used for the detection of domoic acid, performed by IFREMER in partnership with the National Ocean Service of NOAA (USA) in 2010 [IFREMER, 2010].

All sea going instruments described above are connected via a cable to a research vessel which supplies power and enables data transfer.

Therefore, the task of this work is to create a portable, easy to use, size-reduced and efficient in situ sensor system for detecting toxic substances in low concentrations. Additionally, the sensor system (or sea going instrument) must be autonomous in order to avoid any external cable connections; it should be easily transportable and able to run measurements (screen the area) in short time frames, i.e. in a few seconds. Furthermore, that sensor should be able to be integrated in any underwater system, as mooring, AOV, ROV or deployed for underwater ocean observatory.

2. The target

New generation in situ sensors must detect dangerous pollution in sea water in very low concentrations, i.e. in the nmol/l (nM) range and lower. Polycyclic Aromatic Hydrocarbons (PAHs) and biphenyl are selected as target molecules. Its sources in the environment, applications, production quantities, utilization methods and health effects are described in the following section and appendix I. As will be shown below, these pollutants are of global importance. Therefore, construction of an in situ sensor, which is able to detect PAHs and biphenyl in the environment, is of huge importance globally.

2.1 PAHs

PAHs are dangerous environmental pollutants known to have carcinogenic, mutagenic and teratogenic effects [EU, 2002].

Huge amounts of PAHs have been produced in USA and Europe for last few decades. If we take the United States as an example, we can see that in the year 1986, acenaphthene was imported in amount of 4×10^3 kg. Almost 45.4×10^6 liters of creosote oil came from Netherlands, France, West Germany and other countries as well as 84×10^6 kg of coal tar pitch, blast furnace tar, and oil-gas tar came from Canada, Mexico, West Germany and Australia. One year earlier (1985), PAH imports in United States were as follows: 573×10^4 kg anthracene oil, 882×10^3 kg anthracene, 1.040 kg fluoranthene, 57.400 kg pyrene. In the year 1984 - 79.200 kg chrysene, 9.440 kg fluoranthene, 9.31 kg fluorine and 551 kg phenanthrene [HSDB, 2010]. Nevertheless, commercial production of PAHs is not a main source of those compounds in the environment. The primary source of PAHs in the

environment result from the incomplete combustion of wood and fuel [Wenzl *et al.*, 2006; ATSDR] which comes from motor vehicles, gas-burning engines, wood-burning stoves, cigarette smoke, and industrial smoke, charcoal-broiled foods [ATSDR; NIEHS, 2011]. PAHs can be also naturally released into the environment from volcanoes, forest fires, crude oil and shale oil [HSDB, 2010; ATSDR]. PAHs from fires can bind to ashes and move long distances through the air [Baker and Eisenreich, 1990].

Approximately two-thirds of PAHs in surface waters are particle-bound and can be removed by sedimentation, flocculation, and filtration processes. The rest requires oxidation for partial removal [ATSDR]. Utilization of most PAHs involves different kinds of incineration in temperature ranges of 480 ^{o}C - 1.600 ^{o}C. Laboratory waste can be oxidized with concentrated sulfuric acid, potassium dichromate or potassium permanganate. In situ bioremediation is considered ineffective for most PAH removal, but land farming can be successful for degradation of PAHs with three or fewer aromatic rings. Bioreactors could be applied for degradation of PAHs. Studies have shown that during 12 weeks overall PAH degradation rate is 93 %, from which 97 % is for two and three ring PAHs; 90 % four - six ring PAHs [ATSDR]. Particular utilization methods for some PAHs are collected in appendix I.

The PAHs utilization techniques are constantly modified to provide better utilization efficiency but it still does not completely remove those chemicals (from 90 % to 97 %) and not all the manufactured PAHs reach utilization procedure. Therefore, it is very important to develop high efficiency detection techniques of PAHs in order to control amounts which enter the environment and track its sources.

European Parliament identified various PAHs as priority substances in the field of water policy [EU, 2001] and set a regulation of the maximum allowed PAH concentration in food which varies from 1 µg/kg to 10 µg/kg wet weight [EU, 2005]. Usual PAH analyzing technics are all kinds of extraction or chromatographic separation [Wenzl *et al.*, 2006] which are complex, costly, and time consuming (taking up to few days).

Therefore, the design of a PAH sensitive in situ sensor which is able to detect those pollutants “fast and cheap” (in comparison to classical methods for the amount of samples) is of global importance and a challenging task for this thesis. Fourteen selected PAHs and biphenyl have been investigated in this work and are summarized in appendix I.

Similar studies for PAH sensor development have been done before in our group by Murphy [Murphy *et al.*, 1997], Bich Ha [Bich Ha, 2004], and Pfannkuche [Pfannkuche *et al.*, 2012] as well as our colleagues in IFREMER - [Peron *et al.*, 2010]. All existing instruments for identification of PAHs have cable connections to vessels for data and power supply. The aim of this current work is to achieve same results in chemical detection, applying an autonomous in situ sensor with all components minimized in size.

2.2 Biphenyl

Biphenyl as Aromatic Hydrocarbon is of high scientific interest, as it is the starting material for the production of **p**oly **c**hlorinated **b**iphenyls (PCBs), which were once widely used as dielectric fluids and heat transfer agents. Its other uses are dyestuff carrier for textiles, as solvent in pharmaceutical production and in the preservation in citrus fruits (Preservative E230, in combination with E231, E232 and E233) [FSA, 2012], because it prevents the growth of molds and fungus. It is part of the active group in the antibiotic Oritavancin.

It is mildly toxic, has mutagenic potential and may cause damage to the liver and persistent neuronal changes. Biphenyl can be degraded biologically by conversion into nontoxic compounds. Some bacteria are able to hydroxylate biphenyl and its polychlorinated biphenyls (PCBs) [Boehncke *et al.*, 1999].

In ambient air, the concentration of biphenyl ranges from 1 to 100 ng/m^3, while indoor air contains 100-1000 ng/m^3. In Germany elevated levels of biphenyl at 1000 ng/l have been detected in the Rhine River in 1970 [Boehncke *et al.*, 1999] and in Emscher tributary area, while 1600 ng/l of biphenyl have been reported in 1994. This is due to coking

plants located in this area. In 1989, 20-25 x 10^5 kg biphenyl was produced in Germany and 5 x 10^6 kg of biphenyl was produced in Japan each year in 1992 and 1993. U.S. production of biphenyl was 24 x 10^6 kg in 1990 [EPA, 1995].

These incredible amounts of biphenyl production and use cause scientific interest in ability to measure this chemical. Furthermore, it is of a great scientific interest to measure biphenyl in situ. Additionally, the detection of biphenyl may serve as a cross reference for PCBs, which are priority substances in seawater pollution monitoring and control, together with PAHs [Gioia *et al.*, 2008].

3. Raman theory

In 1930, C.V. Raman was the first “non-white”, Asian and Indian to receive the Nobel Prize in physics for his work on scattering of light and discovery of the Raman Effect [Raman, 1930; Raman and Krishnan, 1928].

Raman spectroscopy is based on the inelastic scattering of monochromatic light. Due to interaction with the sample, e.g. the excitation of molecular vibrations, the frequency of photons in monochromatic light changes, causing “Stokes” and “anti-Stokes” scattering. This inelastic scattering is extremely weak compared to the elastic Rayleigh scattering, which has no change in scattered light frequency.

As shown in figure 1, Raman Stokes scattering emits light with lower frequencies compared to the incident photos, therefore it is shifted to the “red” spectral region. Raman anti-Stokes scattering emits light with higher frequencies than the incident photons and is therefore shifted to the “blue” spectral region. The difference in energy absorption / emission is equal to characteristic vibrational energy levels of the molecule, which provides “fingerprint” information of the probed substance. This makes Raman technique extremely useful for the identification of chemicals in food studies [Sowoidnich and Kronfeldt, 2012a], oceanography [White, 2010; White, 2008], biology [Baena and Lend, 2004; Gelder, 2007] and even for security/ military purposes [Mogilevsky *et al.*, 2012].

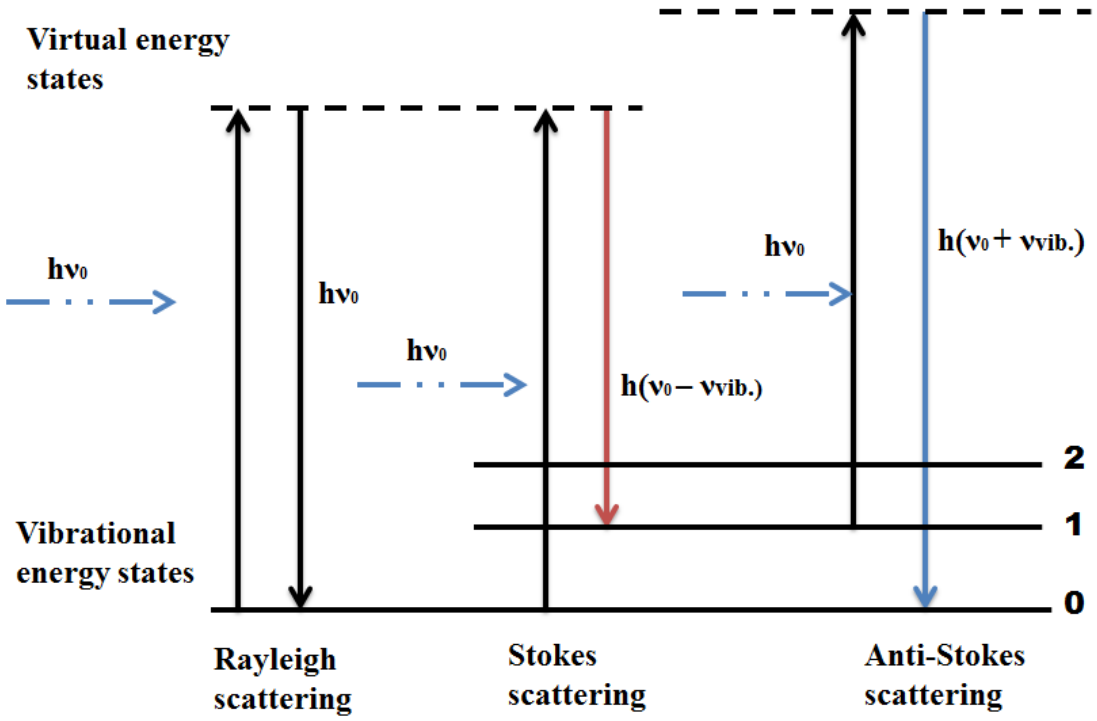

Figure 1: Schematic representation of light scattering from molecules excited by an incident photon with energy $h\nu_0$.

3.1 Classical wave theory

The Raman effect is based on the induction of an electronic dipole moment when a molecule is exposed to the electric field E and its electronic cloud is deformed. The intensity of Raman signal will be determined by the change of the molecular polarizability α. The laser beam can be considered as an oscillating electromagnetic wave with electrical vector E. Upon interaction with the sample it induces an electric dipole moment P, which deforms the shape and size of the electronic cloud of the molecules [Long, 2002]. The relationship between the oscillating dipole moment and the field is described by the following equation:

$$P = \alpha E \qquad (1)$$

The electromagnetic field of the incident light can be expressed as:

$$E = E_0 \cos(2\pi\nu_0 t), \quad (2)$$

where ν_0 is the frequency of the light

Using equation 1, the induced dipole moment is:

$$P = \alpha E_0 \cos(2\pi\nu_0 t) \quad (3)$$

Considering a harmonic oscillation of the molecule, the polarizability temporally changes in the following way:

$$\alpha = \alpha_0 + (\Delta\alpha) \cos(2\pi\nu_{vib.} t), \quad (4)$$

Where α_0 is equilibrium polarizability and $\nu_{vib.}$ is frequency of specific vibrational mode.

Therefore, induced dipole moment can be transformed into the following equation:

$$P = [\alpha_0 + (\Delta\alpha) \cos(2\pi\nu_{vib.} t)] \times E_0 \cos(2\pi\nu_0 t) \quad (5)$$

Finally, the equation can be rearranged to:

$$P = \alpha_0 E_0 \cos 2\pi\nu_0 t + 1/2\, \Delta\alpha\, E_0 [\cos 2\pi(\nu_0+\nu_{vib.})t + \cos 2\pi(\nu_0-\nu_{vib.})t] \quad (6)$$

This equation predicts that the induced dipole moment will oscillate with the following three frequencies: ν_0, $\nu_0+\nu_{vib}$ and $\nu_0-\nu_{vib}$: ν_0 represent the Rayleigh scattering, $\nu_0+\nu_{vib}$ is the anti-Stokes scattering, and $\nu_0-\nu_{vib}$ is the Stokes scattering.

However, the low Raman scattering cross section (10^{-25} - 10^{-30} cm^2) limits its applications [Kneipp, 2007, Kneipp *et al.*, 2006]. For identification of chemicals at low concentration in water bodies, the Raman signal is too weak to be detected even with the most recent Raman equipment. Therefore, several variations of Raman spectroscopy have been developed to enhance the signal. One of the most usual methods to enhance the sensitivity is Surface Enhanced Raman Spectroscopy (SERS) [Kwon *et al.*, 2012b]. Furthermore, to remove fluorescence and background noise, Shifted Excitation Raman Difference (SERDS) [Sowoidnich and Kronfeldt, 2012a,b] can be applied. Resonance Raman is suitable to enhance specific Raman lines (Raman microscopy), and acquire very specific information [Maiwald *et al.*, 2009a]. In this work, SERS and SERDS have been applied to explore the advantages of both methods.

3.2 Surface Enhanced Raman Scattering (SERS)

In 1974, Fleischman and coworkers [Fleischmann *et al.*, 1974] discovered large Raman signal from pyridine adsorbed on electrochemically roughened silver and referred it to the number of molecules that were scattering on the surface. They did not recognize a major enhancement effect. Three years later in 1977 two groups independently noted that the concentration of analyte could not describe such large enhancements of the signal. Each group developed a model of the enhancement effect. Jeanmaire and Van Duyne [Jeanmaire and Duyne, 1977] proposed an electromagnetic effect, while Albrecht and Creighton [Albrecht and Creighton, 1977] described a charge-transfer (chemical enhancement) effect.

3.2.1 Electromagnetic enhancement effect

The electromagnetic enhancement is dominant in SERS and can be as high as 10^{12} for some systems [Kneipp, 2007; Baker and Moore, 2005; Hicks, 2001] while the chemical

effect enhances the Raman signal up to two orders of magnitude. The combination of both effects gives a total SERS enhancement up to 10^{14}.

The power of Raman signal (R_{SERS}) depends on the number of molecules N involved in the process, the laser intensity I_L, the effective Raman cross section of the adsorbed molecule σ^R_{ads}, and enhancement factors $|A(\nu_L)|^2$ – magnification of laser-excitation and $|A(\nu_S)|^2$ – scattered field [Kneipp, 2007; Baker and Moore, 2005]. According to equation 7, the Raman signal is following:

$$R_{SERS} \sim N \times I_L \times \sigma^R_{ads} \times |A(\nu_L)|^2 \times |A(\nu_S)|^2 \quad (7)$$

Where,

$$A(\nu_L) \approx \frac{\varepsilon(\nu_L) - \varepsilon_0}{\varepsilon(\nu_L) + 2\varepsilon_0} \left(\frac{r}{r+d}\right)^3 \quad (8)$$

$\varepsilon(\nu_L)$ and ε_0 are complex dielectric constants of electromagnetic fields, *r* is metals sphere radius and *d* is distance between the molecule and metal particle.

Therefore, electromagnetic enhancement factor becomes as follows:

$$|A(\nu_L)|^2 \times |A(\nu_S)|^2 \approx \left|\frac{\varepsilon(\nu_L) - \varepsilon_0}{\varepsilon(\nu_L) + 2\varepsilon_0}\right|^2 \left|\frac{\varepsilon(\nu_L) - \varepsilon_0}{\varepsilon(\nu_L) + 2\varepsilon_0}\right|^2 \left(\frac{r}{r+d}\right)^{12} \quad (9)$$

This equation shows that enhancement scales are in the power of four of the local metallic nanostructure fields, the enhancement is the strongest when incident laser and Raman scattered fields are in resonance with surface plasmons and lastly, dependence on the distance between molecule and metal particle is essential [Kneipp, 2007; Baker and Moore, 2005].

The early SERS experiments that was done by S. Nie and S. R. Emory [Nie and Emory, 1997], showed that the intensity of SERS depends from polarization of incident light, the orientation of particles and orientation of molecules adsorbed to the particle. Only very few molecules showed strong enhancements of the signal, which is due to “hot spots” created by the metal plasmons. The size of those “hot spots” is three times of average particle size,

which means that particle aggregation and formation of colloid blocks would increase the amount “hot spots” and attached molecules.

One of the substrates – Ag,DMCX:MTEOS, which is applied in this work for sea water investigations has such a structure and the experimental results are in agreement with previously completed studies [Murphy *et al.*, 1999; Kwon *et al.*, 2012a; Kwon *et al.*, 2011].

3.2.2. Chemical enhancement effect

Chemical enhancement effect is not yet completely understood. Even if enhancement factor is only around two orders of magnitude, the chemical effect cannot be separated from electromagnetic effect, as it shows some phenomena that cannot be explained by electromagnetic theory. The study of [Hubental, 2013] propose chemical interface damping mechanism which is caused by electron transfer from the metallic structure of SERS surface to the adsorbate, as a basic mechanism for chemical enhancement effect in SERS.

Two theories (electromagnetic and chemical enhancement) complete each other. For example, SERS is not independent from chemical nature of the adsorbed molecule as it should be in electromagnetic effect. Therefore, chemical enhancement of the signal must also take place. It can be divided on two models: Charge transfer model and adatom model [Vo-Dinh, 1998; Zeman and Schatz, 1987].

Charge transfer model involves chemical bond formation between metal and adsorbate, increasing the value of molecular polarizability. This happens due to overlapping of metal and adsorbed molecule electronic wavefunctions which “initiatestes” charge-transfer process.

If the molecule is adsorbed to the defected sides of a metal surface, the overall signal enhancement is more effective. This may be due to adsorption on special active sites of atomic scale roughness (adatoms) which facilitates charge-transfer mechanism [Vo-Dinh, 1998].

3.3 Shifted Excitation Raman Difference Spectroscopy (SERDS)

Another useful technique for better identification of the Raman bands by removing fluorescence and fixed-pattern noise from Raman signal detection unit, e.g. with CCD detectors, is SERDS. The technique was originally introduced by Shreve in 1992 [Shreve *et al.*, 1992]. SERDS can be applied when Raman spectra are excited by two laser lines closely spaced, i.e. around $\Delta\nu = 10\ cm^{-1}$ in frequency. In this case the Raman peaks shift according to the laser frequencies, while the broad fluorescence background remains unchanged. Subtracting the two spectra can thus remove the fluorescence and provide Raman spectra of better resolution [Schmidt *et al.*, 2011]. Numerous studies [Sowoidnich and Kronfeldt, 2012a,b; Kwon *et al*, 2012b; Ahmad *et al*, 2011; Maiwald *et al*, 2009a] have proved the efficiency of SERDS by resolving highly fluorescent spectra and obtaining measurement results in the concentrations of pyrene in the pM range [Kwon, 2012].

3.4 The combination of Raman techniques

In selected cases the combination of Raman techniques provides high efficiency in order to improve the limit of detection of the investigated chemical. Very good results are obtained applying a combination of SERS and SERDS [Kwon, 2012; Kwon *et al*., 2012 c]. Therefore, such combination was also applied in the current work.

4. Experiments

4.1 SERS and SERS/SERDS basic set-up

The portable Raman/SERS sensor system for sea water investigations in laboratory and in situ experiments, contains four main parts, see figure 2: (A) microsystem diode laser with excitation wavelength of 671 nm for SERS measurements or two laser diodes with excitation wavelength of 670.0 / 671.6 nm for SERS/SERDS measurements; (B) the Raman optode and the substrate, (C) the miniature spectrometer and (D) netbook. Depending on applications, a few parts may be added or changed in the basic set up. There are three different applications of the current set up for the sea going instrument, i.e. in the laboratory, on board, and in situ: see chapters 4.2, 4.3 and 4.4.

In details: One or two laser drivers (1) was applied to control one or two diode lasers: as excitation light sources (2) [Kolomijeca *et al.*, 2012; Maiwald *et al.*, 2009 b,c]. The experimental conditions, e.g. current and temperature are set depending on target laser power, specific for each substrate (not to burn it). Note, that we apply specially developed microsystem 671 nm diode laser instead of the more common 785 nm laser, since the quantum efficiency in this spectral region of CCD-detectors are much better.

The excitation beam passes through a bandpass filter (Semrock, Inc.) (3), which is guided by two dielectric mirrors (4) to a Raman edge filter (Semrock, Inc.) (5), then on to a lens (6) with a focal length of 10 mm, which focuses the light through a quartz glass window (7) onto the substrate (8) and water sample.

The backscattered light from the sample is collected by the same lens and filtered by the Raman edge filter, which blocks the Rayleigh scattered radiation as well as the anti-Stokes scattering. The Raman Stokes signal is then launched by a lens (9) with a focal length of 16 mm into a 100 μm optical fiber (10) which is connected to the detector unit via standard SMA connector. For our experiments, the Raman Stokes light was analyzed by a custom-designed miniature spectrometer (Horiba Scientific) (11), with a dimension of 200 x 190 x 70 mm^3 and a resolution of 8 cm^{-1}. The Raman spectra are detected by a CCD camera (S7031 - 1006, Hamamatsu) with 1024 x 58 pixels, cooled thermoelectrically down to -8 °C. The spectra were recorded using a netbook (different types for each experiment) (12) running "Versaspec" software from Horiba Scientific.

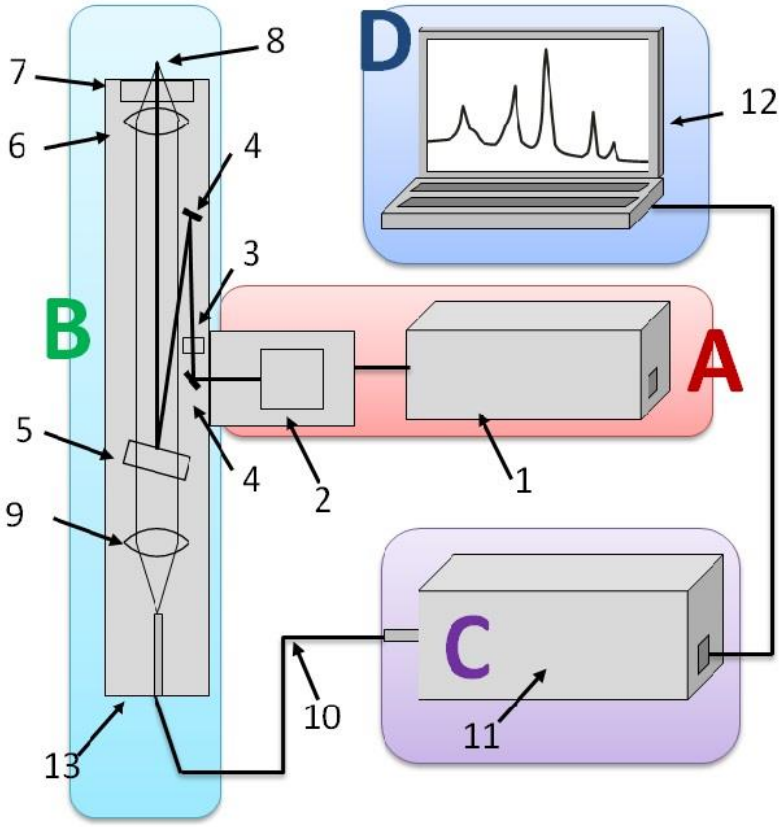

To realize a compact setup and to protect fragile parts of optics, the Raman optical bench (13), e.g. optode, which has a diameter of 25 mm and a length of 180 mm, has been designed and constructed by our group.

Figure 2 : Scheme of the sensor parts: (A) laser, (B) optode, (C) spectrometer, (D) computer; (1) laser driver, (2) microsystem diode laser, (3) bandpass filter, (4) mirrors, (5) Raman edge filter, (6) lens, (7) quartz glass window, (8) substrate and sample, (9) lens, (10) optical fiber, (11) mini spectrometer with CCD camera, (12) netbook, (13) optode.

4.2 Laboratory SERS/SERDS system for water sample investigation

As a first step, hundred seawater and sediment samples were taken from selected locations worldwide, with various laboratory experiments carried out on each sample. The specimens were collected from the North Sea (Svalbard Island, Norway), Atlantic Ocean (East Coast, USA), Pacific Ocean (West Coast, USA; Hawaii, USA), Great Lakes (Buffalo, Niagara Falls, Youngstown, NY, USA), Mediterranean Sea (Barcelona, Spain; Banyuls-Sur-Mer, Marseille, Nice, France), Chesapeake Bay (Baltimore, Washington DC, USA), East China Sea (Qingdao, China), Mississippi River (New Orleans, USA), Aegean Sea (Rhodes, Greece), Baltic Sea (Warnemunde, Germany) and other places from 2010 till 2013. For SERS investigations, the Raman sensor contains a 671 nm microsystem light source with two slightly different emission wavelengths (671.0 nm and 671.6 nm), as mentioned above. The SERDS technique was combined with newly developed gold island SERS substrates [Ahmad and Kronfeldt, 2013], i.e SERS/SERDS measurements were carried out for all water and sediment samples.

4.2.1 Tasks of the experiment

The laboratory experiments were focused towards the ability to make Raman SERS/SERDS measurements with different samples, check the substrates sensitivity in different environments, investigate the efficiency of the combined SERS/SERDS approach, try to detect new Raman bands and refer them to possible pollution sources. The tasks were as follows:

- Perform SERS/SERDS measurements for all collected water samples
- Analyze the data in order to detect PAHs or biphenyl
- Detect further chemicals in water body
- Investigation of 15 selected PAHs and biphenyl in saturation concentration (preparation procedure see in table 1) to obtain reference spectra
- Evaluate substrates for their sensitivity to specific pollutants (different PAHs)

Table 1: Preparation procedure of PAHs and biphenyl in sturation concentration

PAH	Weight/mg	MeOH/ml	Stock sol./mM	From stock sol./µl	H_2O_{dest}/ml	$C_{saturation}$
Acenap	38.6	10	25	20	19.98	25 µM
Aceylene	33.5	10	22	20	19.98	22 µ/M
Ant	9	50	1	17	99.983	170 nM
BaA	1.2	10	0.5	1	19.999	25 nM
BbF	0.3	10	0.1	1.8	19.9982	9 nM
	1.3	50	0.1			
BaP	0.3	10	0.1	3	19.997	15 nM
	1.3	20	0.1	757.5	19.2425	15 nM
BgP	Already in stock sol.		400 (nM)	55.1	19.9448	1 nM
BkF	0.3	10	0.1	1.8	19.9982	9 nM
	1.3	50	0.1	545.4	19.4546	9 nM
Chr	0.2	10	0.1	1.6	19.9984	8 nM
Fla	6.1	20	3	20	99.98	600 nM
Flu	13.8	10	8.3	20	19.98	8.3 µM
Nap	230.8	10	180	20	19.98	180 µM
Phe	68	20	19	20	99.98	3.9 µM
Pyr	8	20	2	20	99.98	4000 nM
Bip	46.3	10	30	20	19.98	30 µM

4.2.2 Experimental conditions

The experiments were carried out at room temperature with a typical sample quantity for each measurement of less than 1 ml. Each sample was investigated with different substrate. Every sample has a record of three measurements:

1. "Blank" - spectrum of artificial[1] sea water
2. "Sample" - spectrum after substrate was immersed into water sample solution at least for 15 min. up to 1 h.
3. "Control" - spectrum of 15 nM pyrene[2] dissolved in artificial sea water.

[1] 30.5 g instant ocean salt dissolved in 1 l of distilled water/filtered through filter paper (grade 595; pore size 4 µm - 7 µm)

[2] Further dissolved from pyrene in saturation concentration (table 1).

The measurements order always remained as described above to prevent contamination of the substrate. Examples of the measurements of the three spectra are presented in chapter 5.1.2.

The combination of SERS /SERDS was applied for achieving the high sensitivity necessary for trace detection in the sub nM regime of numerous substances, for example polycyclic aromatic hydrocarbon (PAHs) or biphenyl, dissolved in sea water or deposited in sediments.

All experiments were carried out under the same experimental conditions:

- Laser wavelengths λ = 671.0 nm, 670.6 nm.
- Laser T = 25 ^{o}C; laser power 30 mW (at I = 325 mA);
- Integration time t = 10 s.

4.2.3 Laboratory set up

The laboratory Raman SERS/SERDS set up is shown in figure 3. It consists of (a) three laser drivers (TuiOptics Inc. (t) and two drivers Thorlabs Inc. (I)); where one is used to control the temperature of the microsystem laser diodes and the other two provides current for both lasers: 671.6 nm and 671.0 nm, which are part of optode (b); miniature spectrometer (c) (described above), analyze the Raman signals and display them on the computer screen, Eee PC 1000HE (d).

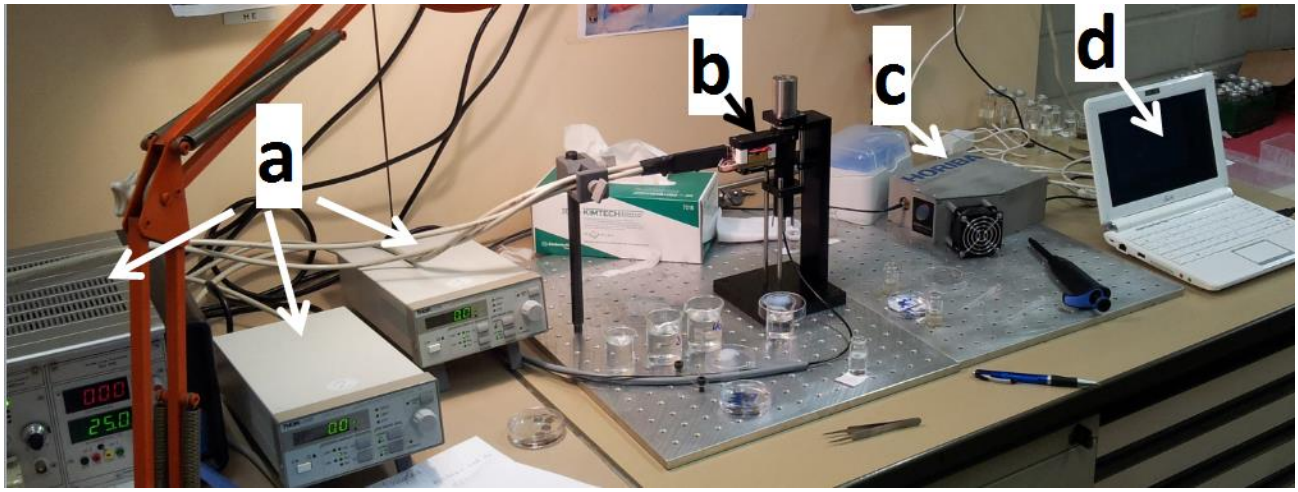

Figure 3: Laboratory Raman set up for water samples investigation – (a) laser drivers; (b) microsystem laser diode and optode; (c) miniature spectrometer; (d) netbook.

The unique microsystem diode laser, with a complete size of 20 mm x 5 mm x 3 mm, suitable for SERDS measurements, was designed and manufactured at Ferdinand-Braun-Institut, Leibniz-Institut für Höchstfrequenztechnik [Maiwald *et al*, 2009b,c] and tested in practical applications by our group at Technical University Berlin [Sowoidnich and Kronfeldt, 2012 a,b; Ahmad *et al.*, 2011; Kwon 2012].

4.2.4 Preparation of gold island SERS substrates

Gold island substrates were prepared according to electroless plating method, by using a mixture of solution from $HAuCl_4$ and H_2O_2. This method allows gold nano particles to aggregate on the surface of the substrates which leads to Raman signal amplification. For a detailed preparation procedure, see [Ahmad and Kronfeldt, 2013].

4.2.5 Water and sediment samples collection

All water and sediment samples were collected in coastal areas (except cruises) in 20 ml glass bottles[3], see figure (4 a), which were securely sealed (with bottle sealing grips, fig. 4 b) to prevent leakage or contamination. It was necessary to take two samples for each in case of sample breakages or the need for re-measuring etc. As reference data; temperature, salinity and GPS position data were taken along with every sample and saved in the laptop, fig. 4 c., applying Pasco Pas*Port* GPS (PS-2175), salinity and temperature sensors (PS-2195), fig. 4 d, and "Data Studio" program to read the measurements. Each measurement for temperature, salinity and GPS position were taken during 1-2 minutes with a frequency of 1 measurement per second. The relative displacement from GPS location (for latitude and longitude) is ~0.2 m in a range of ± 10000 m [Pasport, a].

The salinity sensor measures conductivity in a range from 1000 μS to 100 000 μS and in a temperature range from 0^{o} C to 50^{o} C. The salinity range is from 1 part per thousand (ppt) to 55 ppt ± 10% without calibration [Pasport, b].

[3] VWR international Inc., Vial headspace glass (75.5 x 23 mm; transp. = 1. Class), covered with 20 mm aluminum caps (clear, silicone/alu., 50^{o} shore A, 3 mm).

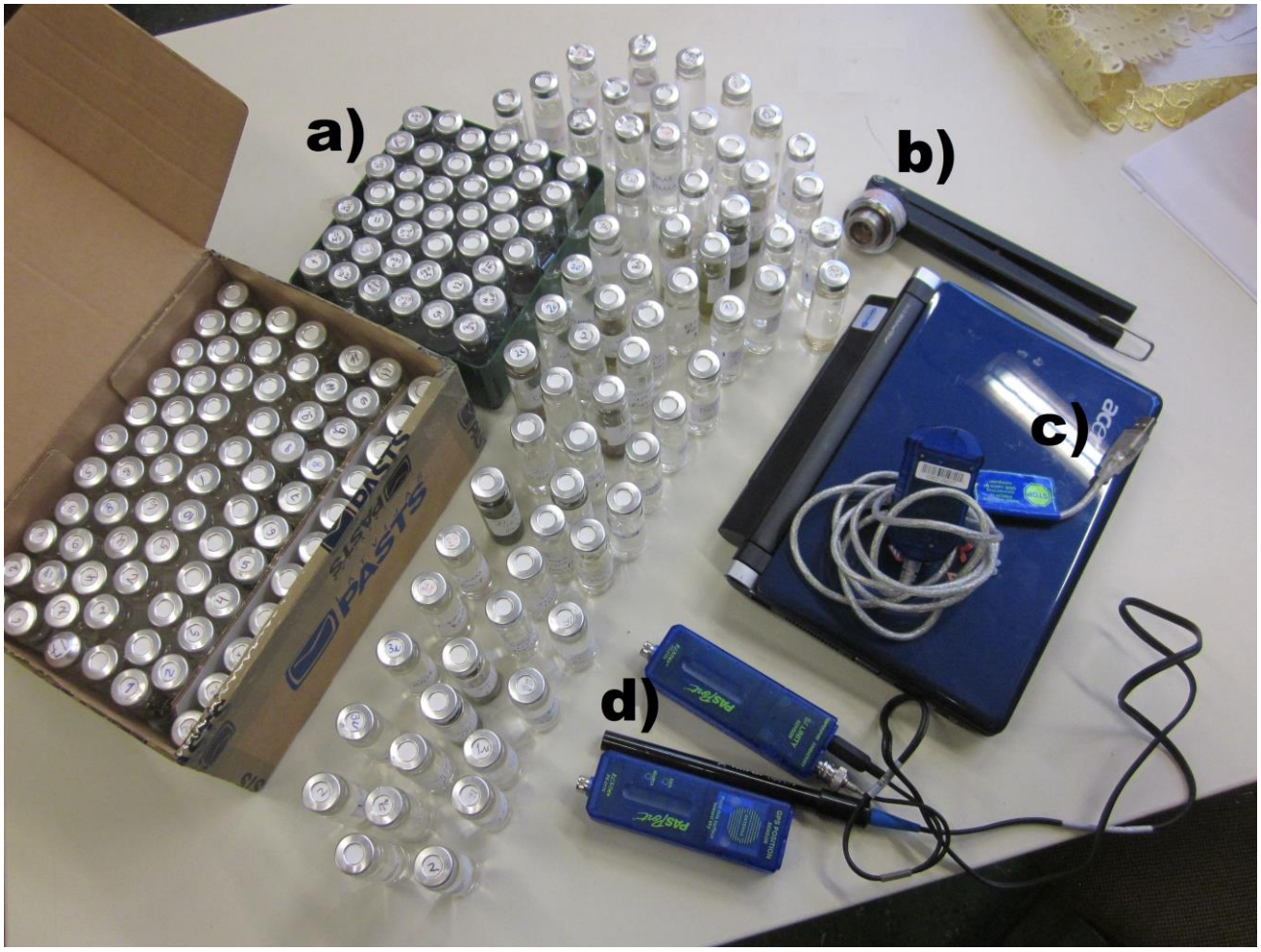

Figure 4: Water samples reference data equipment; a) water samples; b) bottle closing device; c) laptop and adapter; d) salinity / temperature and GPS sensors.

4.3 On board portable Raman system for Arctic test

Since all previous Raman experiments were done in the laboratory with artificial sea water, it remained completely unclear how the set up and SERS surfaces would behave in real field conditions, e.g. experiencing vibrations from the ship, lower temperatures of the water samples, substrates sensitivity and stability in real sea water. Therefore, to carry out pilot studies of the in situ Raman sensor in real field conditions with seawater, "on board" portable Raman system was tested in the Arctic area during three weeks (2011, August 2nd-21st). Various locations were examined onboard James Clark Ross research vessel (British Antarctic survey) [Kolomijeca *et al.*, 2012 a,b].

Arctic region is known for PAHs existence [Sapota *et al.*, 2009]. Main pollution sources in the area is in the form of atmospheric deposition from local mining industries and coal-fired power stations in the Isefjord [Rosie *et al.*, 2004] as well as being transported from other locations via the atmosphere, ocean current and river flow [Barrie *et al.*, 1992; Fellin *et al.*, 1996]. Concentration of PAHs in summer time is the lowest, making investigations more difficult and challenging. Previous studies identified the presence of PAHs in surface sediments from five locations around the fjords (79.4 N -15.4 E), in the concentration range of Σ16PAHs = 36 ng g^{-1} (dray weight) [Sapota *et al.*, 2009].

4.3.1 Description of the cruise

The JCR 253 cruise was joined by me in the beginning of August from Svalbard Island, while the main scientist team joined the cruise one week earlier from Glasgow, Scotland. During the following three weeks, the research area was between 78^{o} N and 10^{o} E. The area of the cruise and ship's track line is presented in figure 5[4].

[4] The picture is kindly provided by Michal Tomczyk, University of Bremen, Germany.

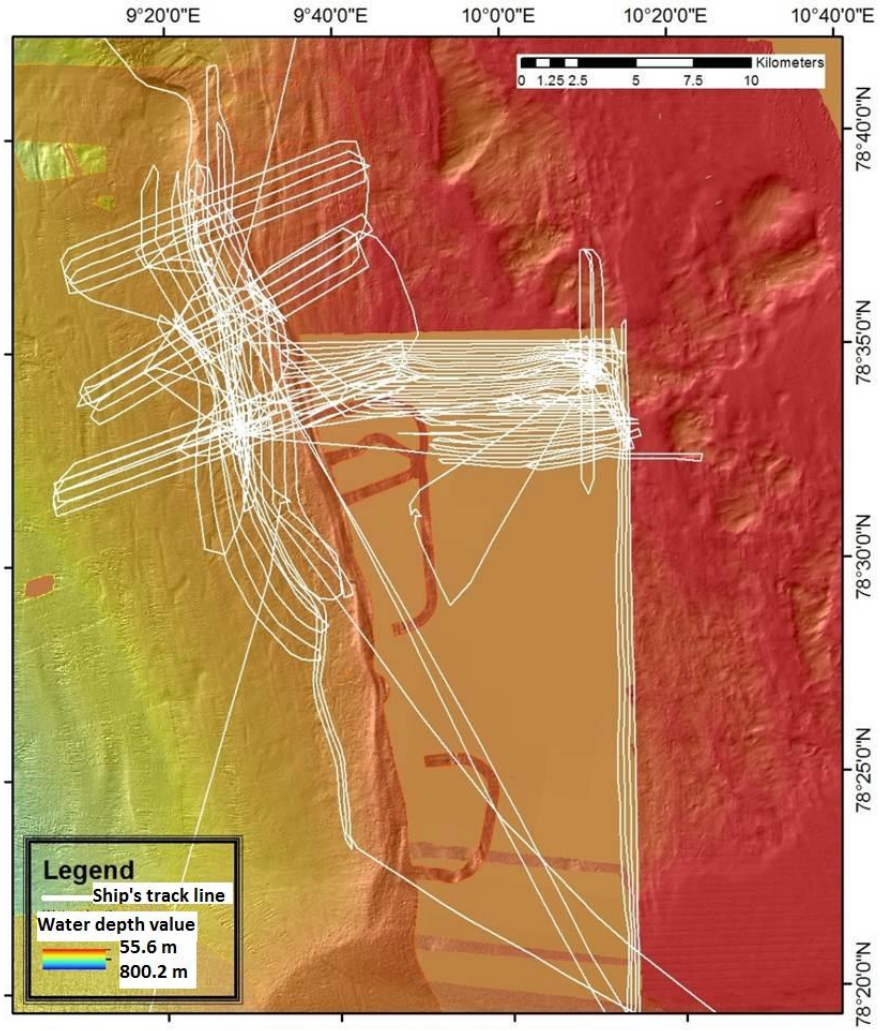

Figure 5: Area of the cruise and ship's track line

All experiments with portable Raman set up were done during night shifts from 10 pm until 10 am (this time of the year the day light is 24 h/day). All laboratory consumables, including all kind of transparent glasses, pipets, gloves, voltage connectors, safety shoes, petri dishes, tweezers, stationary consumables, containers for sea water and waste as well as all chemicals (PAHs and solvents) were collected and sent from Berlin.

4.3.2 Tasks of the experiment

Since Arctic sea trial tests were an intermediate step between laboratory experiments and construction of the sea going instrument, most of the tasks were focused towards Raman sensor equipment and its ability to work in harsh field conditions, e.g. vibrations from the ship, real sea water etc. The main tasks[5] of arctic experiment were as follows:

- Check portable Raman set up under harsh field conditions
- Analyze surface and sediment water from selected locations
- Perform artificial spiking tests with PAHs in real sea water
- Determine in situ limit of detection of the selected PAHs
- Evaluate short-term and long-time substrate stability.

4.3.3 Experimental conditions

Experiments were performed in the laboratory onboard JCR at room temperature of 25 ^{o}C. In total, approximately 40 Ag,DMCX:MTEOS substrates were examined. The substrates were continuously exchanged for different experiments to prevent contamination. Different integration times were applied for most of the measurements: 0.3 s, 0.5 s, 1 s, 5 s, 10 s, 25 s, 35 s, 50 s, in order to find the optimum ratio between (shortest) integration time and (highest) Raman signal. Every result spectrum is averaged from 10. The laser power on the sample was typically: 18 mW (I = 275 mA, t = 25 ^{o}C), Sample flow rate 0.05 ml/s.

[5] All tasks for the Arctic experiment see in the appendix II

4.3.4 On board set-up

To achieve the aims of the experiment, a few additional parts were added to the previously described basic Raman set-up (see fig. 6). The 671 nm laser (1) is fixed in the aluminium housing (2), which is constructed in our workshop; this way the optics and electronics are protected against moisture, dust and physical shocks. The collected Raman signal passes through the fibre optic cable (3) into a miniature spectrometer for further analyzing. The sensor head (4) contains optics for excitation and collection of the signal [Sowoidnich *et al.*, 2012].

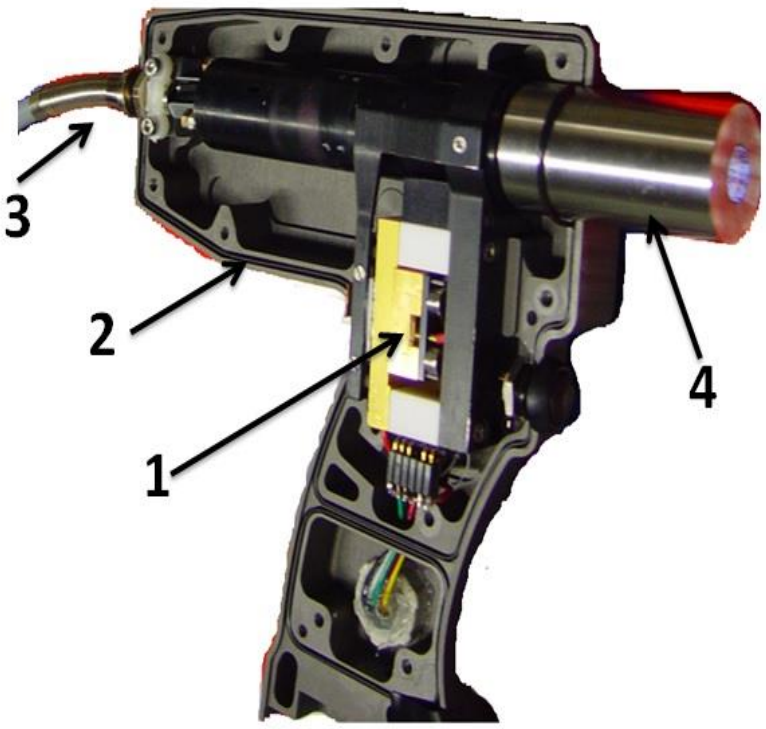

Figure 6: Optode with diode laser in aluminum housing. (1) microsystem diode laser, (2) sensor housing (3) optical fiber (4) optode.

Since water investigations were done on board the ship, a self-constructed flow-through cell system was applied to ensure a constant sample of water flow. The flow through cell, which is schematically depicted in figure 7, was made from a quartz window and a sea water resistant aluminum alloy. The thickness of the sample solution in the cell is 3 mm and the effective volume is 113 µl [Kwon, 2012].

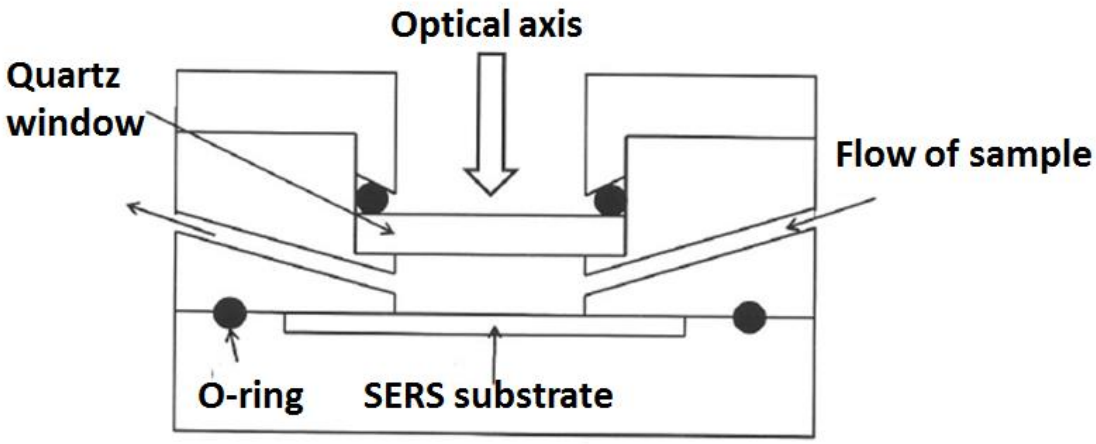

Figure 7: Scheme of flow-through cell [Kwon, 2012].

The peristaltic pump (PP1-05, ISMATEC), as part of the sample supply system, held a constant water flow with a speed rate of 0.05 ml/s. Sample and waste water reservoirs were constantly filled and emptied, making sure there was no contamination with other chemicals. A picture of the complete on board Raman set up is presented in figure 8.

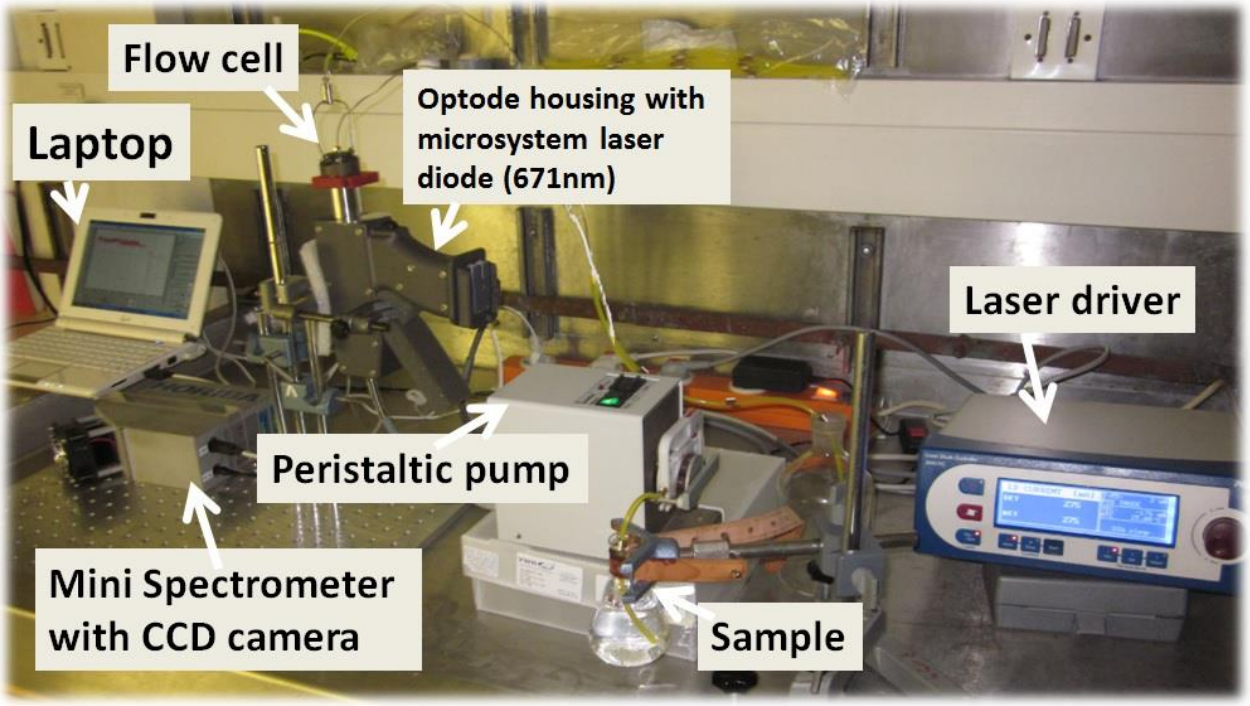

Figure 8: Portable Raman set up on board of James Clark Ross, August 2011.

The equipment, including portable Raman/SERS set up, laser driver (Sacher Lasertechnik Inc.), miniature spectrometer (Horiba Inc.) with CCD camera (Hamamatsu Inc.), peristaltic pump (Ismatec SA), flow through cell, glass holders etc., were carefully collected and tested in Berlin prior to sending them to the ship. The "set up check" involved measuring of laser power dependence from the temperature in a range of 25 ^{o}C – 28 ^{o}C, calculating and testing correct focal position of the laser beam, flow through cell flow speed rate, sensor calibration and test experiments with polluted water, as well as preparation of the "stock" solutions from pure anthracene, pyrene and fluoranthene dissolved in methanol.

4.3.5 Sampling and substrates preparation

Constant supply of surface seawater was ensured by pumping it onboard to the laboratory through a pipe. Surface water and sediment water of twenty locations (see

appendix II) between 78 ^{o}N and 10 ^{o}E were examined with surface water temperatures varying from 3 ^{o}C to 5 ^{o}C.

The sediment samples (locations indicated in appendix II) were taken in a depth of 200 m – 400 m applying gravity corer. Then it was mixed with surface seawater (50 % - 50 %) and heated up to 20 ^{o}C – 40 ^{o}C, in order to make desorption process (of possible pollution) more efficient. Finally sediment water was filtered with laboratory filter paper (pore size 4 μm – 7 μm).

The flow through cell was washed with milli-Q water between the experiments (not involving PAH spiking). In case of the PAH spiking tests, cleaning procedure of equipment involved three steps of clean [1.milli-Q water – 2.Methanol + Acetone mixture (50 % - 50 %) – 3.milli-Q water] and pipe exchange. All spiking tests were carried out with real sea water, which was mixed with PAHs: pyrene (pyr), anthracene (ant) and fluorenthene (fla) in the following order: one by one (e.g. pyr, or ant, or fla) / two of each (e.g., pyr and ant, or ant and fla, or fla and pyr) / all three in different concentrations (pyr, ant and fla) starting with 0.25 nM up to their specific saturation concentrations, i.e. 150 nM anthracene, 400 nM pyrene and 600 nM fluorenthene. All chemicals used in the experiments were purchased from Sigma Aldrich Company.

The substrates were prepared on a base of quartz (d = 10 mm; thickness = 1 mm) applying the sol-gel technique [Murphy, 1999] which was further developed and resulted in the formation of silver colloids, functionalized with DMCX in MTEOS derived sol-gel film: Ag,DMCX:MTEOS [Kwon *et al* 2011; Kwon *et al*, 2012; Kwon, 2012].

Before measurement, the prepared SERS substrates were stored in distilled water. For every measurement, new substrates were used, except for the stability tests.

4.4 Sea going instrument

4.4.1 Electrical Specifications

The main aim of EU project [SENSEnet, 2013] was to develop a fully autonomous sea going instrument that could be fully submersed without any external cables or connections to the sensor from a research vessel. This is achieved by supplying power from a 12 V DC 60 A Lithium Ion Battery (Lithionics, Inc.) that is housed inside the sensor tube (see appendix III) together with all the components. During normal running conditions, the sensor requires 2.75 A (measured with Ammeter) running current. This gives the system a total usage time of approximately 22 h from each charge.

The autonomous sea going instrument (see figure 9) contains:

- A 671nm microsystem laser diode (1) described above
- Junction boxes – IP 55 rated (2)
- Two laser drivers – 12 V DC/3.75 A (Pilot PC500 OEM, Sacher Lasertechnik) (3)
- Changeover switch – 4 pole/10 A Industrial Cam Switches (4)
- Microcomputer – 19 V DC/3.42 A (Acer Aspire Revo R3700) (5)
- Miniature spectrometer/CCD camera – 9 V DC/670 mA/6.03 W (Horiba /Hamamatsu) (6)
- Battery - Lithium Ion 12 V DC, 60 A (Lithionics) (7)
- DC/DC converter – 12/19 V DC/3.42 A/65 W
- DC/DC converter – TSR 1-2490 12/9 V DC/1 A (Traco Power).

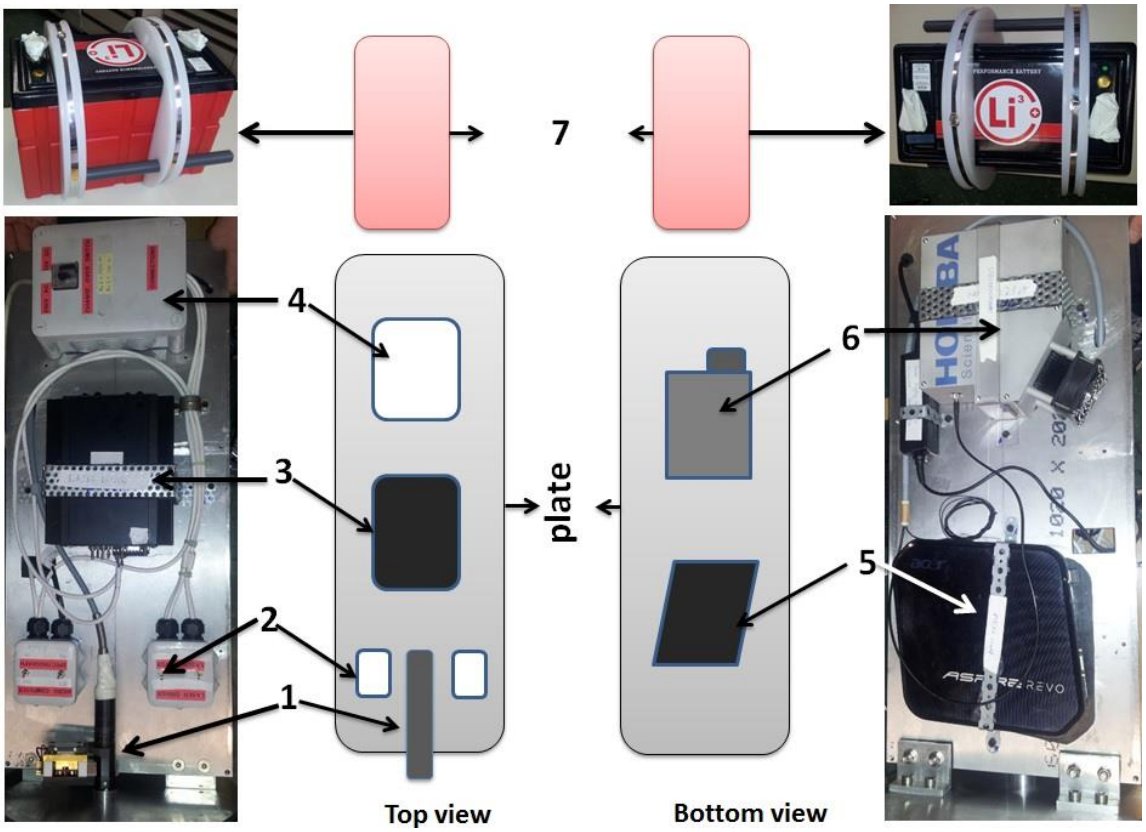

Figure 9: Scheme and photo of self developed sea going instrument (SGI). 1. optode with 671 nm microsystem laser diode ; 2. junction boxes; 3. laser drivers; 4.changeover switch; 5. computer; 6. spectrometer with CCD camera; 7. battery.

The complete sea going instrument has a length of 107.4 cm, diameter of 32 cm and a weight of 70 kg (with all the components inside), equation of V_{tube} is presented below. A Minimum of 40 kg of additional weight must be added to the instrument in order to have a neutral weight in water. The static buoyancy of the SGI is 88 kg[6].

---

6 $V = \pi r^2 h$

$V_{tube} = 3.14 * 16^2 * 107.4 = 86332_{cm^3} = 0.0863_{m^3}$

$Buoyancy_{static} = V_{sgi} * \rho_{sea\,water} = 0.0863_{m^3} * 1025_{\frac{kg}{m^3}} = 88_{kg}$

4.4.2 Battery

The battery (Lithium Ion, Lithionics Inc.) is fully secured inside one end of the housing tube, by specially designed plastic holders to prevent any movement, which could cause serious damage to the sensor due to Lithium Ion properties or by shock damages, see figure 10. They also act as a very comfortable grip for removing the battery. Due to state-of-the-art design, the weight of the battery amounts to 13 kg only. This was an important factor when designing the sea going instrument to keep the weight down to a minimum. Charging is performed by an intelligent battery charger (Input: 90 V ~ 240 V; Output: DC 12 V ~ 20 A, Lithionics), which takes approximately 3-4 hours for a full charge.

Figure 10: Li ion battery with the handle

4.4.3 230VAC Implementation

As can be seen from the electrical schematic diagram (see appendix IV and V), the sensor has been designed to implement 230 V AC single phase mains power (with the addition of some power supplies and a multi socket), if needed for laboratory use or testing purposes without having to depend on the battery supply time. However, in situ experiments which were done in this current study did not require 230 V AC, therefore it can be installed upon request for future applications.

4.4.4 Housing

All the components of the sensor are secured to an aluminum base plate that slides into the water resistant aluminum housing (Develogic GmbH, see appendix III). Both ends are removable, but one side has the optode attached, therefore special care is needed when removing not to de-adjust or damage the laser. Each end is secured to the tube by allen key grub screws (M5) and has special "O Ring" seals to prevent water ingress into the tube.

4.4.5 Electrical Wiring

All electrical parts, connections and terminations have been wired to industry standard (see appendix IV – circuit diagram and appendix V – wiring diagram). The main electrical connection junction box (155 mm x 155 mm x 74 mm) is IP55 (Ingress Protection) rated and controls the mains supply by a 3-position changeover switch mounted on the front. For 12 V DC use, the switch must be in "Position 2". If 230 V AC is implemented, the switch must be in "Position 1". There is full electrical isolation between 230 V AC and 12 V DC supply through this switch. Inside the electrical connection box there is a set of din rail connectors each numbered, (E, 1-12). The first 4 connectors are for 230 V AC use. Connectors numbered 3-6 are a positive 12 V DC rail, connectors 9-12 are a negative 12 VDC rail and connector number 7 is a 9 VDC supply for the spectrometer.

4.4.6 Main Components

The microcomputer requires a 19 V DC supply. Therefore, a DC/DC converter was used to convert 12 V DC to 19 VDC. The spectrometer requires a 9 VDC supply, which is achieved through a Traco Power (model: TSR1-2490) DC/DC 12 to 9 V DC converter component. Even though the current rating for the spectrometer is 670 mA, a 1 Ampere fuse was needed due to the inrush current of the fan motor upon starting the spectrograph.

4.4.7 Fuses

All the main components are protected by appropriate fuse sizes (5 x 20 mm) to prevent damage to any component by a short circuit or any electrical fault. Full discrimination (fuse nearest the fault blows first) has been applied protecting the relevant parts. Series In-Line fuse holders were chosen due to their ease for implementation, replacement of fuses and minimum size. See appendix IV, V:

F1 – Not installed (230 V AC use)
F2 – Main fuse for battery (6.3 A)
F3 – 12/19V DC/DC converter protection (3.15 A)
F4 – Not installed or needed as component is small and cheap to replace (max. rating 1 A)
F5 – Micro Computer protection (4 A)
F6 – Spectrograph protection (1 A)
F7 – Laser Driver protection (3.15 A)
F8 – Laser Driver protection (3.15 A)

4.4.8 Switches

Two further junction boxes (65 mm x 65 mm x 40 mm) were used to house switches, connections and fuse holders. One junction box controls power to the micro computer and Spectrometer through switches SW1 and SW2 respectively by opening and closing the circuit depending on their position. The other junction box controls power to the laser drivers through SW3 and SW4. See appendix IV, V:

SW1 – Micro Computer
SW2 – Spectrometer
SW3 – Laser Driver 1
SW4 – Laser Driver 2

4.4.9 Tasks of experiment for SGI

Since SGI construction is the main task of the current PhD work, it was very important to achieve the main requirements, e.g. make it fully autonomous, mechanically robust and able to work for several hours in different depths down to 100 m. The top priority tasks were:

- Tube leakage tests
- In situ harbor Raman/SERS measurements
- Sea trial tests
- Investigation of water samples in laboratory for cross references.

4.4.10 Conditions and the area of experiment

IFREMER, Seyne-sur-Mer, France kindly provided facilities and opportunities for the final calibration of sea going instrument and testing in the area of the Mediterranean Sea. Therefore, all experimental studies were carried out in France from 01.10.2012 until 07.01.2013. Tube leakage (short term: minutes range and long term: one day range) experiments as well as measurements in fresh water were done in the IFREMER indoor pool at room temperature. In situ measurements were done outdoor in the harbor and in open water areas at different temperatures, weather conditions, and timing of the day. The area of measurements:

- **Pools** (in-door, outdoor): IFREMER (Seyne-sur-Mer, France)
- **Harbor**: Mediterranean Sea (La Seyne-sur-Mer, France: N 43.1054 and E 5.8856)
- **Sea trial**: Mediterranean Sea (Station I: N 43.0052; E 5.0571; Station II (Tamaris Le Lazaret muscle farm): N 43.0053; E 5.0544)

Experimental conditions: Laser 671 nm, temperature 11 ^{o}C – 23 ^{o}C, Laser I = 275 mA, Power ~ 30 mW; integration time 5 s – 60 s, depending on experiment.

5. Results

The work is divided into three main parts: (5.1). Laboratory experiments, (5.2). Pilot studies in the Arctic, (5.3). SGI construction and testing. Thus, the results will be discussed in the same order.

5.1 Laboratory experiments for water samples investigations

In the time period of 2011 – 2013, approximately one hundred water samples were collected at selected locations in Europe, Asia, and America, which are schematically presented in figure 11 (details can be found in chapter 4.2).

The data containing precise geographical position as well as water conditions (salinity and temperature) are collected in appendix VI.

Figure 11: Locations of collected water samples, EU: Norwegian Sea, Mediterranean Sea, Aegean sea, Baltic sea; Asia: East China Sea; America: Atlantic Ocean, Pacific Ocean, Gtreat lakes, Chesapeake bay, and Mississippi River, [Maps of EU and Asia taken from www.nationsonline.org; America: The National Atlas of the USA].

5.1.1 The reference data

The reference data, e.g Raman and SERS / SERDS measurements of chosen PAHs in their pure state or / and saturation concentrations, adsorbed on Ag,DMCX: MTEOS and gold island substrates, are presented in appendix VII.

As we can see from reference measurements (appendix VII), different types of substrates are individually selective to PAHs and biphenyl. Due to adsorption properties of the substrates, Raman bands from the same chemical may appear in slightly different positions with different intensities [Kwon, 2012]. For example, SERS/SERDS spectrum of biphenyl in its saturation concentration (30 μM), adsorbed on gold island substrate, figure 12 (a), looks different than the Raman/SERDS spectrum from pure biphenyl, in figure 12 (b). As we can observe from figure 12, adsorption properties of the substrate may significantly influence Raman spectrum from the same chemical. Therefore, standard Raman measurements cannot be taken as reference data in all cases. According to figure 12 (a), measuring SERS/SERDS signal from biphenyl, dissolved in artificial sea water in saturation concentration, produce intense signals in the area of 488 cm^{-1}, which belong to quartz (it should not be taken into consideration) and Raman signal in the area of 990 cm^{-1}, which is overlapping with the signal from the substrate (fig. 12 a (upper spectrum, in blue)). The rest of the signals, in the area of: 730 cm^{-1}, 1140 cm^{-1}, 1190 cm^{-1}, 1270 cm^{-1}, 1360 cm^{-1} and 1490 cm^{-1} have lower intensities, which are approximately equal. This differs to Raman/SERDS spectrum, in which biphenyl (fig. 12 b) produce four intense peaks in the area of 1000 cm^{-1}, 1030 cm^{-1}, 1270 cm^{-1} and 1600 cm^{-1}. As we can see, the Raman peak intensities of these two measurements are different, which means that with lower concentrations of this chemical in the seawater, only the most intense peaks will be observed and the rest will be hidden in the background noise. Therefore, if Raman measurements will be taken as reference in the experiments where substrates are applied, the expected intense peaks will not appear on the spectra and further analysis will be mistaken. To avoid erroneous measurements, the reference measurements of the specific chemicals must be taken with the same type of the substrate [Ahmad and Kronfeldt, 2013], which was further applied in the investigations.

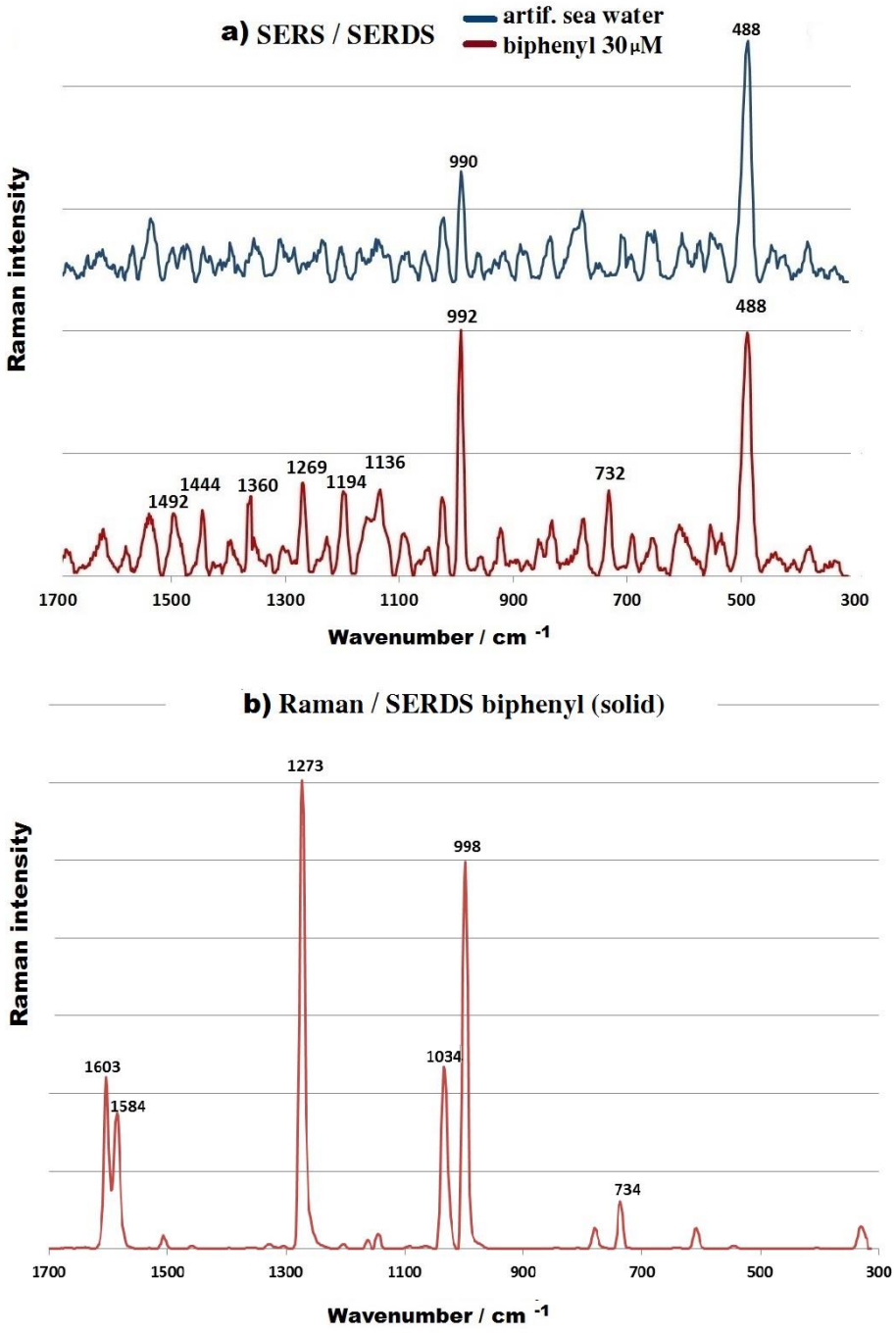

Figure 12: Raman Spectra of biphenyl. (a) SERS/SERDS spectrum of C_s = 30 µM biphenyl dissolved in artificial sea water (red). Gold island substrate, Artificial sea water (blue) serves as "blank" spectrum. (b) Raman/SERDS spectrum of biphenyl, solid phase. Same conditions for all measurement: lasers λ_1 = 671,6 nm and λ_2 = 671, 0 nm; laser power 30 mW; integration time 10s.

Gold island substrates, which was applied for all water samples, is sensitive to the following "light" PAHs (due to properties of the substrate): Acenapthene, Acenapthylene, Biphenyl, Flouranthene, Fluorene, Napthalene, Phenanthrene, and Pyrene (see appendix VII).

5.1.2 Measurements of water samples

Artificial seawater, which was deposited on every substrate for at least 15 min, served as a "blank" measurement and used as internal standard. This is necessary to determine Raman bands coming from the substrate and seawater, e.g. the Raman bands of "no interest". Pyrene was chosen to be a chemical for "control" measurements, due to its ability to produce one intense Raman peak in location 590 cm^{-1} (see figure 13 a). Note, the intensity of the signals from pyrene measurement in saturation concentration (13 a), is ten times higher than the intensity of the signals from sample measurements (13 b). The "control" measurement is necessary to prove that the substrate works, i.e. if Raman band in location 590 cm^{-1} is not observed, the measurement has to be repeated. The order of every measurement was as follows: "blank" spectrum, "sample" and "control" measurements. This order remained unchanged to avoid sample contamination.

Three measurement sets for water sample (location 78.3394 N and 9.3407 W, Arctic) is presented in figure 13 (b): the spectrum of artificial seawater in blue; the spectrum of the sample in red; and the spectrum of 15 nM pyrene (dissolved in artificial seawater) in green.

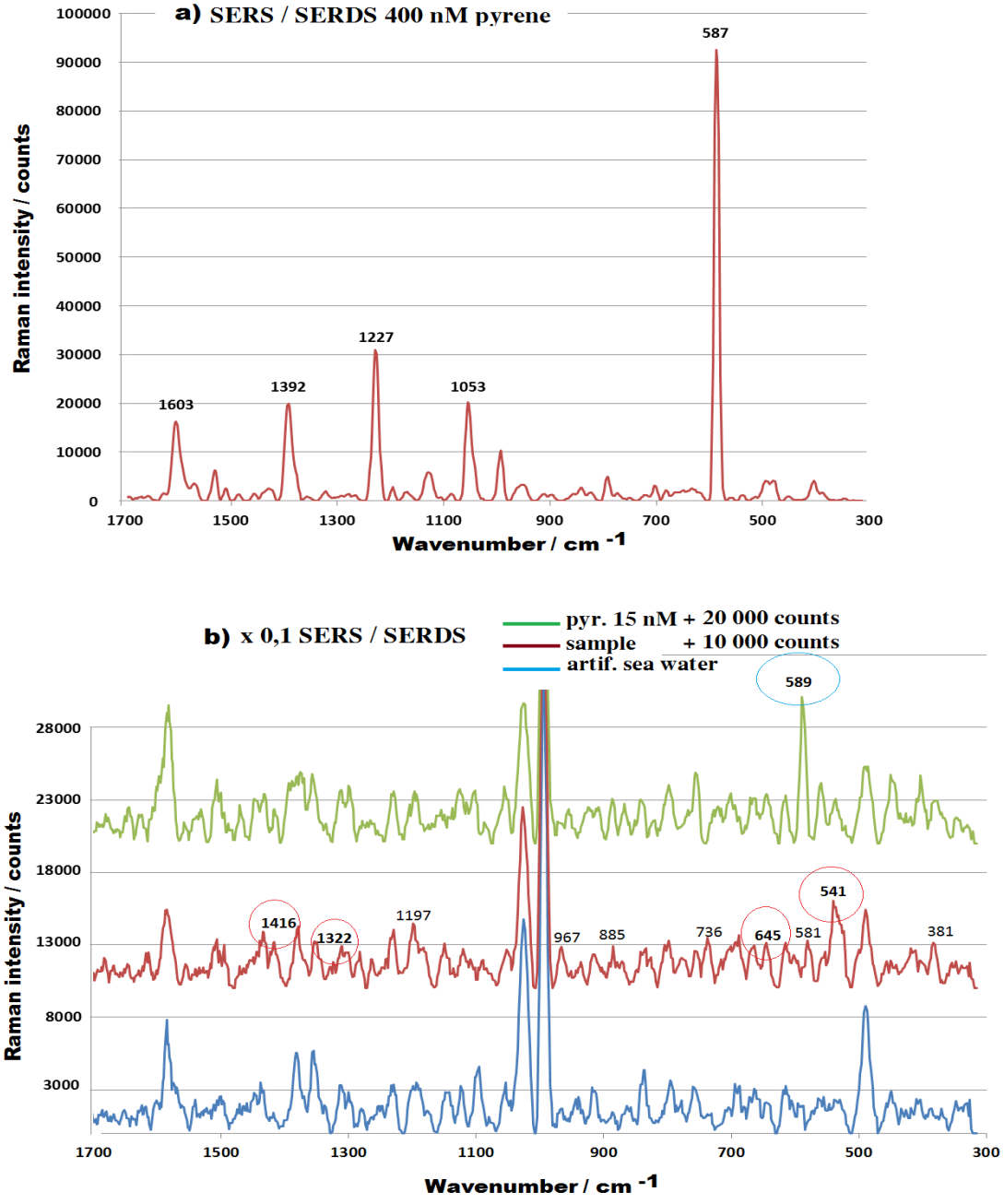

Figure 13: SERS / SERDS spectra of a) 400 nM pyrene, dissolved in artificial sea water (in red); b) artificial sea water (in blue), water sample, location 78.3394 N and 9.3407 W, Arctic, taken 06.08.11, (in red) and 15 nM pyrene, dissolved in artificial sea water (in green), all three measurements are taken with the same gold island substrate. Lasers: λ_1 = 671, 6 nm and λ_2 = 671, 0 nm; Laser power 30 mW; integration time 10 s.

As we can see from the measurement of the sample, various Raman bands appear. It is very difficult to say exactly which chemicals are present in real seawater and how they react with the substrate. Therefore, only eight previously mentioned "reference" chemicals might be searched for its possible presence.

Every "unknown" Raman peak is compared with the reference table (appendix VII). The locations in the table, which are marked in bold, represent intense peaks.

Since concentration of the pollutants in the seawater is expected to be much lower than during experiments in the laboratory, only the most intense Raman signals are expected to appear in real seawater.

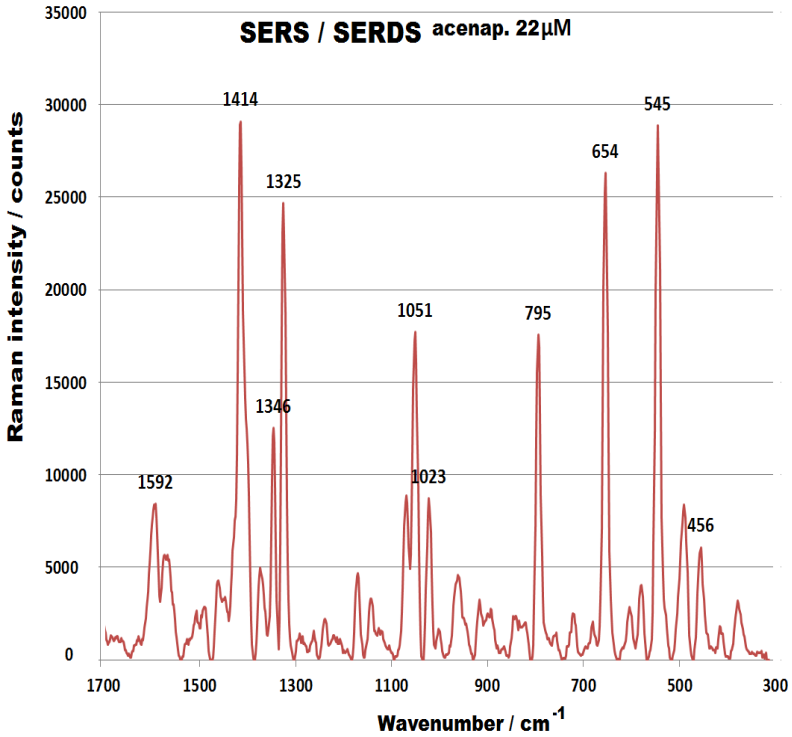

Comparing Raman bands, which are obtained from the sample in figure 13 b, four peaks in the locations 1416 cm^{-1}; 1322 cm^{-1}; 645 cm^{-1}; and 541 cm^{-1}, are matching with intense Raman bands, obtained from acenapthylene (see figure 14).

Figure 14: SERS / SERDS spectrum of 22 µM acenapthylene dissolved in artificial sea water on gold island substrate. Lasers: λ_1 = 671, 6 nm; and λ_2 = 671, 0 nm. Laser power 30 mA, integration time 10 s.

In figure 14, we can observe the SERS/SERDS spectrum of acenapthylene, dissolved in artificial seawater in its saturation concentration (22 µM). The four most intense Raman bands are produced in the locations of 1414 cm^{-1}, 1325 cm^{-1}, 654 cm^{-1}, and 545 cm^{-1}, which are similar to the signals, found in the real seawater sample. Small Raman shifts (1 - 15 wave

numbers) can occur due to adsorption properties of different substrates, see [Kwon, 2012; Ossig *et al*., 2013].

Every water samples was investigated as described previously. Readings of all detected wave numbers, as well as possible PAHs, are collected in the last column of appendix VI.

Examples of randomly extracted water samples (from appendix VI) are presented in table 2. All readings contain data of the *place* where sample was taken, *date* (as we know, pollution concentration may change depending on the time of the year), *temperature*, *GPS* location and water *salinity* – some fresh water[7] samples were also taken and measured, as can be seen. In some cases, salinity of the water sample is lower than "normal" seawater salinity, i.e. 35 ‰. This means that the sample was taken directly in the input of fresh water into the sea: in the point where fresh water meets seawater. This is stock water from the city cannels, or input from the rivers. Consequently, in such samples many Raman bands appear, which can be referred also to PAHs and biphenyl.

As we can see from table 2, significant PAH peaks can be found in one or various locations. Of course, the more Raman bands that can be referred to a particular PAH, the higher possibility that a pollutant is there. In some cases more than one type of PAH can be detectible in the same water sample, which is logical, because those pollutants are likely to appear in the mixtures.

Reviewing water sample results from table 2 and appendix VI, we can see that fluoranthene, acenapthene and biphenyl appears in the samples more often than another

[7] An interesting example of fresh water sampling is the two Great Lakes in North America: Erie and Ontario, which are two, last once out of five before entering the Atlantic Ocean through the St. Lawrence River. The samples were also taken from bottom and upper Niagara River, which connects both Great Lakes. The importance of sampling in this area is that the great lakes are the largest group of fresh water lakes on Earth, which contains 21% of the world's surface water [LUHNA, 2003], therefore pollution of the lakes will be transferred as input to the Atlantic Ocean. However, serious pollution was not detected (see appendix VI).

PAHs – it can be described ether with high sensitivity of the substrates to this particular pollutants, or, more likely, with higher amounts of these chemicals in the samples. However, results of water samples do not follow a systematical sequence, and different types of PAHs can be found in different areas, or different PAHs in two samples from the same area.

I would like to remind that only eight of certain PAHs and biphenyl can be detected with gold island substrate. Therefore, the remaining "unknown" Raman bands, which are detected in the samples, belong to the chemicals which are not investigated in this work.

Table 2: Example of possible PAHs in the sea water samples

Place	**Date**	**Tempe-rature, °C**	**Salinity, ‰[8]**	**GPS, N**	**GPS, W**	**Vibrations detected, cm^{-1}**	**PAHs**
Erie canal, Lockport cave, NY, USA	23.04.11	9.09	0	43.17	78.69	664 796 1373	Fla
Hudson river, NYC, USA	02.05.11	11.73	4.2	40.74	74.01	786 1412 1434 1582 1278 1582	Fla Bip
Water Stock, Svalbard, Arctic	27.07.11	2.03	0	78.20	15.89	666 1254 *1412* 1434 1590 1353 *1412*	Fla Phe
North Sea, Arctic	06.08.11	3.79	35	78.34	9.34	540 645 967 1324	Acenap

[8] permille (parts per thousand) (‰), which is approximately grams of salt per kilogram of solution.

						1416 738 1199 1263 540 1199 1416	Bip Phe
North Sea, Arctic	08.08.11	5.49	35	78.34	9. 33	662 782 1373 1417	Fla
North Sea, Arctic	17.08.11	4.49	35	78.34	10.11	666 1083 1446 1606	Fla
East China Sea, Qingdao, China	04.06.12	20.0	35			538 1049 1414	Aceylene
East China Sea, Qingdao, China	04.06.12	22.48	35	36.09	120.46	489 735 659 1437 1591	Bip Fla
Aegean Sea, Rhodes Greece	06.12	23.3	35	36.41	28.19	560 670 1444 1588	Fla
Mediterranean Sea, harbour Six Fours, France	01.01.13	13.54	35	43.10	5.80	600 *1018* 709 *1018* 990 *1266* 1501 *1018* *1266*	Acenap Phe Bip Fla

5.2 Arctic test

Pilot studies in the Arctic has been a challenging task which provided necessary information about the work efficiency of the portable Raman sensor, stability, suitability of the substrates in field conditions and ability to run long term Raman tests (12 hours range). Numerous Raman and SERS spectra were taken during 12 hour shifts every day for three weeks. Since every experiment involved a change of integration time, starting from 0.3 s to 50 s or 64 s and each spectrum was averaged from 10 measurements, therefore every experiment set took approximately 30 min - 40 min. Only a few typical spectra out of thousands are presented in this work due to repetition of results or specific focus on the given task.

5.2.1 Discussion of results

Raman and SERS measurements were carried out for analyzing surface and sediment water. Typical examples of SERS spectra from real surface water (location 78.2912 N and 10.1453 E), sediment water (location 78.59167 N; 9.38312 E, depth: 407 m), and artificial sea water are presented in figure 15 (a), (b) and (c), respectively.

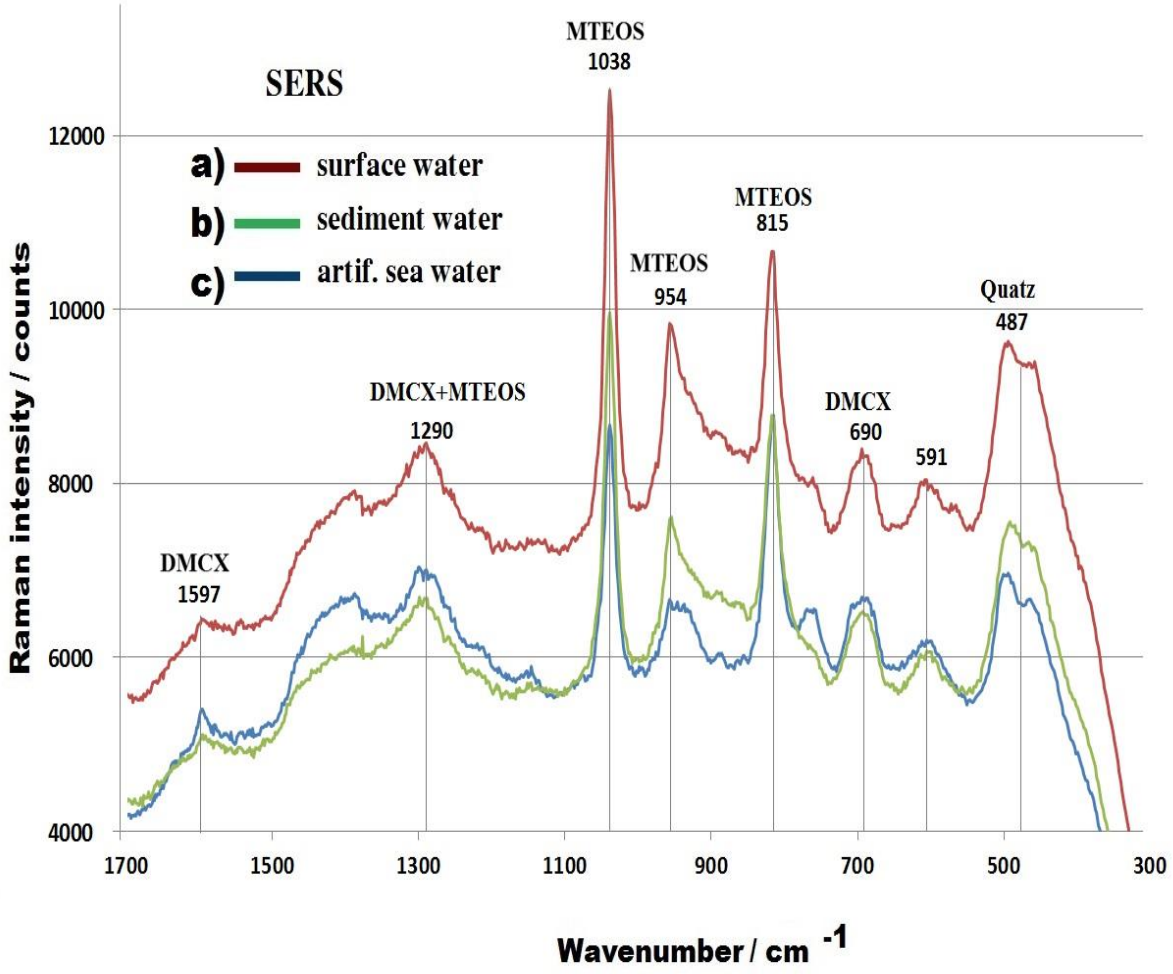

Figure 15: SERS spectra of a) real sea water from surface, location: 78.2912 N and 10.1453 E; b) sediment water, sediment sample location 78.59167 N; 9.38312 E and depth: 407 m; c) artificial sea water. Laser power 18 mW. All SERS spectra are made with the same Ag,DMCX:MTEOS substrate - averaged from 10 spectra. Integration time 10 s.

Within 10 s, various Raman peaks appear, but most of them (1597 cm^{-1}, 1290 cm^{-1},1038 cm^{-1}; 954 cm^{-1}; 815; 690 cm^{-1}) come from the sol-gel DMCX:MTEOS substrate [Kwon, 2012] or from the quartz window in the optode at 490 cm^{-1}. Raman signal at 591 cm^{-1} can come from strongly shifted, overlapped DMCX and MTOES. This means that pollution in the particular location is not recorded, i.e concentration of PAHs or other chemicals, which

adsorbs to the surface of the substrate is lower than 1 nM. But in some areas (approximately 1 % of the spectra) strongly pronounced Raman signals can be detected. An example of such measurements is presented in figure 16 (a). Real surface water (fig. 16 a), from the location 78.3345 N and 10.0399 E, produce eight unknown Raman signals comparing to the sediment water (fig. 16 b), with sediment sample location at 78.6177 N and 9.4227 E and at a depth of 308 m. Note, that both spectra are taken with the same substrate in only 10 s integration time. The "unknown" signals are in the area of: 1390 cm^{-1}, 1270 cm^{-1}, 1230 cm^{-1}, 1000 cm^{-1}, 850 cm^{-1}, 710 cm^{-1}, 620 cm^{-1}, and do not belong to the substrate (marked with the star) or to the quartz in the optode (marked with the cross). The Raman signals from the surface water will be further analyzed.

For comparison, figure 16 (c) shows conventional Raman spectrum of surface water, which produce such low peaks, that it is impossible to detect any chemicals in water. One signal in the conventional Raman spectrum comes from quartz, at 490 cm^{-1}, which is part of the equipment. This spectrum proves a need to apply SERS technique for achieving better results.

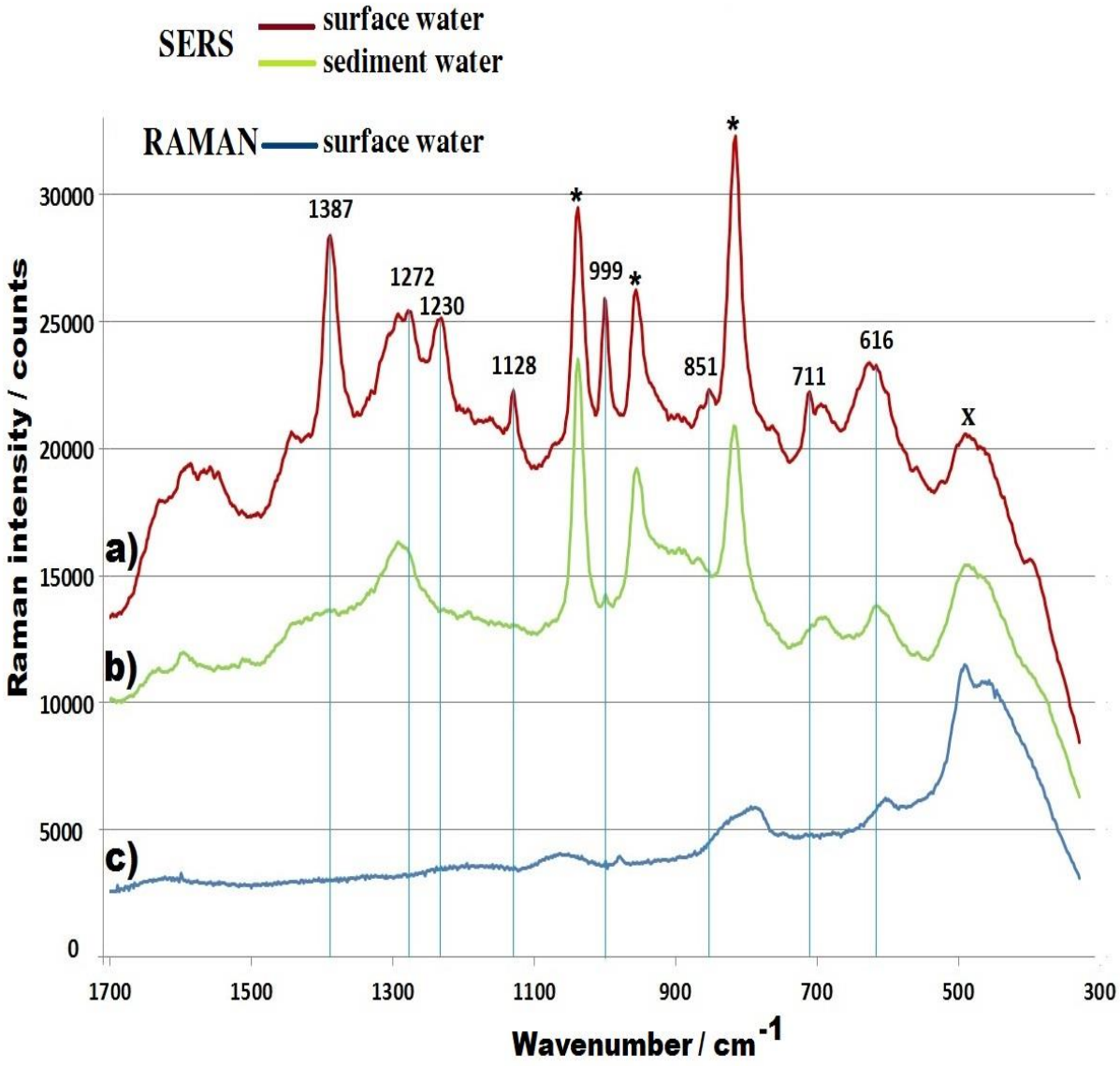

Figure 16: Raman and SERS spectra. a) SERS: Surface sea water (red), b) SERS: sediment water (green) and c) conventional Raman spectra of surface water (blue). Surface sea water location 78.3345 N and 10.0399 E. Sediment sample location 78.6177 N and 9.4227 E; depth 308 m. Laser power 18 mW. All SERS spectra are made with the same Ag,DMCX:MTEOS substrate - averaged from 10 spectra. Integration time 10 s.

As we can see, surface water from location 78.3345 N and 10.0399 E (fig. 16 a) produces various Raman bands. Although, the origin of these signals probably came from oily products, which are released from vessels, it takes the current Raman sensor 10 s to detect it. The conclusion about pollution origin is made based on the fact that strong Raman signals appear suddenly and are not constantly recorded. This can happen due to the ships movement at the same time when pollutants are released; therefore the sensor is able to "catch" it.

However, the interpretation of results brings various discussions, because even if we take into consideration previous studies, which were done in the arctic area (see chapter 4.3), it is still not completely clear what exact pollutants and chemicals exist in the water and how current substrates react with them.

The data from the cruise can be compared with existing references in order to predict certain types of possible pollution. In our case, fourteen PAHs and biphenyl have been chosen.

For simplicity, all eight unknown Raman bands from figure 16 (a) are collected in the table 3. Ag,DMCX:MTEOS substrates have direct measurements with four PAHs [Kwon, 2012], but as we can see from appendix VII, the SERS signals from the substrate produce similar results as Raman measurements, therefore in this special case Raman spectra can be applied as reference.

In table 3, various PAH pollution may be expected in the sample. A strong probability has benzo(a)pyrene (reference Raman (a) and Raman/SERDS (b) spectra see in figure 17) and biphenyl (reference Raman spectra see in figure 12), because the position of intense Raman bands which are produced by the sample, matches exactly the position of expected intense signals from these pollutants. Of course the presence of other mixed PAHs is very possible, including PAHs that are not investigated in this work.

However, the applied sensor is well suited in this "screening" area method, to provide fast information (10 s) and the type of pollution in the water.

Table 3: Sea water pollution (possible). In bold': strong Raman signal; Capital letter: Raman signal; small letter: possibly stronly shifted Raman signal

PAHs	**Abbreviation**	**Wavenumbers cm^{-1}**							
Raman peak position		**1387**	**1272**	**1230**	**1128**	**999**	**851**	**711**	**616**
Anthracene	**Ant**	X				X			
Benzo(a)anthracene	**Baa**	**X'**	X			X		x	
Benzo(a)pyrene	**Bap**	**X'**		**X'**					
Benzo(ghi)perylene	**Bgp**	**X'**	x	x		x			
Benzo(k)fluoranthene	**Bkf**		X						
Chrysene	**Chr**	**X'**							
Fluorenthene	**Fla**		X		X	x	x		
Fluorene	**Flu**	X		**X'**		x	X		
Naphthalene	**Nap**	**X'**				x			
Phenanthrene	**Phe**							**X'**	
Pyrene	**Pyr**			X					
Biphenyl	**Bip**		**X'**			**X**			

As we can see from figure 17, the Raman spectrum of benzo (a) pyrene is taken with an integration time of 1 s, due to structural characteristics of the sample (yellow needle like crystals), which produces very high fluorescence, fig.17 a, (so high, that if the integration time is only 3 s, the spectrum goes to complete saturation). To remove such fluorescent back ground, a Bap sample was measured applying SERDS technique (fig.17 b). Note, that the spectrum in figure 17 (a) and 17 (b) is the same measurement. The reason that Raman signals are slightly shifted (2-5 cm^{-1}) is due to reconstruction algorithm in the SERDS program (Matlab): expected effect [Kwon, 2012].

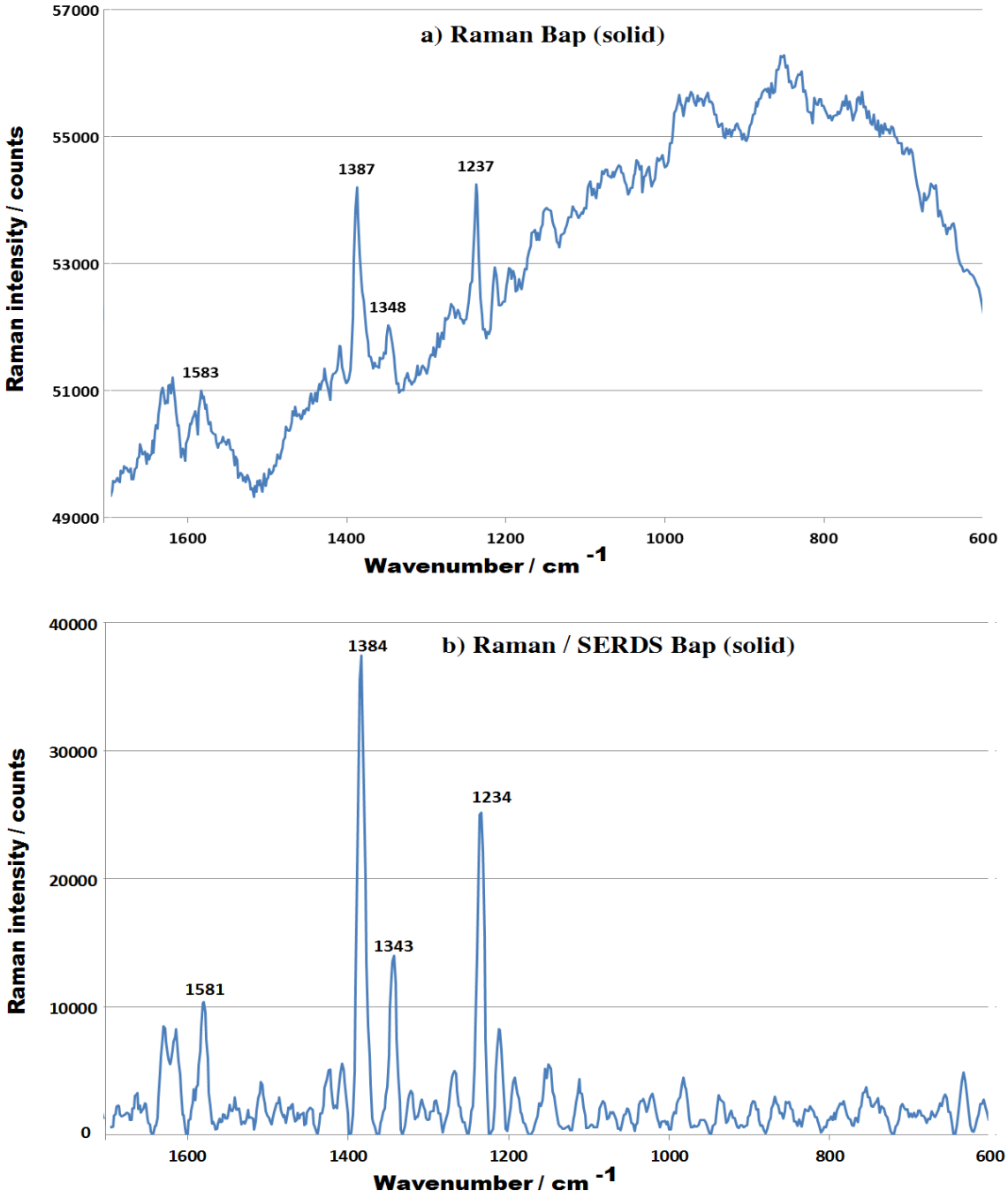

Figure 17: Raman spectrum of Benzo(a)pyrene. a) Raman spectrum of Bap, Laser λ = 671, 0 nm; b) Raman/SERDS spectrum of Bap. Lasers: λ_1 = 671, 6 nm; and λ_1 = 671, 0 nm. Laser power 30 mW, integration time 1 s.

5.2.2 Spiking tests with mixtures of two and three PAHs

If pollution is present in surface water, it can be in a form of mixtures of several types such as PAHs, PCBs[9], DDT[10], pesticides, oil spills and other kinds of pollutants. The Ag,DMCX:MTEOS substrate is proved to be sensitive to PAHs and biphenyl, which can be a cross reference to PCBs (due to the same structure of basic component). But it still remains unclear how the substrate reacts with remaining pollutants or in mixtures. Moreover, it is necessary to make reference spectra with polluted real seawater (spiked water), in order to see if the substrate is able to detect pollution in real field conditions.

As current work is focused on PAHs, the spiking tests were done with a mixture of two and three PAHs, to see the behavior of Ag,DMCX:MTEOS substrates.

Figure 18 represents a typical spectrum of surface seawater from location 78.0382 N and 9.0181 E, spiked with anthracene (Ant) and pyrene (Pyr) in three concentrations: (a) (near) saturation concentration (150 nM (Ant) - 400 nM (Pyr)), (b) "medium" concentration (7.5 nM (Ant) – 8 nM (Pyr)) and (c) "low" concentration (0.25 nM (Ant) - 0.3 nM (Pyr)). Spectrum (d) serves as a reference of substrate in milli-Q water.

Here we can see from the figure 18, pollution is detectible and the intensity of Raman bands is proportional to their concentrations. Raman band at 1384 cm^{-1} could be referred to several chemicals in surface water, but since the intensity of this peak increase is according to increasing concentrations of pollutant, we must refer it to a combination of strongly shifted anthracene (1395 cm^{-1})[11] and pyrene (1401 cm^{-1}), as both provides intense peaks in those locations. The Raman band at 1237 cm^{-1} comes from pyrene (1234 cm^{-1}); position 995 cm^{-1} is typical for anthracene (1002 cm^{-1}) as well as 761 cm^{-1} (752 cm^{-1}). Signals which come from the substrate are marked with a star and can be seen in the "blank sample" measurement of the milli-Q water.

---

[9] PCB – **p**oly**c**hlorinated **b**iphenyls
[10] DDT – **d**ichloro**d**iphenyl**t**richloroethane
[11] Reference measurements are taken from [Kwon, 2012] and can be found in appendix VII

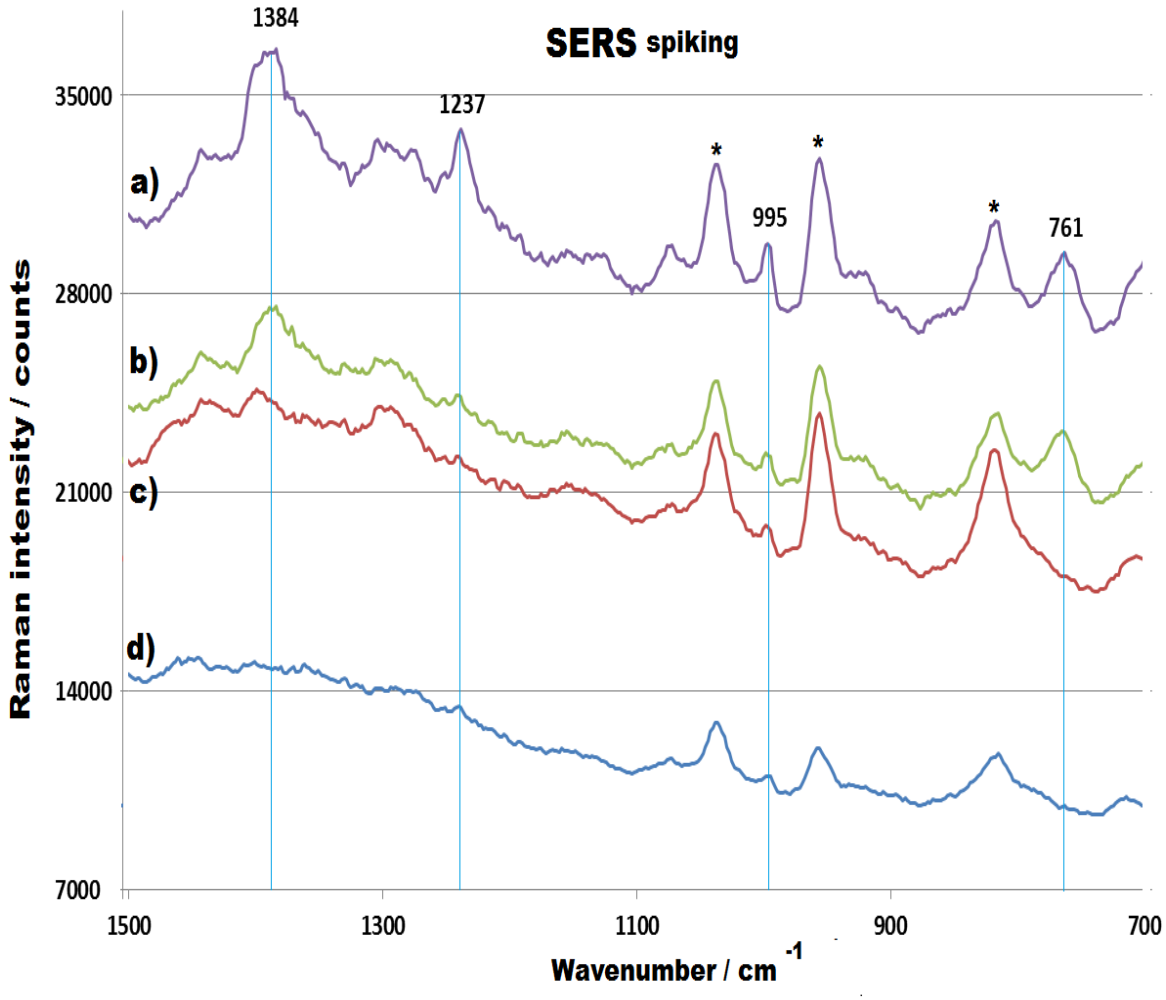

Figure 18: Spiking test: misture of anthracene and pyrene in real surface water. (a) anthracene (150 nM) - pyrene (400 nM); (b) anthracene (7.5 nM) – pyrene (8 nM); (c) anthracene (0.3 nM) – pyrene (0.25 nM); (d) milli-Q water as blank sample. Real water location 78.0382 N and 9.0181 E. All spectra were done with the same Ag,DMCX:MTEOS substrate. Integration time 25 s, laser power 18 mW. Averaged from 10 spectra.

Further experiments involve mixing of three pollutants: fluorenthene, pyrene and anthracene with real surface seawater from the same location (78.0382 N and 9.0181 E). Spectrum (a) in figure 19 represents anthracene (Ant), fluoranthene (Fla) and pyrene (Pyr) mixture in saturation concentrations (150 nM (Ant) - 600 nM (Fla)- 400 nM (Pyr)); spectrum

(b) in “medium” concentrations (7.5 nM (Ant) - 8 nM (Fla)- 8 nM (Pyr)); (c) in “low” concentrations (0.3 nM (Ant) - 1 nM (Fla) - 0.25 nM (Pyr)) and (d) is blank reference spectrum of the substrate in milli-Q water. The reason that blank spectrum has such high intensity and almost overlapping with the spectrum of highly polluted sample, is that “blank” spectrums are always taken first, prior to any measurements in order to avoid contamination of the substrate. Consequently “fresh” substrate is the most active (see “substrate stability” in following chapter) and the overall intensity of the spectrum is high.

According to stability tests (chapter 5.2.3), the polluted sample, which is measured last, is supposed to have the lowest overall intensity and low background noise due to loss of the substrate sensitivity in contact with sea water. But in the same time, as more chemicals are adsorbed to the surface of the substrate during the experiment, the Raman signals become more intense. Therefore, the effect of the substrate sensitivity loss is fully compensated by the adsorption process and spectrum from highly polluted sample appears as most intense. But such a tendency is not always observable (as we did not see it in previously described measurements) due to the timing of preparing samples and making readings (in some cases it takes more time to prepare the sample and make the experiment, so the substrates sensitivity loss effect cannot be directly observed).

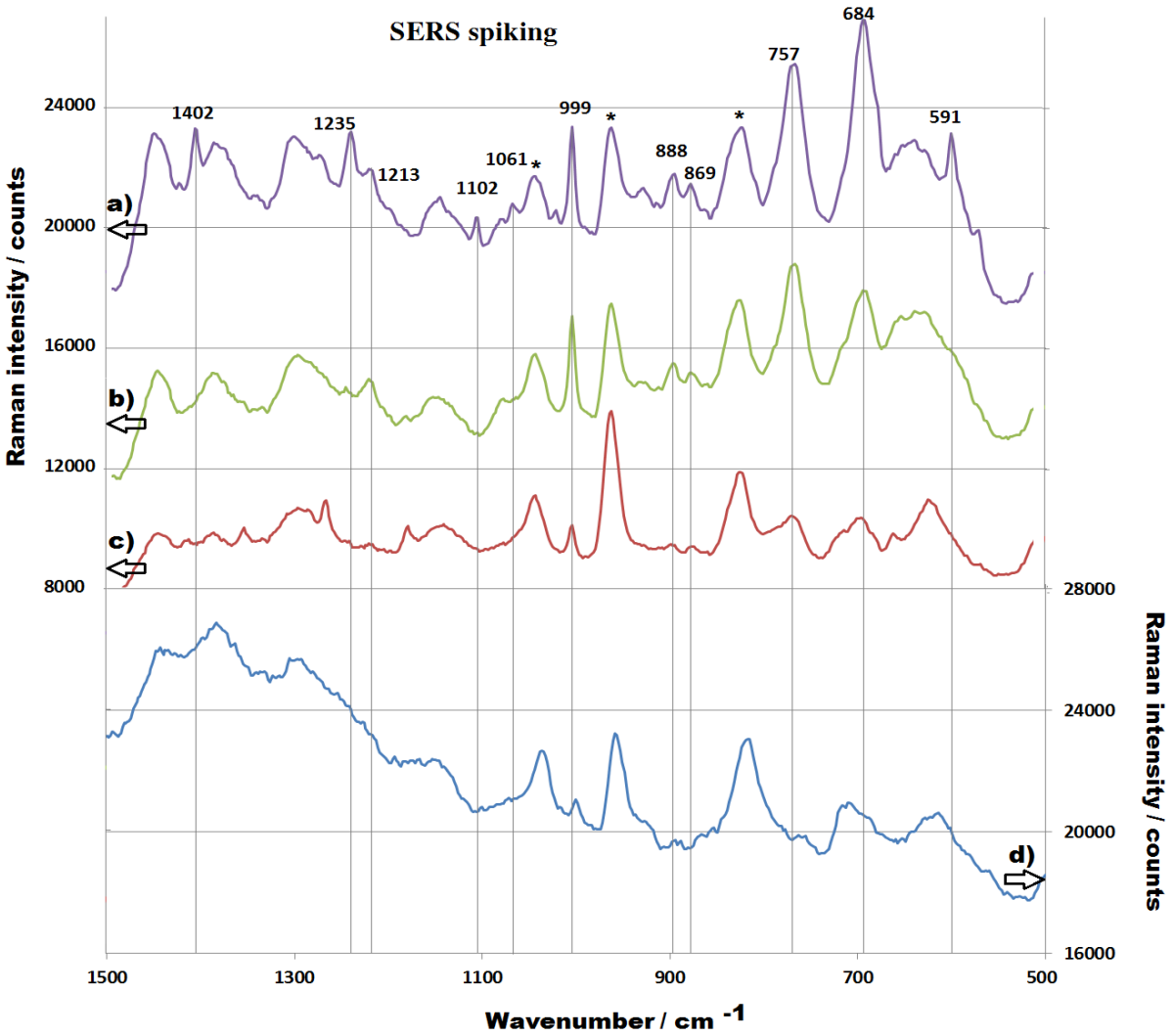

Figure 19: Spiking test: mixture of Anthracene, fluoranthene and pyrene in real surface water. (a) anthracene (150 nM) – fluorenthene (600 nM) - pyrene (400 nM); (b) anthracene (7.5 nM) – fluorenthene (8 nM) - pyrene (8 nM); (c) anthracene (0.3 nM) – fluorenthene (1 nM) - pyrene (0.25 nM); (d) milli-Q water as blank sample. Real water location: 78.0382 N and 9.0181 E. All spectra were done with the same Ag,DMCX:MTEOS[12] substrate. Integration time 10 s, laser λ = 671 nm; power 18 mW. Averaged from 10 spectra.

[12] Raman signals, which come from the substrate, are marked with a star.

Eleven signals from a given sample were detected in 10 s and collected in table 4. Most of the Raman bands can be clearly referred to certain pollution as described in the table. Because peak at 1213 cm^{-1} shows a very strong shift of Raman signal (30 wavenumbers), comparing with the theoretical position of anthracene (1183 cm^{-1}), this is probably not the source and can be preferable to the chemicals in the seawater. As well as two low Raman signals: at 888 cm^{-1} and 869 cm^{-1}, comes from seawater and cannot be referred to any of added PAHs. The peak at 999 cm^{-1} can be observed in the "blank" spectrum, but since the intensity of the peak increase according to pollution concentration, we can refer it to anthracene.

The signal in the position at 757 cm^{-1} and 684 cm^{-1} are so high, that Raman bands can be clearly observed even in smallest concentrations (e.g, 0.3 nM for anthracene and 1 nM for fluorenthene), which provide low in-situ limits of detection. Laboratory experiments defined calculated LODs for individual components, applying SERS as following: pyrene – 0.3 nM, anthracene – 1 nM and fluoranthene -1.2 nM [Kwon, 2012]. Surprisingly, onboard tests for pollution mixtures showed even lower directly measured and observable LODs and better results, as we can clearly observe Raman signals from 0.3 nM anthracene (at 757 cm^{-1}) and 1 nM fluoranthene (at 684 cm^{-1}).

Also as can be seen from the table, Raman shifts difference between onboard and laboratory measurements are 0 to 13 wavenumbers. While the difference between Raman and SERS reading in the laboratory of the same chemical in pure or/and dissolved state, is typically 1 to ±5 wavenumbers [Kwon, 2012] for Ag,DMCX:MTEOS substrate and in some cases can be as much as 15 wavenumbers [Ossig *et al.*, 2013], for the Ag nanoparticle substrates.

Table 4: Raman signals from spiking test: mixture of three PAHs

Detected wavelength cm^{-1}	**1402**	**1235**	**1213**	**1102**	**1061**	**999**	**888**	**869**	**757**	**684**	**591**
PAH	Ant Pyr	Pyr	Ant (?)	Fla	Pyr	Ant	-	-	Ant	Fla	Pyr
Theoretical Wavelength, Appendix VII cm^{-1}	1395 1392	1227	1183	1102	1062	1002			754	671	596
Difference, cm^{-1}	+7 +10	+8	+(30)	0	-1	-3	-	-	+3	+13	-5

5.2.3 Stability

Ag,DMCX:MTEOS substrates were tested for short- (hour range) and long- (weeks range) time stability in order to check their ability to work in long lasting field experiments. For the short - time stability test, one substrate was inserted in the flow-through cell and exposed to sediment water (sediment sample location 78.0558 N and 9.0534 E; depth 339, 61 m) up to 22 h, with an integration time of the measurement set at 25 s. The measurement results from 1^{st}, 10^{th} and 22^{nd} hour are presented in figure 20: (a), (b), and (c) respectively. As we can observe, the main sensitivity loss (ΔI) of 800 counts (2%) is during the first 10 hours. After this time the substrate (within the limits of accuracy) remains unchanged. The loss of

the substrate sensitivity presumably happens due to a reaction of silver nano particles aggregates from the porous top layer of the surface with chloride ions from the sea water[13].

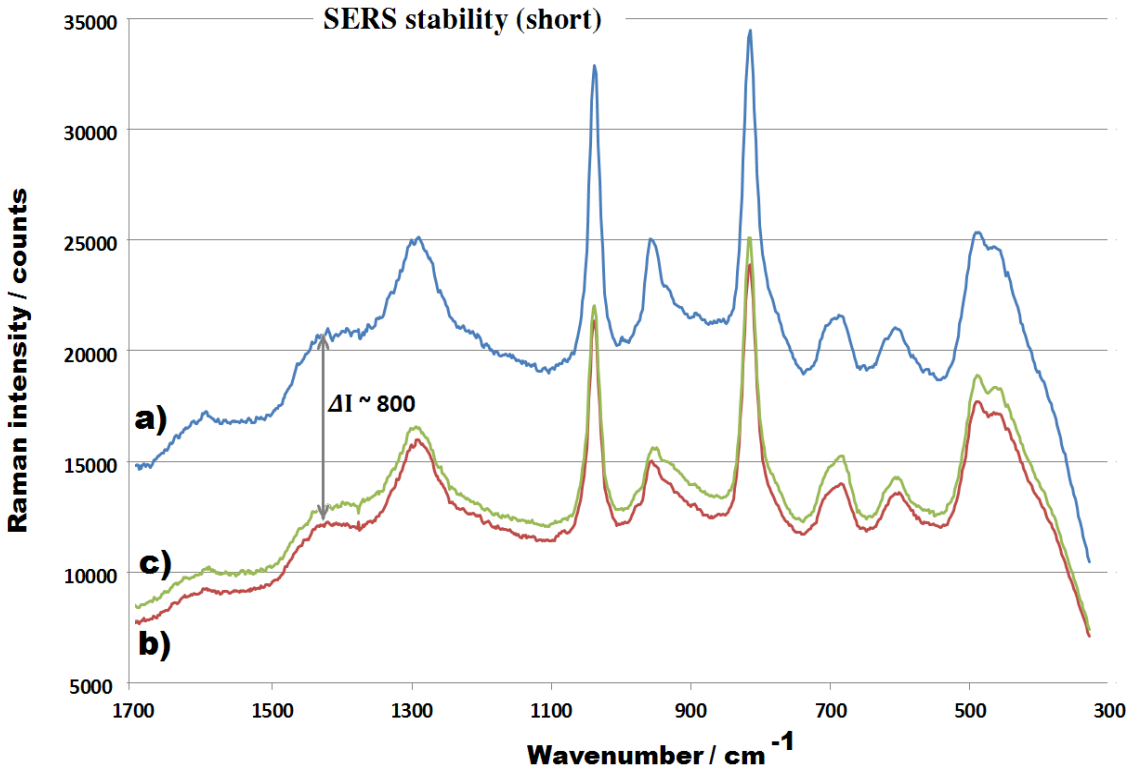

Figure 20: Ag,DMCX:MTEOS substrates short time stability test. (a) SERS sediment water 1st hour, (b) SERS sediment water 10th h , (c) SERS sediment water 22nd h. Sediment location 78.0558 N and 9.0534 E; Depth 339,61 m. Integration time 25 s, laser λ = 671 nm; power 18 mW. Averaged from 10 spectra.

In order to check the substrates long time stability and optimum storing conditions, the following experiment was performed: seawater sample was measured with two Ag,DMCX:MTEOS substrates: (a) and (b) spectra in figure 21. Substrate (a) was stored for 7 days in real sea water, but substrate (b) in sweet water. After 7 days, measurements were repeated.

[13] $Ag^+ + NaCl = AgCl + Na^+$

Results show that the sensitivity of the substrate drops ΔI ~ 9000 counts (20 %), if it is stored in sea water (a'), as expected. The signal from "sweet water" substrate (b') after 7 days of storage has very low intensity difference, e.g. Δi ~ 2000 (max) 5% – 0 (min) counts, comparing to the first measurement (b).

As we can see, Raman signals can still be well observable even after the absolute intensity of the spectra drops, which means that the Ag,DMCX:MTEOS substrates are stable, especially suitable for measurements in sweet water.

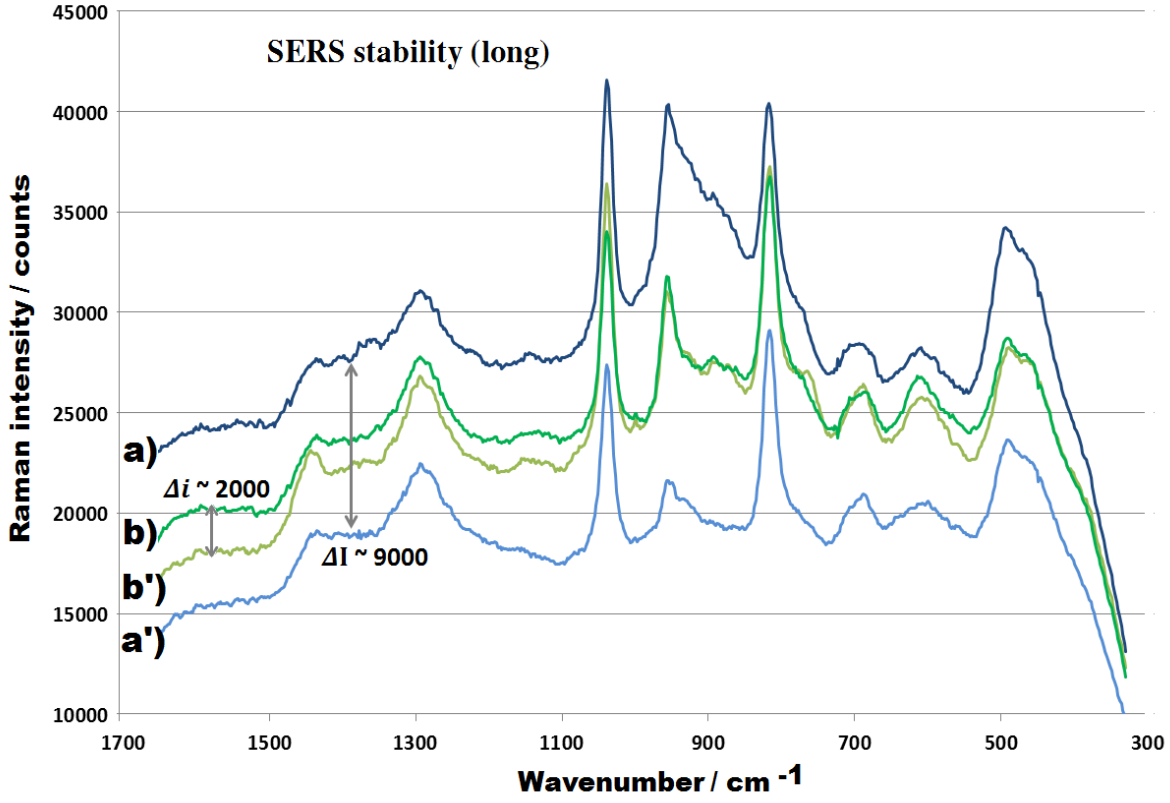

Figure 21: Ag,DMCX:MTEOS substrates long range stability test. (a) and (b) are surface sea water day 1: different substrates; Surface see water spectra after storing the substrate in real sea water (a') or in milli-Q water (b') for 7 days; Location of the samples (a and b): 78.0339 N and 9.0340 E; location of the samples (a'; b'): 78.0336 N and 9.0591 E. Integration time 25 s; Laser λ = 671 nm; power 18 mW. Averaged from 10 spectra.

5.3 In situ tests with the Sea Going instrument

Construction of the sea going instrument took place at Technical University Berlin. All parts of the instrument were mounted and fixed on a base plate in the tube, while the final assembly was done in the IFREMER Center in La Syene sur Mer, France. The computer screen is only attached for setting the parameters of the program which must then be removed prior to closing the tube. The complete Sea going instrument is presented in the figure 22.

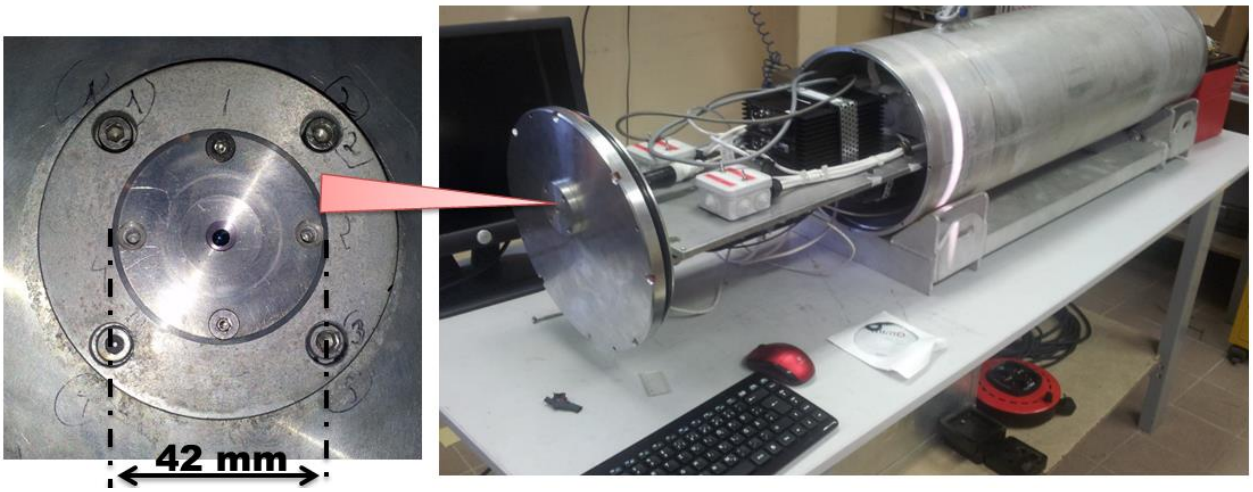

Figure 22: Sea going instrument with a window for laser optical path and substrate

Two tube leakage tests were done in IFREMER's indoor pool[14]. During the first test the tube was placed in fresh water for 10 mins. No leakage was detected.

For the second test, the tube was left in the fresh water for 23 h without any leakage. Figure 23 shows the test, which was done under normal room conditions.

[14] Pool size = 4m x 3 m; depth 2 m

As we can see the tube was lifted by an electric hoist. 60 kg of additional weight was added so that the tube had negative buoyancy and could be submersed (see static buoyancy calculation in chapter 4.4.1).

After construction, installation and testing of all the parts, the SGI was ready for its first in situ experiments.

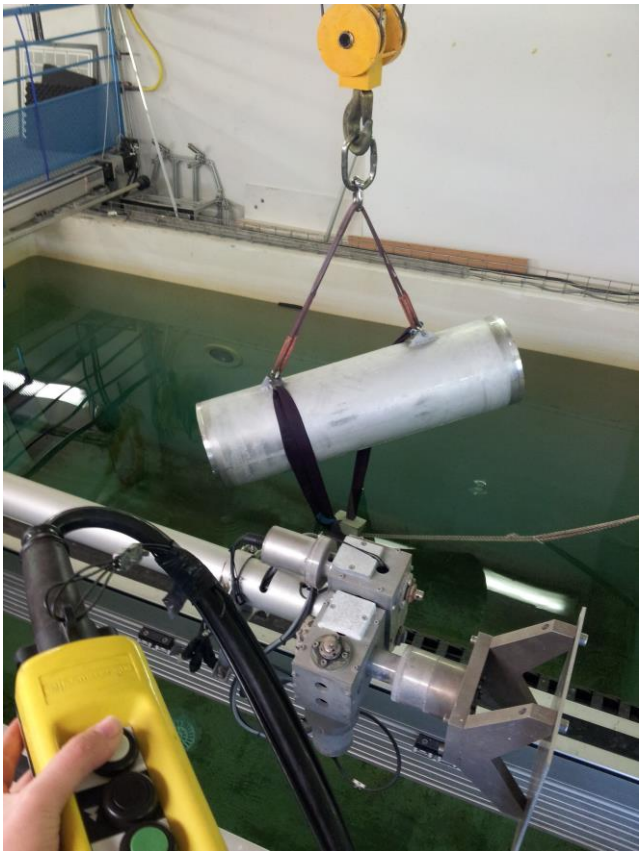

Figure 23: Housing leakage test in IFREMERs pool

5.3.1 Calibration of the sensor

Before each experiment, material containing polystyrene was measured with "normal" Raman for 5 s, in order to calibrate the sensor. This is due to the fact that Raman shift of all the measurements is expressed in pixel numbers. Selected Raman signals coming from polystyrene was transferred from a particular pixel number into a known wavenumber.

Figure 24 shows the same Raman spectrum of polystyrene that is taken before sea trials, at 7.01.13, expressed in pixel numbers (actual measurement) and in wavenumbers (after evaluation).

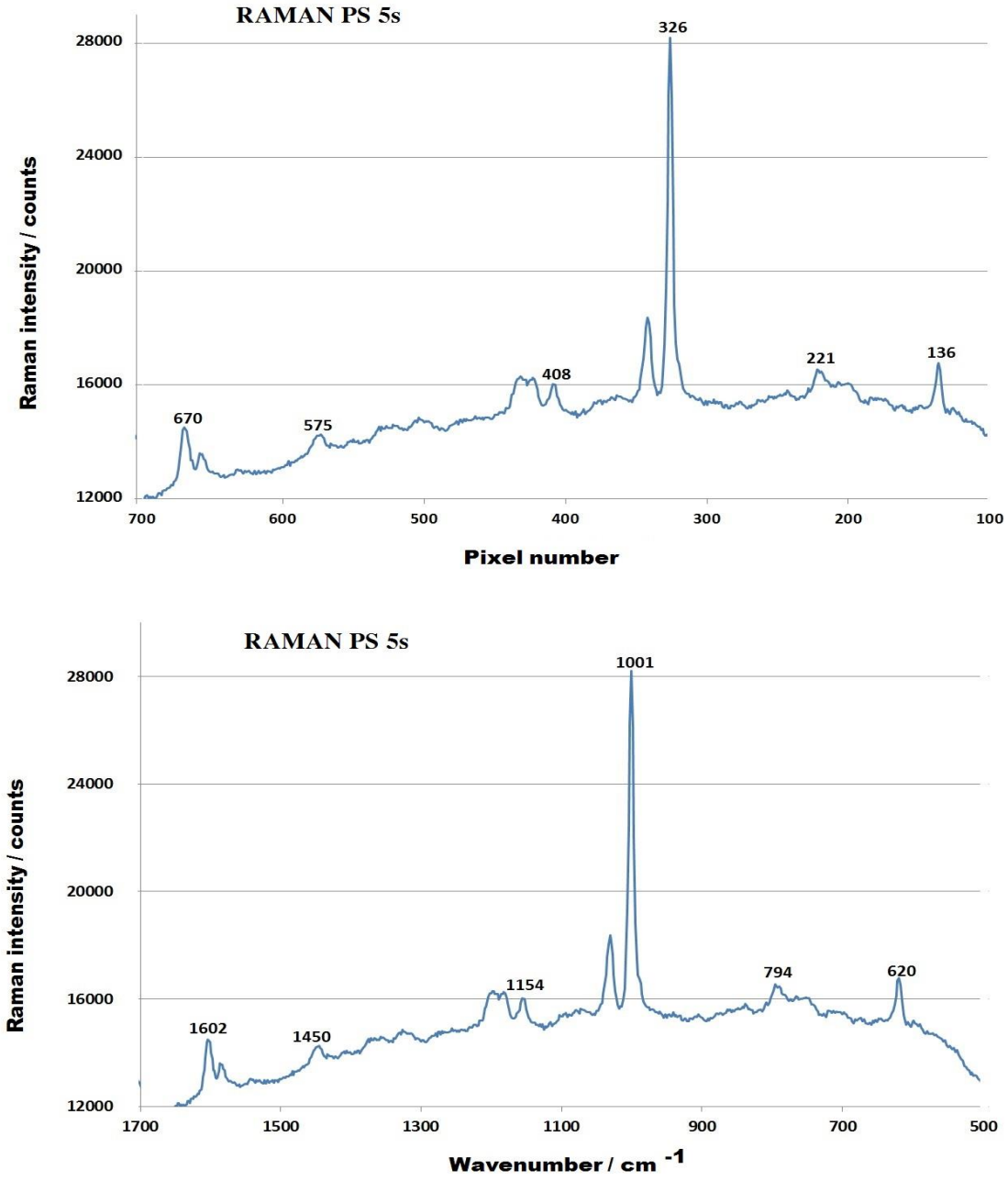

Figure 24: Raman specrum of polystyrene (PS). Spectrum is taken 7.01.13 (directly before cruise). Laser 671 nm, laser power 30 mW; integration time 5s.

5.3.2 In situ harbor experiments

For the first time, in situ experiments of an autonomous Raman/SERS sensor system was carried out during 23.11.2012 – 19.12.2012 in La Seyne Sur Mer harbor, near IFREMER center.

This area of experiments was chosen for a reason. Previous studies showed promising results: to detect PAHs (and heavy metals) in the Mediterranean Sea, bio integrator network (RINBIO) was applied by IFREMER [Andral, 2009]. In the summer of 2004, 92-man made cages containing mussels were distributed along the French Mediterranean coast for a time period of three months. During this time, the mussels bio accumulated toxic and dangerous substances in their body. PAHs were analyzed using high-performance chromatography, combined with a fluorescence detector [Andral *et al.*, 2004]. Significant amounts of PAHs, mostly fluoranthene, (1 µg/kg – 10 µg/kg) were found in its higher concentrations near Toulon anchorage, Languedocian lagoons and Hyeres zone [Andral, 2009; Andral *et al.*, 2004]. This data was applied as cross a reference for further Raman/SERS measurements.

Raman/SERS experiments were done during day and night (in order to reduce fluorescence from sun light) with SGI immersed in the seawater at a depth of 0.5 - 1 m (see figure 25). Water samples were taken from same locations in order to investigate them in the laboratory for additional cross-references.

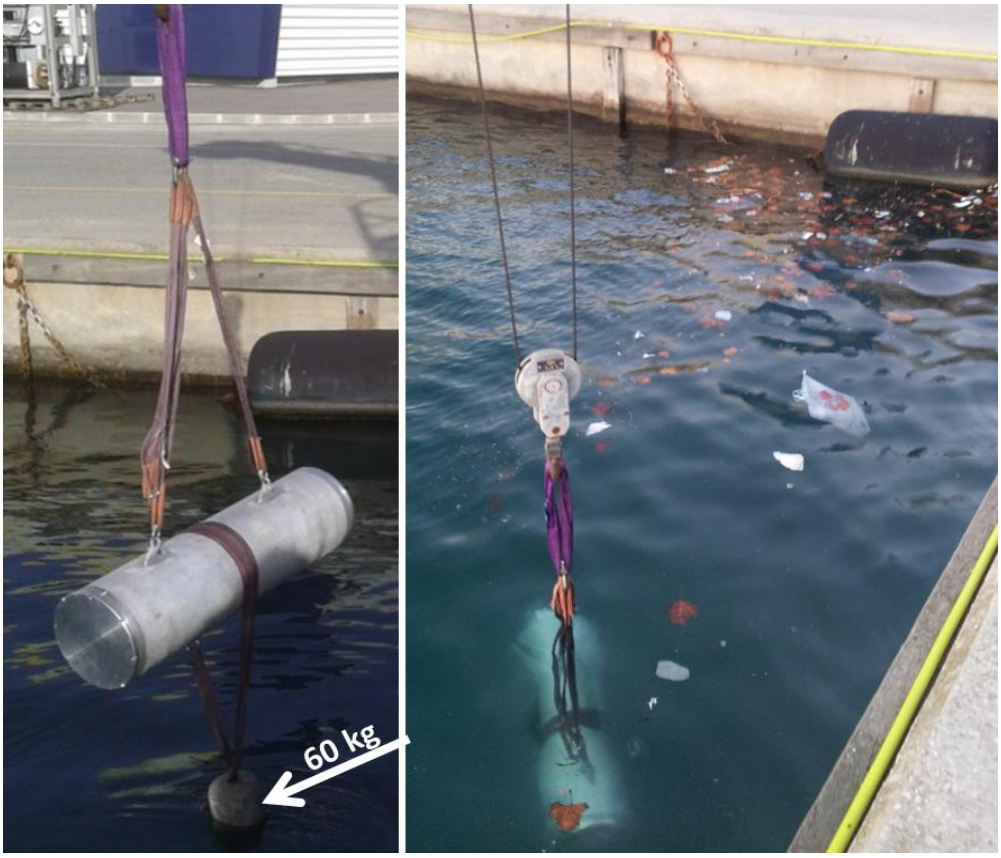

Figure 25: In situ tests in La Seyne Sur Mer harbor

Measurement of Raman spectra in the harbor (location 43.1054 N and 5.8856 E), without a substrate, can detect salt ions of SO_4^{2-} in the position 980 cm^{-1}, which can be observed within 25 s, with zoom in 10 s. Raman spectra are presented in figure 26. The detection of salt ions in the seawater is an important step to provide a reference for sensitivity of the developed instrument and proof of its function.

All in situ measurements with SGI are single Raman spectrum (only one CCD readout) and not averaged from 10 (as Arctic experiments), because if the sample is not uniform (as in laboratory conditions), flow will change with time, and Raman signals that appear only once, will be automatically excluded by the program as a spike (signal from the equipment), making results incomplete. This is the reason that spectra, which are taken in higher integration times, may contain spikes, as can be seen in figure 26.

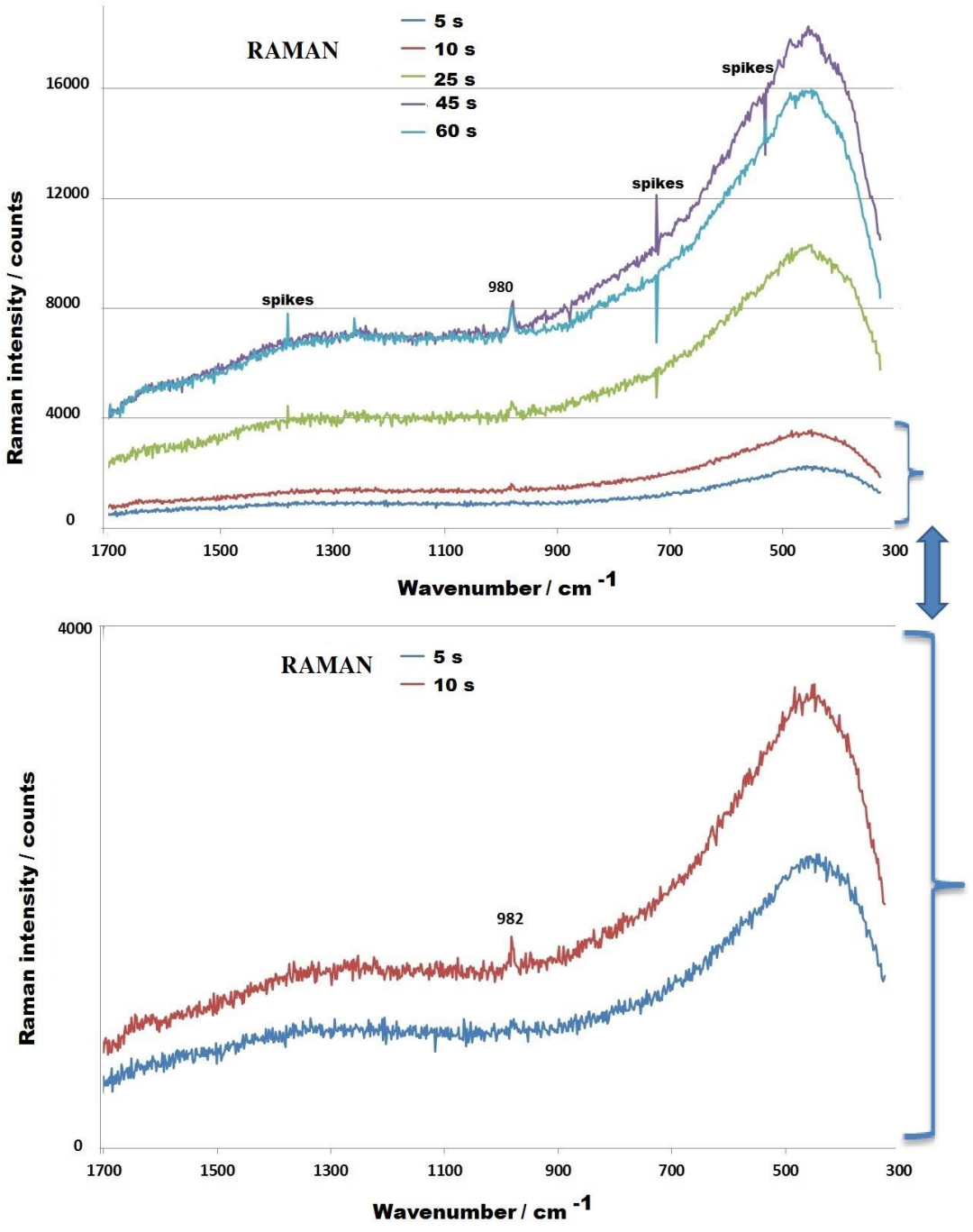

Figure 26: Raman spectra of real sea wate at different integration times from 5s-60s. Laser 671 nm, laser power 30 mW.

After applying gold island substrates, various signals appear within 10 s. Figure 27, shows Raman/SERS in situ measurements of real seawater in the harbor, for a time period of 25 minutes. As we can see, the intensity of Raman signals is not constant during the measurement. This is due to the adsorption/desorption process of the chemicals from the water to/from the surface of the substrate. The absolute intensity of Raman signals increase during the first 1-15 minutes; after this time intensity of Raman signals are decreasing. This effect is due to gradual sensitivity loss of the gold island substrate in contact with seawater [Ahamad and Kronfeldt, 2013].

In the first minutes of measurement (fig. 27), two intense signals appear in the positions of 500 cm^{-1} and 700 cm^{-1}. The Raman signal at the area of 500 cm^{-1} belongs to the quartz, but since the intensity of this signal is significantly higher in the first few minutes of the measurement, it must overlap with the signal from pollution. The only pollutant that gives intense signal in this area (488 cm^{-1}) is biphenyl, but in the area of 700 cm^{-1} - flouranthene (662 cm^{-1}), see appendix VII. The reason that high peaks from pollution are observed only during the first few minutes could be explained by the substrate adsorbing pollutants from the surface of the water (where oily chemicals will be present more likely) and later those pollutants are “washed off” from the substrate.

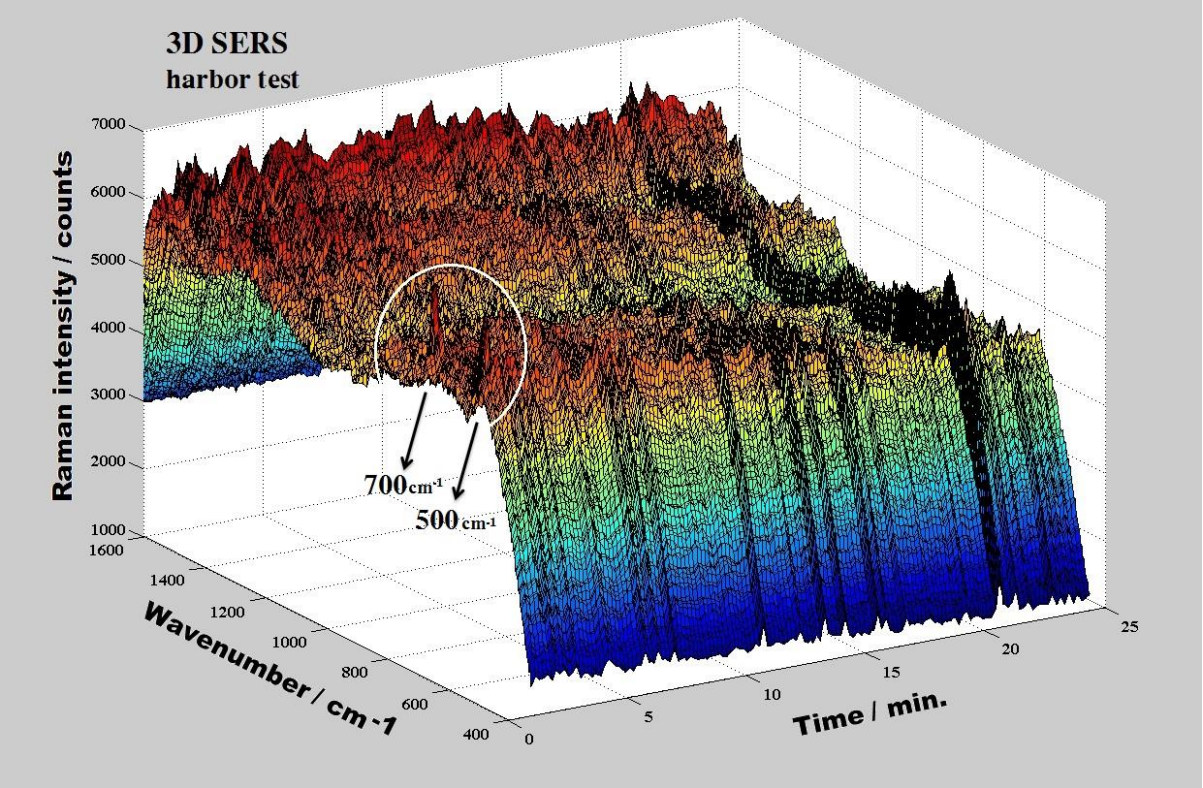

Figure 27: 3D, Raman/SERS measurements of real sea water in the harbor on gold island substrates. laser power 30 mW; λ = 671 nm. 10 s integreation time, experiment done on 29.11.12, 17:45-18:09.

Investigating 2D diagram (see figure 28 a) of the discussed measurement (Raman/SERS in the harbour, 10 s integration time, taken on 29.11.12), we can identify various Raman signals which are collected and referred to PAHs and biphenyl in table 5.

A week later (5.12.12) the same[15] experiment was carried out, but applying a different gold island substrate and reducing the integration time to 5 s, see figure 28 b.

It is a very remarkable fact that the same Raman/SERS signals are obtained in both experiments.

[15] in the harbor (location 43.1054 N and 5.8856 E) same time of the day (17:45 – 17:47) in order to achieve the same fluorescence conditions

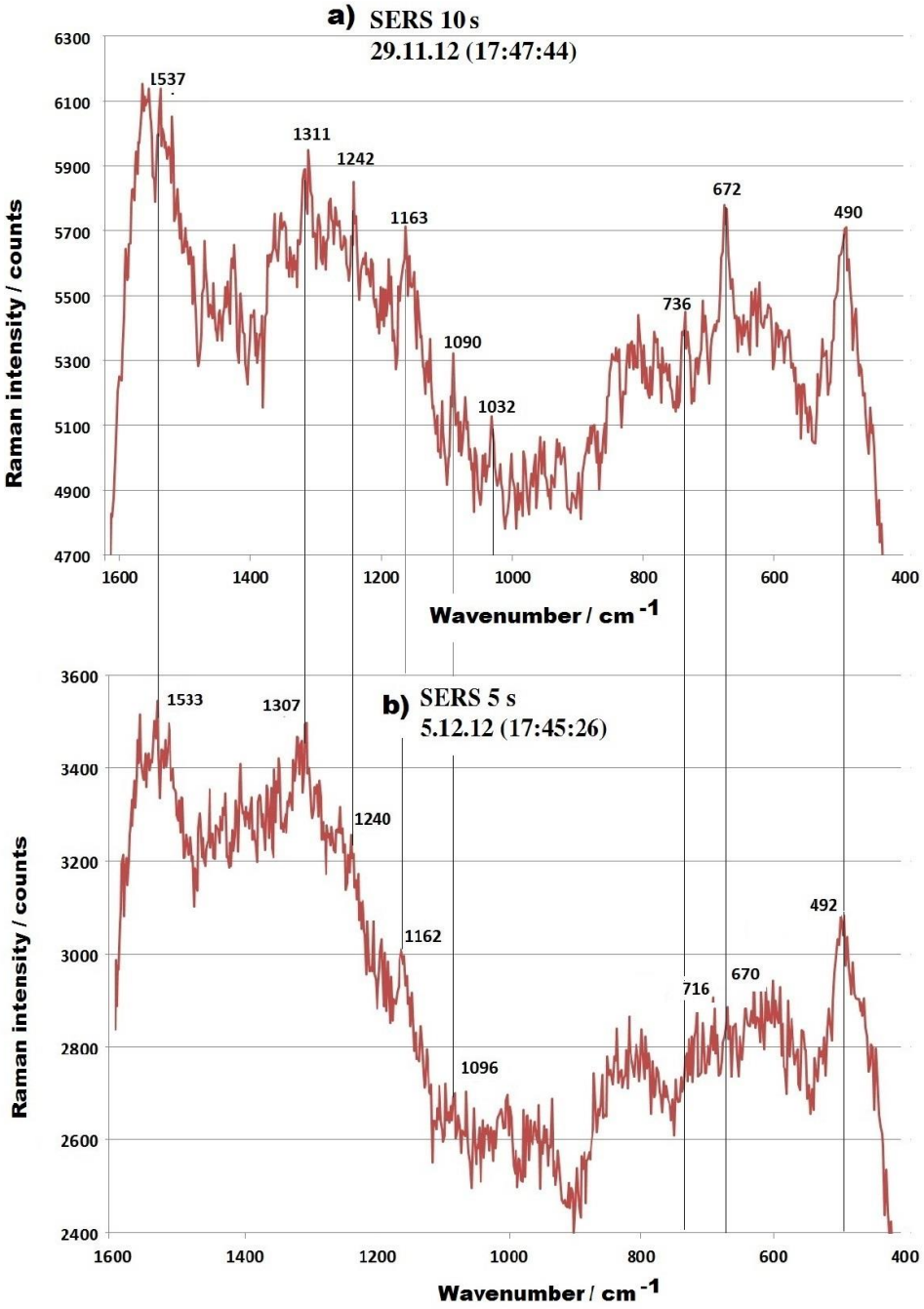

Figure 28: Raman/SERS measurements of real sea water in the harbor on gold island substrates (different), laser power 30 mW; λ = 671 nm. (a) 10 s integreation time, experiment done on 29.11.12, 17:47:44; (b) 5 s integration time, experiment done on 05.12.12, 17:45:26.

The signals of interest (from fig. 28) are collected in table 5.

Raman signal at 490 cm^{-1} belongs to quartz or biphenyl (as discussed above). If PAHs are present in the harbor water, the most expected according to current experiments, are fluranthene, biphenyl and fluorene. Note, that fluoranthene, representing the sum of PAHs (1 µg/kg - 10µg/kg dry weight) and biphenyl (1 µg/kg dry weight) was detected in this area in 2009 [Andral, 2009].

Table 5: Raman/SERS signals from in situ test in the harbor

Detected wavelength cm^{-1}	1533/7	1307/11	1240/2	1163	1090/6	1032	716/36	670/2	490/2
PAH	Flu	Flu	Flu (?)	Bip (?)	Fla	Acenap Phe	Bip	Fla	Bip
Theoretical wavelength, appendix VII	1544	1304	1227	1136	**1092**	1026 1028	732	**662**	**488**
Difference	-9/7	+3/7	+13/15	+27	**-2/+4**	+7 +4	-16/+4	**+8/10**	**+2/4**

5.3.3. Sea trial in the Mediterranean

After successful experiments in the harbor, the SGI was ready to be exposed in harsh offshore conditions for further sea trials. Two measurement stations around Toulon area[16] were chosen for experiments in order to use previously obtained results during RINBIO project [Andral, 2009; Andral et al., 2004] as a cross-reference. Station I is an open sea field with strong movement, especially in the upper water layer (0.5 m) to which the SGI was exposed, therefore measurements from this area were done in very harsh offshore conditions. Station II, Tamaris Le Lazaret muscle farm, is located in a bay with standing water. Since station II is a food production area; it is a point of interest for pollution measurements.

[16] Station I: N 43.0052; E 5.0571; Station II (Tamaris Le Lazaret muscle pharm): N 43.0053; E 5.0544

As the developed sensor is fully autonomous in its operation, this allowed all sea trials to be done on a Rigid Inflatable Boat (RIB) powered by an outboard engine (see figure 29 a). All experiments were performed during daytime. In order to prevent direct sunlight on the optical window of the SGI, an additional part was constructed: "the roof" of the sensor (figure 29 b). The SGI, with a complete weight of over 100 kg[17], was immersed in the water by using a davit crane (figure 29 c). All the parameters for driving the 671 nm laser, measuring and recording spectra, were programmed on land prior to the cruise and left running for a few hours between closing and opening the SGI (before and after the cruise). The gold island substrates were changed directly on the boat in between the measurements, as this does not require opening the SGI.

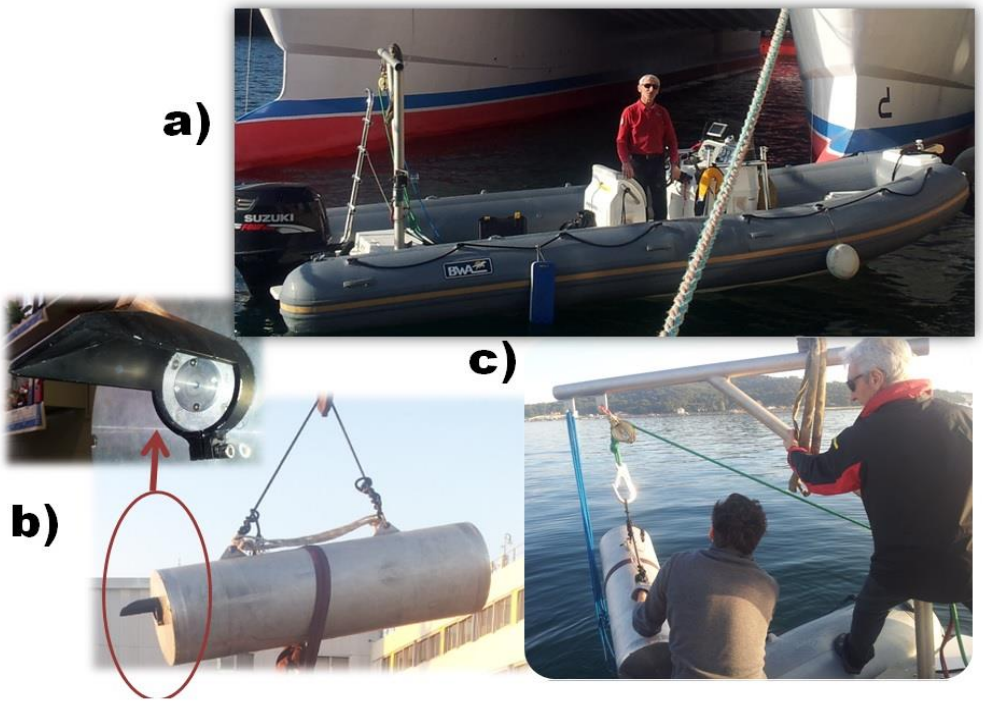

Figure 29: Test sea trial. a) The boat of the sea trial; b) SGI and sunlight screening part c) the process of experiment[18].

[17] Weight of SGI is 70 kg + additional minimum weight of 40 kg to prevent floating
[18] Francois Roland and Eric Emery amercing SGI into the water

A 3D diagram from continuous SERS measurements of real sea water from station I, during 12 minutes, with integration time of 10 s is presented in figure 30 a. As we can see, the intensity of the signal varies with time. This happens due to ad-/de-sorption of chemicals from seawater to/from the surface of the substrate, as already discussed.

During the first 10-30 seconds, Raman signal is very intense due to high sensitivity of the "fresh" substrate. After this time the top layer of the gold nano-particles (which are not covered with the sol gel) in the surface of the substrate degrade from contact with the seawater, slightly decreasing the substrates sensitivity.

However, the effect of overall sensitivity loss for the substrate is compensated for the first 10 minutes with the chemical adsorption process, which happens faster than desorption. After this time sensitivity loss of the substrate is higher than the adsorption process and signals start to decrease.

Simply saying, for the first 30 seconds, Raman signal is very high due to the "fresh" substrate. From the 1^{st} to 10^{th} minute of the experiment, overall intensity of the spectra increases, due to fast chemical adsorption from the seawater. After the 10^{th} minute, intensity of the spectra starts continuously decreasing due to the substrates sensitivity loss in contact with seawater.

Four spectra have been chosen and presented in a 2D diagram, figure 30 b, which were taken with 3 minutes time difference and extracted from the measurements. A reference spectrum of fresh "mains supply" water, which was taken in IFREMERs indoor pool is also displayed.

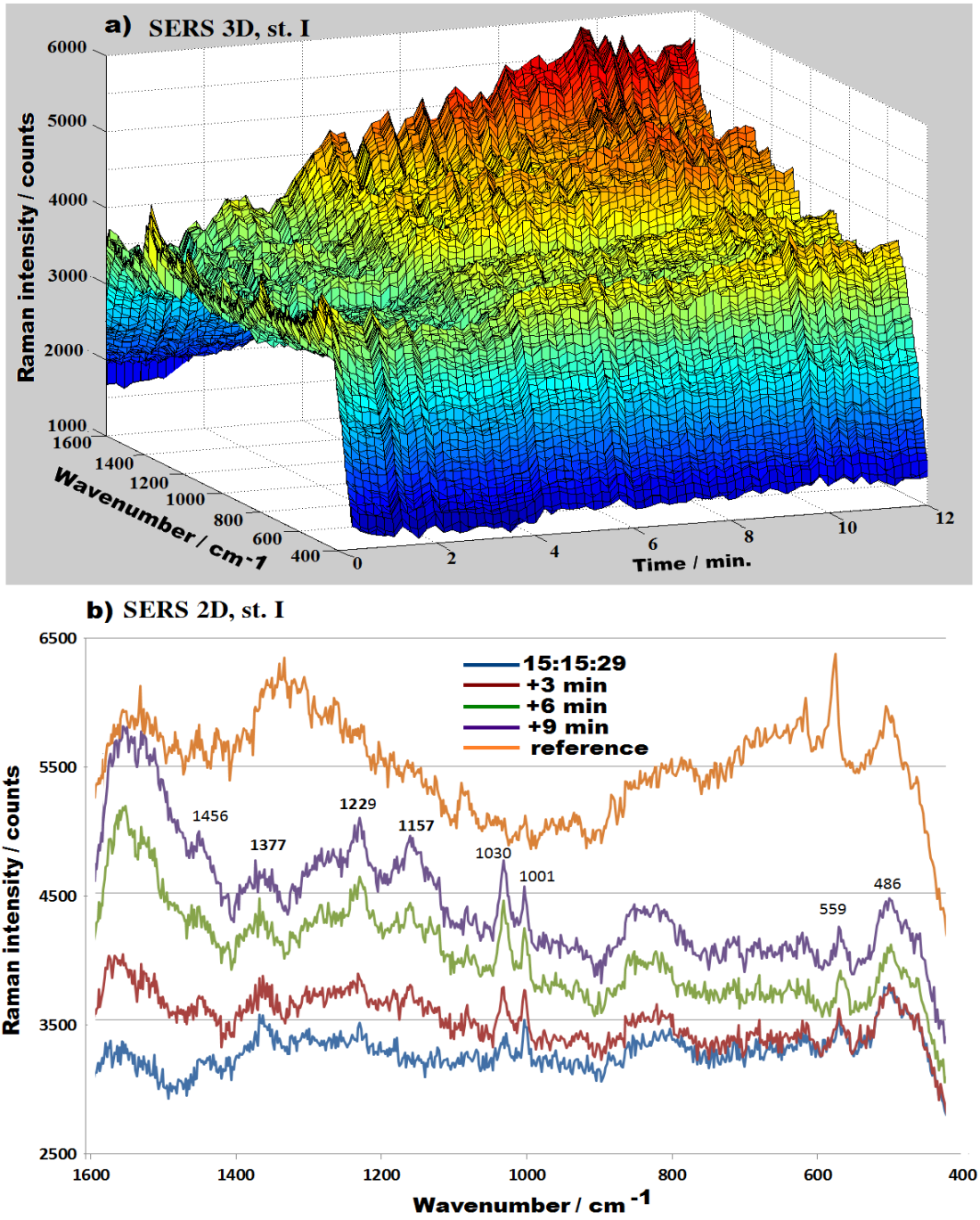

Figure 30: SERS spectra a) real surface water in station I: 07.01.13; continous measurement, 3D; b) real surface water in station I : 07.01.13; 15:15:29; "+3 min" = 15:18:12; "+6 min" = 15:21:26; "+9 min" = 15:24:39; and reference spectra of fresh tab water: 08.01.13; 13:53:38; gold island substrates Laser λ = 671 nm, laser power 30 mW; 10 s integration time.

As we can see, all spectra have high background noise due to fluorescence and very few Raman bands are sharp. Eight of them can be observed (see table 6): 486 cm^{-1}, 559 cm^{-1}, 1001 cm^{-1}, 1030 cm^{-1}, 1157 cm^{-1}, 1229 cm^{-1}, 1377 cm^{-1}, 1456 cm^{-1}. Three out of eight Raman bands can be excluded due to its repetition in the reference spectrum, such as: 486 cm^{-1} (quartz peak[19]), 559 cm^{-1} and 1456 cm^{-1}.

The most intensive Raman signals are in the positions 1001 cm^{-1} and 1030 cm^{-1}, nevertheless, they also have to be excluded because all the measurements of water samples with SERDS setup (which is more sensitive) shows that gold island substrates produce two intense peaks in the area of 1000 cm^{-1} - 1030 cm^{-1} (see chapter 5.1).

According to the reference table from appendix VII, Raman band in the location 1157 cm^{-1} does not belong to any of the 15 PAHs or biphenyl, which are investigated in this work. The peak in position 1229 cm^{-1} and 1377 cm^{-1} can belong to pyrene, but as we know pyrene produces strong Raman signal in the area of 587 cm^{-1}, we cannot see such a signal. Raman band in the position 1377 cm^{-1} is very typical for naphthalene. It can also belong to fluoranthene.

Table 6: Raman signals from sytation I

	Detected Raman bands, cm^{-1}							
	1456	**1377**	**1229**	**1157**	**1030**	**1001**	**559**	**486**
Produced by	Refernce spectrum (fig.28b)	Pyrene Naphthalene fluoranthene	pyrene	----	Gold island substr.	Gold island substr.	Refernce spectrum (fig.28b)	Refernce spectrum (fig.28b)
Origin	---			----	Silane layer [Ahmad and Kronfeldt 2013]	Silane layer [Ahmad and Kronfeldt 2013]	----	quartz

[19] the same intensity in all readings

One of the Raman signals - 1229 cm^{-1} from figure 30 (station I), that does not belong to the gold island substrate, has been analyzed for absolute (fig. 31 a) and net (fig. 31 b) intensity change. Absolute intensity (fig. 31 a) of the signal is very high during the first ~30 seconds, when the substrate just came in contact with seawater. Net intensity (fig. 31 b) of the signal is lowest because the chemical did not have time to adsorb (well) yet. From the 1st minute until 10th, both (overall and net) intensities increase. Starting from the 10th minute of the measurement, both (overall and net) intensities slowly continuously start decreasing.

The strong intensity change variation in figure 31 represents the ad-/de-sorption process of the chemical during the experiment.

Current results fully match the previous observation of figure 30 a.

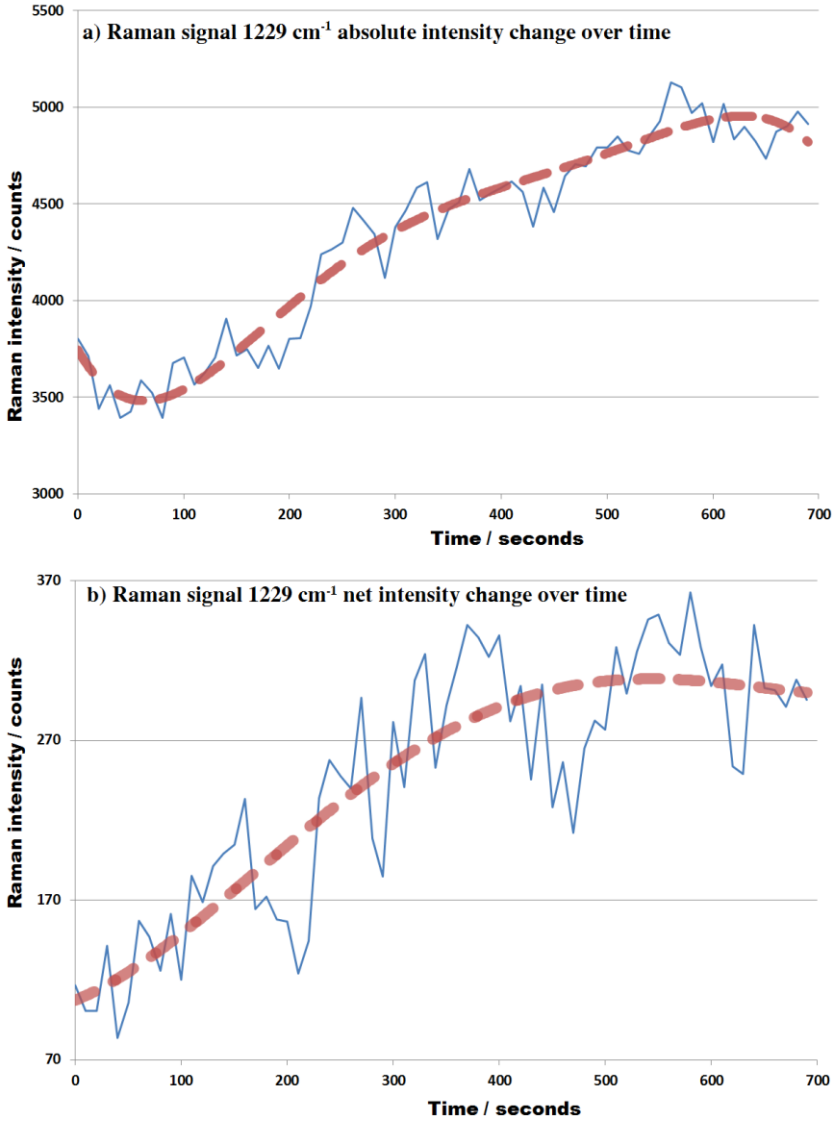

Figure 31: Raman signal 1229 cm^{-1} a) absolute intensity change and b) net intensity change

3D continuous measurements from muscle farm “Tamaris”, Station II, is presented in figure 32 (a), note that the time scale is in seconds due to a short experiment time (4 minutes).

As was seen in previous results from station I (figure 30, 31 a), first readings are more intense – this is the time when the SGI just came in contact with the seawater, but after ~30 seconds, spectra stabilize with further increases in sensitivity, starting from four minutes.

In the 2D diagram of one chosen reading (at 15:50:31, station II), as well as reference spectrum of fresh “mains supply” water (taken the next day (08.01.13; 13:53:38) in the IFREMER indoor pool) is presented in figure 32 b.

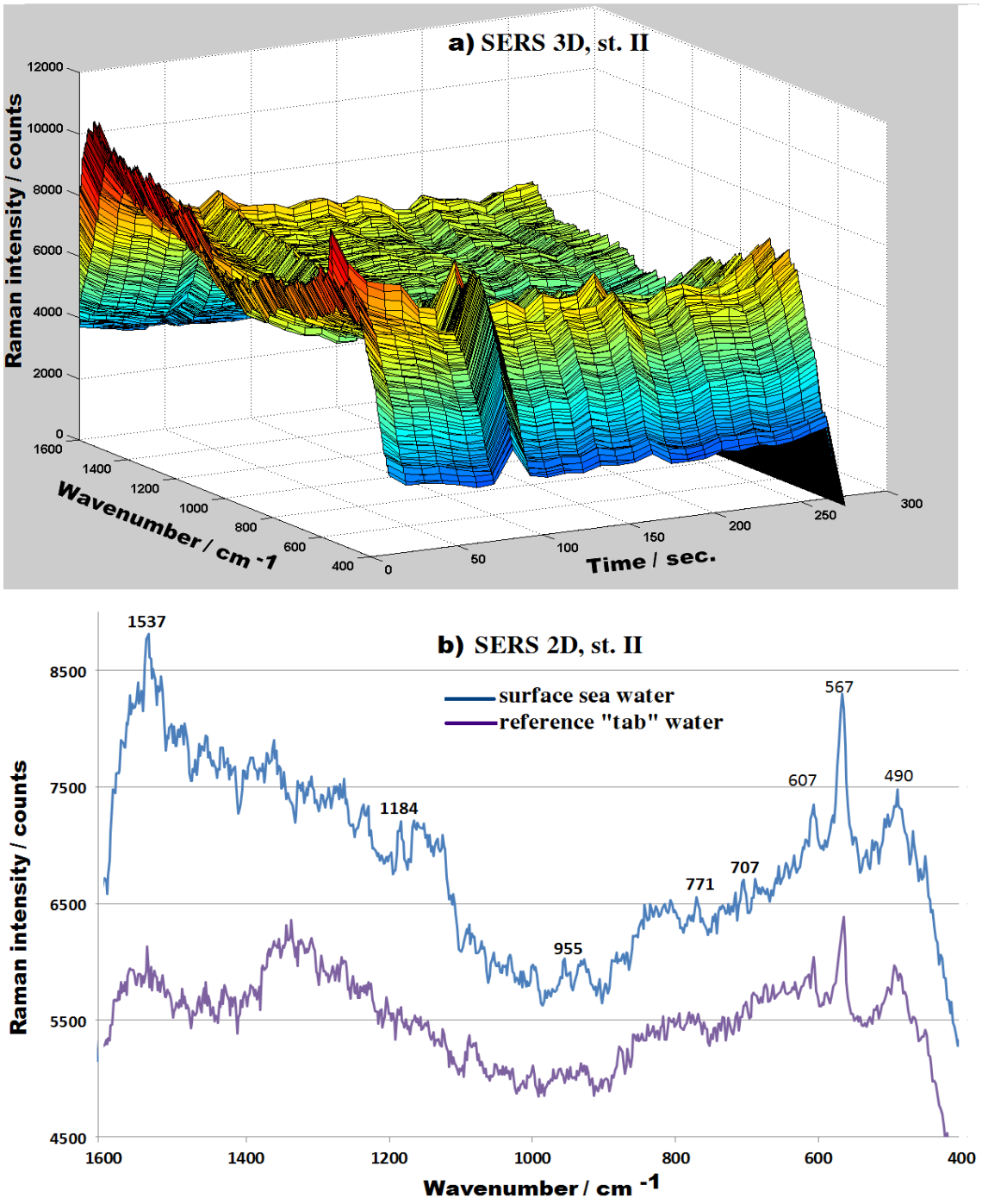

Figure 32: SERS spectra of a) real sea water, station II: 07.01.13; continuos measurement, 3D; b) Real sea water, station II (in blue): 07.01.13; 15:50:31; 2D and reference spectra (in purple): 08.01.13; 13:53:38. Gold island substrates. $\lambda = 671$ nm, laser power 30 mW; 10 s integration time.

As we can see from figure 32, the most intensive Raman signals in positions 490 cm^{-1} (quartz signal), 567 cm^{-1} and 607 cm^{-1} have to be excluded because they repeat in the reference measurement, consequently these Raman signals do not come from expected pollution.

The remaining signals are not strongly pronounced, however they can be referred to specific chemicals, see table 7. For example: position 707 cm^{-1} and 1184 cm^{-1} are significant for phenanthrene (**701**, 1198), 771 cm^{-1} remains unknown, 955 cm^{-1} can be referenced to acenapthene (960); 1184 cm^{-1} may be produced by phenanthrene (1198) or biphenyl (1194) 1537 cm^{-1} – fluorine (1544).

Table 7: Raman signals from station II

	Raman signlas, cm^{-1}							
	1537	**1184**	**955**	**771**	**707**	**607**	**567**	**490**
Produced by	flu	phe	acenap	----	phe	-----	-----	quartz
Theory [appendix VI]	1544	1198	960		**701**	In the ref. spec.	In the ref. spec.	490
difference	7	14	5		6			0

5.3.4 SERS/SERDS measurements of water sample taken from station I and II

Measurement of the water sample taken from station I during sea trials is presented in the figure 33 (in red). Artificial sea water served as reference spectrum (figure 33 in blue). A few Raman signals from the sample were detected, two of them could be referenced to fluoranthene, and they are in the position: 566 cm^{-1} and 651 cm^{-1}. Both Raman signals in these positions are expected to be intense. Raman bands, which were measured during sea trials, did not appear. This can be explained by the strong movement of the water in station I. In this case the surface of the water (where sample was taken) could contain different chemicals and concentrations of possible pollutants which could be spread uneven comparing to the water layer where SGI was immersed.

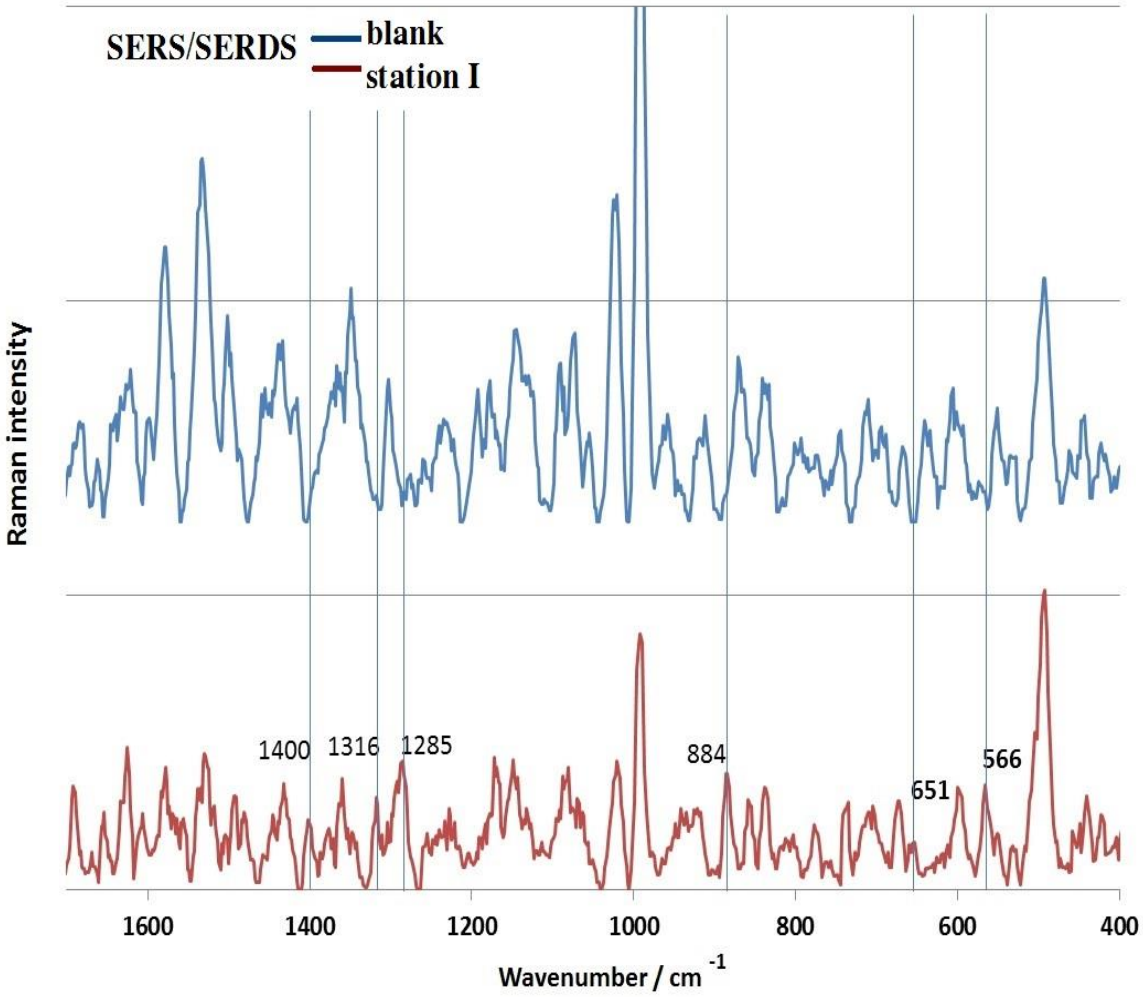

Figure 33: SERS/SERDS spectrum of water sample from station I (in red) and reference specrum (in blue). Gold island substrate, lasers: λ_1 = 671,6 nm and λ_2 = 671, 0 nm; laser power 30 mA; integration time 10 s.

Measurement of the water sample, which was taken from station II during sea trial, is presented in figure 34 (in red). Artificial sea water served as reference spectrum (figure 34 in blue). In the location of station II, water was standing and had almost no movement, as result we can see three (out of five) Raman signals repeat comparing to in situ measurements (see chapter 5.3.3), these are: 775 cm^{-1}, 942 cm^{-1} and 1185 cm^{-1}. Additionally three peaks, which

are typical for fluoranthene were detected in the positions: 660 cm^{-1}, 795 cm^{-1} and 1605 cm^{-1}. As well as one Raman band that is very typical for fluorine, in the position 1740 cm^{-1}.

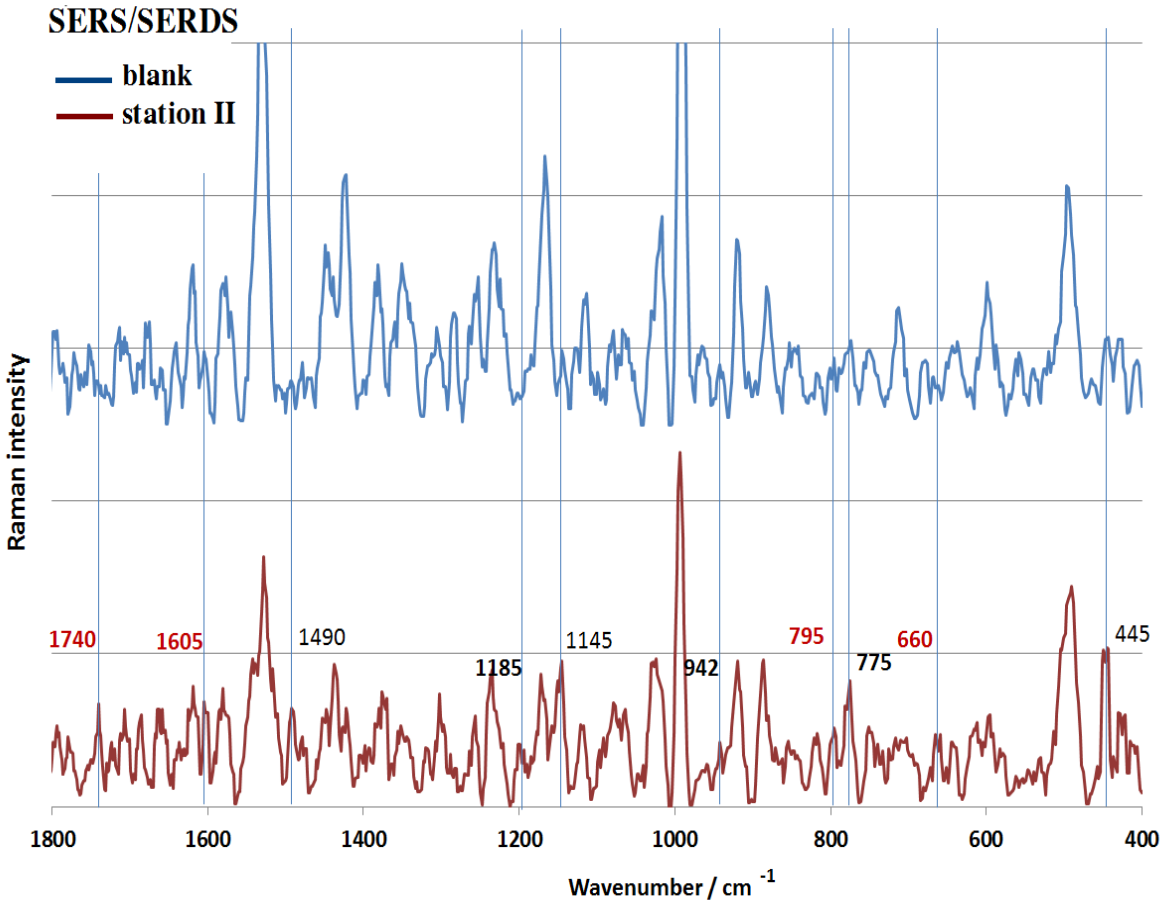

Figure 34: SERS/SERDS spectrum of water sample from station II (in red) and reference specrum (in blue). Gold island substrate, lasers: λ_1 = 671,6 nm and λ_2 = 671, 0 nm; laser power 30 mA; integration time 10s.

6. Summary and outlook

Summary

For the first time, an autonomous sea going in situ Raman and SERS (surface enhanced Raman spectroscopy) detector for chemical monitoring at nM level in seawater was developed and successfully tested at selected locations in the Mediterranean Sea.

To achieve this goal, basic laboratory experiments were carried out with water samples collected from the North Sea, Atlantic Ocean, Pacific Ocean, Great Lakes, Mediterranean Sea, Chesapeake Bay, East China Sea, Mississippi River, Aegean Sea, and Baltic Sea between 2010 and 2013. Applying a specially designed microsystem diode laser with two emission wavelengths (λ_1 = 671.0 nm, λ_2 = 671.6 nm), SERS and combined SERS/SERDS (shifted excitation Raman difference spectroscopy) investigations were performed with an integration time of 10 s only using gold island substrates. Results of the laboratory experiments provide information about substrate behavior in different water bodies, e.g. ability to measure characteristic Raman signals and refer them to certain pollutants – PAHs or biphenyl (see appendix VI). The most prominent Raman signals, indicating a high degree of pollution, appeared in water samples taken from harbors, city stokes, and nearby factories. Frequently, characteristic Raman signals from fluoranthene, biphenyl, acenapthtylene and pyrene could be detected as pollution mixture, sometimes as single pollutants.

Based on these initial investigations, a portable 671 nm on-board Raman/SERS sensor was developed and adapted for measurements under harsh offshore conditions. To gather valuable information for in situ measurements with real seawater, the system was tested in the Arctic area (78° N, 10° E) during three weeks in August 2011. Thirteen surface water and six sediment water specimens from selected locations have been examined on board James Clark Ross research vessel. Ag,DMCX:MTEOS substrates, based on sol-gel

layer coating technique, have been applied due to their special sensitivity for PAH detection. Measured visible limits of detection (LOD) for anthracene and fluoranthene in real seawater, being in the mixture, were obtained lower than calculated LODs during laboratory experiments for single chemical in artificial seawater: anthracene 0.3 nM and lower (laboratory: 1 nM), and fluoranthene 1 nM and lower (laboratory: 1.2 nM). Substrate stability tests showed that sensitivity loss of Ag,DMCX:MTEOS during the first 10 h is only 2 %. After 7 days, the intensity can decrease up to 20 % if the substrate is stored in seawater and up to 5 % when stored in fresh water. These results demonstrate that the substrates are capable for weeklong experiments in seawater and especially suited for long-term experiments in fresh water.

Finally, a cutting-edge autonomous sea going 671nm Raman/SERS instrument that could be fully submersed without any external cables or connections to the sensor from a research vessel, was constructed and tested in the Mediterranean Sea. In situ experiments in the harbor of La Seyne-sur-Mer, France (43° N, 5° E) verified the ability to measure various Raman signals from the seawater, typically in only 10 s. Raman measurements, without application of the SERS substrates, showed signals from the salt ions (SO_4^{2-}) in seawater using integration times of 10 s only. After applying gold island substrates, characteristic signals from fluoranthene and biphenyl could be detected. Offshore tests were conducted in two stations near Toulon, France: Station I exhibiting harsh offshore conditions and strongly moving water; Station II with mild conditions and standing water (Tamaris Le Lazaret muscle farm). At both locations, the in situ measurements showed different Raman signals, which can be attributed to selected PAHs (as pyrene, naphthalene, fluoranthene, phenanthrene). Reference investigations in the laboratory from collected water samples, taken from station I and II confirmed the offshore results showing essentially the same Raman signals as detected in situ.

Outlook

The developed autonomous 671 nm Raman/SERS sea going instrument is able to measure any Raman active molecules and substances. Consequently, future applications of the current techniques and equipment are very wide. Target chemicals (in current example PAHs) can be changed without modifications of equipment and techniques. Here, different types of SERS substrates can be applied according to the individual measurement tasks. This is very convenient due to the ability to measure nutrients, minerals, pollutants or other chemicals with the same sensor in any water body (e.g. fresh, salty, wastewater), at different experimental conditions (temperature, pressure, movements). Moreover, due to the robustness of the developed instrument, the measurements can be done in harsh offshore conditions.

The autonomous sea going instrument is a new technological platform for various applications and can be further adapted to any buoy station, mooring system, autonomously operated vehicle (AOV), cruise or cargo vessel. It can be installed on a network of alarm sensors for long term surveillance of small or intermediate ocean areas and offers the possibility for deep-sea-investigations (depth monitoring) with improved pressure housing down to 10 000 m water depth.

References

[Adams *et al.*, 2000] N.G. Adams, M. Lesoing, V.L. Trainer. Environmental conditions associated with domoic acid in razor clams on the Washington coast. *Journal of Shellfish Research*, 19: 1007–1015, 2000.

[Ahmad and Kronfeldt, 2013] H. Ahmad, H.D. Kronfeldt. High Sensitive Seawater Resistant SERS Substrates Based on Gold Island Film Produced by Electroless Plating. *Marine Science*. 3(1): 1-8, 2013

[Ahmad *et al.*, 2011] H. Ahmad, A. Kolomijeca, K. Sowoidnich, H.D. Kronfeldt. Application of Shifted Excitation Raman Difference Spectroscopy (SERDS) for In-situ Investigations in the Deep Sea. *Proceedings of the Ninth ISOPE Ocean Mining Symposium*: 78 - 82, 2011.

[Andral, 2009] B. Andral. Reseau Integrateurs Biologiques RINBIO 2009. Evaluation de la qualite des eaux base sur l'utilisation de stations artificielles de mousles en Mediterranee: results de la champagne, 2009.

[Andral *et al.*, 2004] B. Andral, J.Y. Stanisiere, D. Sauzade, E. Damier, H. Thebault, F. Galgani , P. Boissery. Monitoring chemical contamination levels in the Mediterranean based on the use of mussel caging. *Marine Pollution Bulletin*, 49 (9-10): 704-712, 2004.

[Albrecht and Creighton, 1977] M.G. Albrecht, J.A. Creighton. Anomalously Intense Raman Spectra of Pyridine at a Silver Electrode. *Journal of the American Chemical Society*, 99 (15): 5215-5217, 1977.

[ATSDR] U.S. Department of Health and Human Services. Agency for Toxic Substances and Disease Registry. PHAs: production, import/export, use and disposal[20].

[ATSDR, 1990] U.S. Department of Health and Human Services. ATSDR: Agency for Toxic Substances and Disease Registry. Public Health Statement, Polycyclic Aromatic Hydrocarbons. Atlanta, GA, 1990.

[Aygun and Kabadayi, 2005] S.F. Aygün, and F. Kabadayi. Determination of benzo[a]pyrene in charcoal grilled meat samples by HPLC with fluorescence detection. *International Journal of Food Sciences and Nutrition*, 56(8): 581-585, 2005.

[20] On-line: http://www.atsdr.cdc.gov/toxprofiles/tp69-c4.pdf

[Babin *et al.*, 2005] M. Babin, J.J. Cullen, C.S. Roesler, P.L. Donaghay, G.J. Doucette, M. Kahru, M.R. Lewis, C.A. Scholin, M.E. Sieracki, H.M. Sosik. New Approaches and Technologies for Observing Harmful Algal Blooms. *Oceanography*, 18(2): 210-227, 2005.

[Baena and Lend, 2004] J.R. Baena, B. Lend. Raman spectroscopy in chemical bioanalysis. *Chemical Biology*, 8:534–539, 2004.

[Baker and Moore, 2005] G.A. Baker, D.S. Moore. Progress in plasmonic engineering of surface-enhanced Raman-scattering substrates toward ultra-trace analysis. *Analytical and Bioanalytical Chemistry*, 382: 1751-1770, 2005.

[Baker and Eisenreich, 1990] J.E Baker, S.J. Eisenreich. Concentrations and fluxes of polycyclic aromatic hydrocarbons and polychlorinated biphenyls across the air–water interface of Lake Superior. *Environmental science and technology*, 24:342-352, 1990.

[Barrie *et al.*, 1992] L.A. Barrie, D. Gregor, B. Hargrave, R. Lake, D. Muir, R. Shearer, B. Tracey, T. Bidelmant. Arctic contaminants: sources, occurrence and pathways. *Science of the Total Environment*, 122: 1–74, 1992.

[Best, 2012] Mari Best. University of Victoria. Information obtained during conversation. Short Course 1- In situ sensors for experimentation and exploration in the deep-sea, Banyuls, France, February 2012.

[Bich Ha, 2004] N. T. Bich Ha: Surface-nhanced Raman Scattering (SERS) for in-situ Analysis of Mixture of Polycyclic Aromatic Hydrocarbons (PAHs) in Sea-water. PhD thesis. Berlin, Germany: Technical University Berlin, 2004.

[Boehncke *et al.*, 1999] A. Boehncke, G. Koennecker, I. Mangelsdorf, A. Wibbertmann. Biphenyl. Concise International Chemical Assessment Document 6. Fraunhofer Institute for toxicology and Aerosol Research, Hanover, Germany, 1999.

[Brewer *et al*, 2011] P.G. Brewer, W. Ussler, E. Peltzer, P. Walz, W. Krikwood, K. Hester. Accurate in situ observation of deep-sea sediment dissolved methane profiles in hydrate bearing provinces. *Proceedings of 7th international Conference on Gas and Hydrates*, 17-21, 2001.

[Browell, 1977] E.V. Browell. Analysis of laser fluorosensor systems for remote algae detection and quantification. NASA Technical Note TN D-8447, 1977.

[Bundy *et al.*, 1996] K.J. Bundy, D. Berzins, P. Taverna. Development of polarographic sensor for heavy metal detection sensing applications. *Proceeding of the HSRC/WERC Joint Conference on the Environment*, 1996.

[Collin *et al.*, 2003] G. Collin, H. Höke, H. Greim. Naphthalene and Hydronaphthalenes. Ullmann's Encyclopedia of Industrial Chemistry Wiley-VCH, Weinheim, 2003.

[Collin *et al.*, 2006] G. Collin, H. Höke and J. Talbiersky . Anthracene. Ullmann's Encyclopedia of Industrial Chemistry, Wiley-VCH, Weinheim, 2006.

[Daisy et al., 2002] B.H. Daisy, G.A. Strobel, U. Castillo. Naphthalene, an insect repellent, is produced by Muscodor vitigenus, a novel endophytic fungus. *Microbiology* , 148 (11): 3737–3741, 2002.

[DPH, 2009] Delaware Health and social Services. Devision of Public Health. Benzo [a] Pyrene[21], 2009.

[DS^{3}F]: Deep-Sea and Sub-Seafloor Frontier[22], Seventh Framework Program, project number: (244099).

[ECO-USA, 1990] Toxicological Profile for Chrysene[23]. Agency for Toxic Substances and Disease Registry, 1990.

[EP, 2013] *Journal Environmental Pollution*. Editor-in-Chief W. Manning. University of Massachusetts, Amherst, USA, 2013.

[GSI, 2010] GSI Environmental Engineering Inc. Chrysene[24], 2010.

[EPA, 1995]: United States Environmental Protection Agency. Biphenyl fact sheet: Support document[25], EPA749-F-95-003a, 1995.

[EPA, 1990]: United States Environmental Protection Agency. Fluorene[26], 1990.

[EPA, 2012a] EPA: United States Environmental Protection Agency. Laws, regulation, Treaties (Permitting) [27], 2012.

[EPA, 2001a] United States Environment Protection Agency. Acenapthylene[28], 2001.

[21] On-line: http://dhss.delaware.gov/dph/files/benzopyrenefaq.pdf
[22] On line: http://www.deep-sea-frontier.eu/
[23] On-line: http://www.eco-usa.net/toxics/chemicals/chrysene.shtml
[24] On-line: http://www.gsi-net.com/en/publications/gsi-chemical-database/single/137.html
[25] On line: http://www.epa.gov/chemfact/biphe-sd.pdf
[26] On line: http://www.epa.gov/osw/hazard/wastemin/minimize/factshts/flourene.pdf
[27] On line: http://water.epa.gov/aboutow/owow/permitting.cfm

[EPA, 2012 b] United States Environment Protection Agency. Integrated Risck Information System. Acenapthylene[29], 2012.

[EPA, 2001b] United States Environment Protection Agency, Acenapthene[30], 2001.

[EPA, 2012c] United States Environment Protection Agency. Integrated Risk Information System. Fluorene[31], 2012 .

[EPA, 2012d] United States Environment Protection Agency. Integrated Risck Information System. Anthracene[32], 2012.

[EPA, 2012e] United States Environment Protection Agency. Integrated Risk Information System. Benzo [k] Fluoranthene[33], 2012.

[EU, 2001] "Decision2455/2001/EC of the European Parliament and of the Council of 20 November 2001 establishing the list of priority substances in the field of water policy and amending Directive 2000/60/EC". *Official Journal of the European Community*, L331/1-5, 2001.

[EU, 2002] "Polycyclic Aromatic hydrocarbons –Occurrence in foods, dietary exposure and health effects". European Commission, Scientific Committee on Food, Dec.4, 2002.

[EU, 2005] "Commission regulation (EC) No 208/2005 of 4 February 2005 amending Regulation (EC) No 466/2001 as regards polycyclic aromatic hydrocarbons". *Official Journal of the European Union*, L34/3-5, 2005.

[EU, 2007-2011] Catalogue of EU funded projects in Environmental research, FP 7 - Theme – 6 Environment (including climate change), 2007-2011.

[28] On-line http://www.epa.gov/osw/hazard/wastemin/minimize/factshts/acnphthy.pdf
[29] On-line http://www.epa.gov/iris/subst/0443.htm
[30] On-line http://www.epa.gov/osw/hazard/wastemin/minimize/factshts/acnphthe.pdf
[31] On-line http://www.epa.gov/iris/subst/0435.htm
[32] On-line http://www.epa.gov/iris/subst/0434.htm
[33] On-line http://www.epa.gov/iris/subst/0452.htm

[Faust, 1993] R. A. Faust. Toxicity Summary for Fluoranthene[34]. Health Sciences Research Division. Oak Ridge National Laboratory, 1993.

[Faust, 1994] R. A. Faust. Toxicity Summary for Benzo [ghi] Perylene[35]. Health Sciences Research Division. Oak Ridge National Laboratory, 1994.

[Fellin *et al.*, 1996] P. Fellin, L.A. Barrie, D. Dougherty, D. Toom, D. Muir, N. Grift, L. Lockhart B. Billeck. Airmonitoring in theArctic: results for selected persistent organic pollutants for 1992. *Environonmental Toxicology and Chemistry*, 15 (3): 253–261, 1996.

[Fleischmann *et al.*, 1974] M. Fleischmann, P. Hendra, A. McQuillan. Raman spectra of pyridine adsorbed at silver electrode. *Chemical Physics Letters*, 26(2):163-166, 1974.

[FSA, 2012] Food Standert Agency[36] current EU approved additives and their E numbers, (last update) 2012.

[Gelder *et al.*, 2007] J. De Gelder, K. De Gussem, P. Vandenabeele, L. Moens. Reference database of raman spectra of biological molecules. *Journal of Raman Spectroscopy*, 38: 1133-1147, 2007.

[GEOHAB, 2008]: Global Ecology and Oceanography of Harmful Algal Blooms[37], 2008.

[GESAMP, 2013]: joint Group of Experts on the Scientific Aspects of Marine environmental Protection[38], 2013.

[Gioia *et al.*, 2008] R. Gioia, L. Nizzetto, R. Lohmann, J. Dachs, C. Temme and K.C. Jones. Polychlorinated Biphenyls (PCBs) in Air and Seawater of the Atlantic Ocean. *Environmental Science and Technology*, 42 (5): 1416–1422, 2008.

[GOOS, 2008] Global Ocean Observing System. The oceanographic component of GEOSS, the Global Earth Observing System of Systems[39], 2008.

[Gostilo *et al.*, 2000] V. Gostilo, A. Sokolov, S. Danengirsh, V. Kondrashov, A. Loupilov, V. Fedotenkov, A. Pchelintsev, S.N. Nekrestjanov, V.F. Kireyev, O.Y. Pichteyev, V.P. Ivanov, D.V. Likov. Floating monitoring station for measurements of radionuclides

[34] On-line: http://cira.ornl.gov/documents/FLUORANT.pdf
[35] On-line: http://cira.ornl.gov/documents/Benzoghiperylene.pdf
[36] On line: http://www.food.gov.uk/policy-advice/additivesbranch/enumberlist#.UTdVyFc9GZk
[37] On line: http://www.geohab.info/index.php?option=com_content&view=article&id=23&Itemid=77
[38] On line: http://www.gesamp.org/
[39] On line: www.ioc-goos.org

volumetric activity in water reservoirs. *Nuclear Science Symposium Conference Record*. IEE, 2000.

[Greisbaum *et al*., 2002] K. Griesbaum, A. Behr, D. Biedenkapp, H.W. Voges, D. Garbe, C. Paetz, G. Collin, D. Mayer, H. Höke. Hydrocarbons. Ullmann's Encyclopedia of Industrial Chemistry Wiley-VCH, Weinheim, 2002.

[Grovel *et al.*, 2003] O. Grovel, Y.F. Pouchus, J.F. Verbist. Accumulation of gliotoxin, a cytotoxic mycotoxin from Aspergillus fumigatus, in blue mussel. *Toxicon*, 42: 297-300, 2003.

[Gruner *et al.*, 1991] K. Gruner, R. Retuer, H. Smid. A new sensor system for airbone measurements of maritime pollution and hydrographic parameters. *GeoJournal*, 24(1): 103-117, 1991.

[HERMIONE, 2012] Hotspot Ecosystem Research and Men's Impact On European Seas[40]; Uropean Commission's Framework Seven Programme, contract number 226354, 2009-2012.

[Hicks, 2001] C.J. Hicks, SERS: Surface Enhanced Raman Spectroscopy. MSU CEM 924, 2001.

[HSDB, 2001] U.S. Department of Health and Human Services. Hazardous Substances Data Bank (HSDB, online database). National Library of Medicine Bethesda, MD, 2001.

[HSDB, 2010] Hazardous Substances Data Bank[41]. Toxicology data file on the National Library of Medicine's (NLM) Toxicology Data Network (TOXNET®), (last update) 2010.

[Hubental, 2013] F. Hubental. Does the excitation of a plasmon resonance induce a strong chemical enhancement in SERS? *Journal of Raman Spectroscopy*. ID: JRS-13-0110. In print, 2013.

[IFREMER] Institute Francais de Recherche pour l'exploitation de la mer[42]. Public institute of an industrial and commercial nature (EPIC).

[IFREMER, 2010] Institute Francais de Recherche pour l'exploitation de la mer: Annual report 2010[43].

[40] On line: http://www.eu-hermione.net/
[41] On line: http://www.nlm.nih.gov/pubs/factsheets/hsdbfs.html#
[42] On line: http://wwz.ifremer.fr/institut

[IOW] The Leibniz Institute for Baltic Sea Research[44], Warnemünde, Germany.

[IPCS, 1999] International Program on Chemical Safety. Benzo [b] Fluoranthene[45], 1999.

[Jeanmaire and Duyne, 1977] D.L. Jeanmaire, R.P. van Duyne. Surface Raman Electrochemistry Part I. Heterocyclic, Aromatic and Aliphatic Amines Adsorbed on the Anodized Silver Electrode. *Journal of Electroanalytical Chemistry,* 84: 1–20, 1977.

[Jonson and Coletti, 2002] K.S. Jonson, L.J. Coletti. In situ ultraviolet spectrophotometry for high resolution and long-term monitoring of nitrate, bromide and biosulfide in the ocean. *Deep Sea Research I,* 49: 1291-1305, 2002.

[Kazetouni *et al.*, 2002] N. Kazerouni, R. Sinha, C.H. Hsu, A. Greenberg, N. Rothman. Analysis of 200 food items for benzo[a]pyrene and estimation of its intake in an epidemiologic study. *Food and Chemical Toxicology*, 40(1):133, 2002.

[Kneipp, 2007] K. Kneipp. Surface-Enhanced Raman scattering. *Physics Today*, 40-46, November 2007.

[Kneipp *et al.*, 2006] K. Kneipp, H. Kneipp, H. G. Bohr. Single-Molecule SERS Spectroscopy. Physics and Applications, *Topics Applied Physics*, 103: 261-278, 2006.

[Kolomijeca *et al.*, 2012 a] A. Kolomijeca, Y.H. Kwon, H.D. Kronfeldt. A Portable Surface Enhanced Raman (SERS) Sensor System Applied for Seawater and Sediment Investigations on an Arctic Sea-trial. *Proceedings of the Twenty-second International Offshore and Polar Engineering Conference*, 1398 – 1402, 2012.

[Kolomijeca *et al.*, 2012 b] A. Kolomijeca, Y.H. Kwon, H.D. Kronfeldt. Surface-enhanced in-situ Raman-sensor applied in the arctic area for analyses of water and sediment. Advanced Environmental, Chemical, and Biological Sensing Technologies IX, 8366, *Proceedings of SPIE*, 2012.

[43] On line: http://wwz.ifremer.fr/institut/content/download/48330/689394/file/Rapport%20Annuel%20final%20-%20anglais.pdf

[44] On line: http://www.io-warnemuende.de/research-vessels.html

[45] On-line: http://www.inchem.org/documents/icsc/icsc/eics0720.htm

[Kwon, 2012] Y.H. Kwon: Surface-Enhanced Raman Scatering (SERS) Suraces for in-situ trace analysis of PAHs in water by Shifted Excitation Raman Difference Spectroscopy (SERDS). PhD thesis. Berlin, Germany: Technical University Berlin, 2012.

[Kwon *et al.*, 2011] Y.H. Kwon, A. Kolomijeca, K. Sowoidnich, H.-D. Kronfeldt. High Sensitivity Calixarene SERS Substrates for the continuous In-situ Detection of PAHs in Sea-water. Advanced Environmental, Chemical, and Biological Sensing Technologies VIII, 8024, *Proceedings of SPIE*, 2011.

[Kwon *et al.*, 2012a] Y.H. Kwon, K. Sowoidnich, H. Schmidt, H.D. Kronfeldt. Application of Calixarene to High Active Surface-Enhanced Raman Scattering (SERS) Substrates Suitable for In-Situ Detection of Polycyclic Aromatic Hydrocarbons (PAHs) in Sea-Water. *Journal of Raman Spectroscopy*, 43(8): 1003 – 1009, 2012.

[Kwon *et al.*, 2012b] Y.H. Kwon, R. Ossig, A. Kolomijeca, F. Hubenthal, H.D. Kronfeldt. Naturally grown silver nanoparticle ensembles for 488 nm in-situ SERS/SERDS-detection of PAHs in water. Advanced Environmental, Chemical, and Biological Sensing Technologies IX, 8366, *Proceedings of SPIE*, 2012.

[Kwon *et al.*, 2012 c] Y.-H. Kwon, R. Ossig, A. Kolomijeca, F. Hubenthal, H.-D. Kronfeldt. Naturally grown silver nanoparticle ensembles for 488 nm in-situ SERS/SERDS-detection of PAHs in water. Advanced Environmental, Chemical, and Biological Sensing Technologies IX, 8366, *Proceedings of SPIE*, 2012.

[Lam and Ho, 1989] C.W.Y. Lam, K.C. Ho. Red tides in Tolo Harbor, Hong Kong. Red tides: Biology, environmental science and toxicology. *Elsevier* 49–52, 1989.

[LE, 2011] Law & Your environment[46]. Plan guide to environmental law, 2008-2011.

[Lee and Shim, 2007] B.M. Lee and G.A. Shim. Dietary exposure estimation of benzo [a] pyrene and cancer risk assessment. *Journal of Toxicology and Environmental Health* (A), 70(15-16):1391-1394, 2007.

[Long, 2002] D.A. Long, The Raman Effct: A Unified Treatment of the Theory of Raman Scattering by Molecules. John Willey & Sons Ltd., 2002.

[LUHNA, 2003] The LUHNA book. K.L. Cole, F. Stearns, G. Guntenspergen, M.B. Davis, K. Walker. Historical Landcover Changes in the Great Lakes Region[47], chapter 6, 2003.

[46] On line: http://www.environmentlaw.org.uk/rte.asp?id=111
[47] On line: http://landcover.usgs.gov/luhna/chap6.php

[MARS, 2013] The Monterey Accelerated Research System[48] - ocean cabled observatory, MBARI 1996-2013.

[MARUM, 2013] Center of Marine Environmental Science. University of Bremen[49], Germany. (last update) 2013.

[Maiwald *et al.*, 2009a] M. Maiwald, H. Schmidt, B. Sumpf, R. Güther, G. Erbert, H.-D. Kronfeldt, G. Tränkle. Microsystem Light Source at 488 nm for Shifted Excitation Resonance Raman Difference Spectroscopy. *Applied Spectroscopy*, 63, No. 11, 1283 – 1287, 2009.

[Maiwald *et al.*, 2009b] M. Maiwald, H. Schmidt, B. Sumpf, G. Erbert, H.-D. Kronfeldt. Microsystem light source at 671 nm for shifted excitation Raman difference spectroscopy. Advanced Environmental, Chemical, and Biological Sensing Technologies VI, 7312, *Proceedings of SPIE*, 2009.

[Maiwald *et al.*, 2009c] M. Maiwald, H. Schmidt, B. Sumpf, G. Erbert, H.-D. Kronfeldt, G. Tränkle. Microsystem 671 nm light source for shifted excitation Raman difference spectroscopy. *Applied Optics*, 48(15): 2789 – 2792, 2009.

[MBARI, 2013] Monterey Bay Aquarium Research Institute[50]. ROV Doc Ricketts. 1996 - 2013.

[MEECE, 2010] Marine Ecosystem Evolution in a changing environment[51]. European Seventh Framework Program, contract number: 2012085, 2010.

[Mogilevsky *et al.*, 2012] G. Mogilevsky, L. Borland, M. Brickhouse, A.W. Fountain III. Raman Spectroscopy for Homeland Security Applications. *Internationa Journal of Spectroscopy*, Id: 808079, 2012.

[Mulas *et al.*, 2006] G. Mulas, G. Malloci, C. Joblin, D. Toublanc. Estimated IR and phosphorescence emission fluxes for specific polycyclic aromatic hydrocarbons in the Red Rectangle. *Astronomy and Astrophysics*, 446 (2): 537, 2006.

[48] On line: http://www.mbari.org/mars/default.html
[49] On line: http://www.marum.de/en/Research.html
[50] On line: http://www.mbari.org/dmo/vessels_vehicles/Doc_Ricketts/Doc_Ricketts.html
[51] On line: http://www.meece.eu/

[Murphy *et al.*, 1997] T. Murphy, H. Schmidt, H. D. Kronfeldt. Detection of Chemicals in sea-water using Surface-Enhanced Raman Scattering (SERS). In Remote Sensing of Vegetation and Water and Standardization of Remote Sensing Methods, G. Cecchi, T. Lamp, R. Reuter, K. Weber, Editors, *SPIE*, 3107: 281-287, 1997.

[Murphy *et al.*, 1999] T. Murphy, H. Schmidt, H.D. Kronfeldt. Use of sol-gel techniques in the development of surface-enhanced Raman scattering (SERS) substrates suitable for in-situ detection of chemicals in sea-water. *Applied Physics*, 69: 147 – 150, 1999.

[NEPTUNE, 2013] The NorthEast Pacific Time-Series Undersea Networked Experiments [52]. Undersea observatory, Ocean Networks Canada, 2013.

[Nie and Emory, 1997] S. Nie and S.R. Emory. Probing Single Molecules and Single Nanoparticles by Surface-Enhanced Raman Scattering. *Science*, 275 (21): 1102-1106, 1997.

[NIEHS, 2011] The National Institute of Environmental Health Sciences. Report on Carcinogens, Twelfth Edition [53], 2011.

[NJDH, 1998] New Jersey Department of Health and senior services: Hazardous substances fact sheet: Acenaphthene[54], 1998.

[NJDH, 2008] New Jersey Department of Health and senior services: Hazardous substances fact sheet. Benz [a] Anthracene[55], 1998-2008.

[NJDH, 2001] New Jersey Department of Health and senior services: Hazardous substances fact sheet. Benzo [b] Fluoranthene[56], 1995-2001.

[NOAA, 2013]: National Oceanic and Atmospheric administration. National Ocean Report. Ocean Observations[57], USA, 2013.

[NOCS, 2013] National Oceanography Center[58]. Natural environment research Council, UK, 2013.

[52] On line: http://www.neptunecanada.ca/about-neptune-canada/
[53] On line: http://ntp.niehs.nih.gov/ntp/roc/twelfth/profiles/PolycyclicAromaticHydrocarbons.pdf
[54] On-line: http://nj.gov/health/eoh/rtkweb/documents/fs/2958.pdf
[55] On-line: http://nj.gov/health/eoh/rtkweb/documents/fs/0193.pdf
[56] On line: http://nj.gov/health/eoh/rtkweb/documents/fs/0208.pdf
[57] On line: http://coastwatch.noaa.gov
[58] On line: http://noc.ac.uk/

[NTP, 2001] National Toxicology Program: Department Of Health And Human Services. Report on carcinogens[59]. Twelfth edition, 2001.

[OSHA, 2007] United States department of Labor. OSHA: Occupational Safety and Health Administration. Phenanthrene[60], 2007.

[OSHA, 2012] United States department of Labor. OSHA: Occupational Safety and Health Administration. Pyrene[61], 2012.

[Ossig *et al.*, 2013] R. Ossig, A. Kolomijeca, Y.H.Kwon, F. Hubenthal, H.D. Kronfeldt. SERS signal response and SERS/SERDS spectra of fluoranthene in water on naturally grown Ag nanoparticle ensembles. *Journal of Raman Spectroscopy*, 44: 717-722, 2013.

[Pasport, a] Pasport GPS position sensor PS-2175[62]. Instruction manual 012-09919A.

[Pasport, b] Pasport Salinity sensor PS-2195[63]. Instruction sheet 012-10546A.

[Pepper *et al.*, 1996] I.L. Pepper, C.P. Gebra, M.L Brusseau. Pathogens in the environment. Pollution Science. Academic Press NY: 279-299, 1996.

[Peron *et al.*, 2010] O. Peron, E. Rinnert, F. Colas, M. Lehaitre, C. Compere. First Steps of in Situ Surface-Enhanced Raman Scattering During Shipboard Experiments. *Applied Spectroscopy*, 64(10): 1086-1093, 2010.

[Pfannkuche *et al.*, 2012] J. Pfannkuche, L. Lubecki, H. Schmidt, G.Kowalewska, H.-D. Kronfeldt. The use of surface-enhanced Raman scattering (SERS) for detection of PAHs in the Gulf of Gdańsk (Baltic Sea). *Marine Pollution Bulletin*, 64(3): 614 – 626, 2012.

[Prien *et al.*, 2006] R. Prien, D.P. Connelly, C.R. German. In situ chemical analyser for the determination of dissolved Fe (II) and MN (II). *Ocean Sciences Meeting*, Honolulu, HI, USA. OS44B-06, 2006.

[Raman, 1930] C. V. Raman. the molecular scattering of light. Nobel lecture[64], 1930.

[59] On-line: http://ntp.niehs.nih.gov/ntp/roc/twelfth/profiles/PolycyclicAromaticHydrocarbons.pdf
[60] On-line: http://www.osha.gov/dts/chemicalsampling/data/CH_261000.html
[61] On-line: http://www.osha.gov/dts/chemicalsampling/data/CH_265100.html
[62] On-line: http://www.conatex.com/mediapool/betriebsanleitungen/BAE_1077052.pdf
[63] On-line: http://www.conatex.com/mediapool/betriebsanleitungen/BLE_1124103.pdf
[64] On-line: http://www.nobelprize.org/nobel_prizes/physics/laureates/1930/raman-lecture.pdf

[Raman and Krishnan, 1928] C.V. Raman, and Krishnan. A new type of secondary radiation. *Nature*, 121(3048): 501-502, 1928.

[RMD] Ravatite Mineral Data[65].

[Rosie *et al.*, 2004] N.L. Rosie, C.L. Rosie, J.F. Boyle, P.G. Appleby. Lake−sediment evidence for local and remote sources of atmospherically deposited pollutants on Svalbard. *Journal of Paleolimnology*, 31: 499–513, 2004.

[Sapota *et al.*, 2009] G. Sapota, B. Wojtasik, D. Burska, K. Nowinski. Persistent Organic Pollutants (POPs) and Polycyclic Aromatic Hydrocarbons (PAHs) in surface sediments from selected fjords, tidal plains and lakes of the North Spitsbergen. *Polish Polar Research*, 30 (1): 59-76, 2009.

[SCRIPPS, 2013] SCRIPPS Institution of Oceanography[66]. UC San Diego, USA, 2013.

[Schmidt et al, 2001] H. Schmidt, D.P Kaiser, M. Maiwald. Method for generating and for detecting a Raman spectrum. Patent 20120162641.

[Senkan and Castaldi, 2003] S. Senkan and M. Castaldi. Combustion. Ullmann's Encyclopedia of Industrial Chemistry, Wiley-VCH. Weinheim, 2003.

[SENSEnet, 2013] International sensor developing network[67]. European Seventh Framework Program, project ID 237868, 2009-2013.

[SEPA] Scottish Environment Protection Agency. Pollution Release Inventory. Benzo [ghi] Perylene[68].

[Soehl and Yi Wu, 2012] A. Soehl, and C. Yi Wu. Great Lakes Commission. Minnesota Pollution Control Agency Assessment of Benzo(a)pyrene[69], 2012.

[Shreve *et al.*, 1992] A.P. Shreve, N.J. Cherepy, and R.A. Mathies. Effective rejection of fluorescence interference in Raman spectroscopy using a shifted excitation difference technique. *Applied Spectroscopy*, 46: 707-711, 1992.

[65] On-line: http://webmineral.com/data/Ravatite.shtml
[66] On line: http://sio.ucsd.edu/
[67] On line: http://www.eu-sensenet.net/
[68] On-line: http://apps.sepa.org.uk/spripa/Pages/SubstanceInformation.aspx?pid=236
[69] On-line: http://www.epa.gov/ttnchie1/conference/ei20/session10/asoehl_pres.pdf

[Sowoidnich and Kronfeldt, 2012a] K. Sowoidnich, and H.-D. Kronfeldt. Shifted excitation Raman difference spectroscopy at multiple wavelengths for in-situ meat species differentiation. *Applied Physics B*, 108(4): 975–982, 2012.

[Sowoidnich and Kronfeldt, 2012b] K. Sowoidnich, H.D. Kronfeld. Fluorescence rejection by shifted excitation Raman difference spectroscopy at multiple wavelengths for the investigation of biological samples. *ISRN Spectroscopy*, Id: 256326, 2012.

[Sowoidnich *et al.*, 2012] K. Sowoidnich, H. Schmidt, H.-D. Kronfeldt, F. Schwägele. A portable 671 nm Raman sensor system for rapid meat spoilage identification. *Vibrational Spectroscopy*, 62: 70 – 76, 2012.

[TDN, 1998] U.S. Department of Health and Human Services. Toxicology Data Network. Benzo [ghi] Perylene[70], 1998.

[UNEP, 2004] United Nation Environment Program. Guidance for a Global Monitoring Program for persistent organic Pollutants. UNEP Chemicals, Geneva, Switzerland. 105 p., 2004.

[UNESCO, 1992] United Nations Educational, Scientific and Cultural Organization. Report of the twenty-second session[71], Vienna, 9-13 March 1992.

[VENUS, 2013] Victoria Experimental Network Under the Sea[72]. Coastal network, part of the Ocean Networks Canada Observatory, 2013.

[Vo-Dinh, 1998] T. Vo-Dinh. Surface-enhanced Raman spectroscopy using metallic nanostructures. *Trends in analytical chemistry*, 17(8): 557-582, 1998.

[Wenzl *et al.*, 2006] T. Wenzl, R. Simon, J. Kleiner, and E. Anklam. Analytical methods for polycyclic aromatic hydrocarbons (PAHs) in food and the environment needed for new legislation in the European Union. *Trends in Analytical chemistry*, 25(7):716-725, 2006.

[West, 2006] L. West. World Water Day: A Billion People Worldwide Lack Safe Drinking Water. 2nd UN World Water Development Report, March 26, 2006.

[70] On-line: http://toxnet.nlm.nih.gov/cgi-bin/sis/search/a?dbs+hsdb:@term+@DOCNO+6177
[71] On line: IMO/FAO/UNESCO/WMO/WHO/IAEA/UN/UNEP Joint Group of Experts on the Scientific Aspects of Marine Pollution. Session
[72] On-line: http://venus.uvic.ca/

[White, 2008] S. N. White. Laser Raman spectroscopy as a technique for identification of seafloor hydrothermal and cold seep minerals. *Chemical Geology*, 2008.

[White, 2010] S.N. White. Qualitative and Quantitative analysis of CO2 and CH4 dissolved in water and seawater using Laser Raman Spectroscopy. *Applied Spectroscopy*, 64: 819-827, 2010.

[WHO, 2002] World Health Organization. Some Traditional Herbal Medicines, Some Mycotoxins, Naphthalene and Styrene. *IARC: Monographs on the Evaluation of Carcinogenic Risks to Humans*, 82 : 367, 2002.

[WHOI, 2013] Woods Hole Oceanographic Institution[73]. Remotely Operated vehicle Jason / Media, 2013.

[Wotton, 2012] R. S. Wotton. Life in Water. An Internet Book[74]. UCL Division of Biosciences, 2001-2012.

[Zeman and Schatz, 1987] E. J. Zeman, and G. C. Schatz. An accurate electromagnetic theory study of surface enhancement factors for Ag, Au, Cu, Li, Na, Al, Ga, In, Zn, and Cd. *Physical Chemistry*, 91(3), 634-643, 1987.

[Zielinski *et al.*, 2001] O. Zielinski, R. Andrews, J. Gobel, M. Hanslik, T. Hunsanger, R. Reuter. Operational airbone hydrographic laser remote sensing. Lidar remote sensing of Land and Sea. *EARSel Proceedings*, 1: 53-60, 2001.

[Zelinski and Brehm, 2007] O. Zelinski, R.Brehm. Hyperspectral multi-parameter sensing for marine environmental security. *International Ocean Systems*, 11(6):19-21, 2007.

[Zielinski *et al.*, 2009] O. Zielinski, J.A. Busch, A.D. Cembella, A. Kohler. Detecting marine hazardous substances: A review on sensors for pollution, toxins and pathogens. *Ocean science*, 5(1)-21, 2009.

[Zielinski *et al.*, 2006] O. Zielinski, T. Hengstermann, N. Robbie. Detection of oil spills by airbone sensors. Springer. Berlin Hidelberg NY: 255-271, 2006.

[73] On line: http://www.whoi.edu/page.do?pid=8423
[74] On line: http://www.ucl.ac.uk/~ucbt212/

Appendix I

PAHs and biphenyl

Nr.	Name Abbreviation Formula	Production/use/comments	Danger to health/ Disposal method
1	Acenahpthene Acenap $C_{12}H_{10}$	**Commercially**: Coal tar consists of about 0.3% of this compound. **Used** on a large scale to prepare naphthalic anhydride, which is a precursor to dyes and optical brighteners [Griesbaum *et al.*, 2002] **has been found** in cigarette smoke, in the exhaust from automobiles and in wood preservatives [EPA, 2001b]	**Health:** Irritate skin, eyes, nose, throat, longs. May effect liver and kidneys [NJDH, 1998] **Disposal**: rotary kiln incineration at t = 820-1.600^{0}C
2	Acenaph- thylene Aceylene $C_{12}H_8$	**Commercially**: occurs as about 2% of coal tar. It is produced industrially by dehydrogenation of acenaphthene [Griesbaum *et al.*, 2002] **Used** to make dyes, plastics and pesticides [EPA, 2001a]	**Health:** No data on human carcinogenicity, inadequate data in animal carcinogenicity. Positive results in a Salmonella typhimurium forward mutation assay [EPA, 2012a]. **Disposal**: rotary kiln incineration at t = 820-1.600^{0}C
3	Anthracene Ant $C_{14}H_{10}$	**Commercially**: from coal tar **In laboratory**: by Elbs reaction **Used**: mainly as precursor to dyes [Collin *et al.*, 2006], it is organic semiconductor; also used in wood preservatives, insecticides, and coating materials Found in space [Mulas *et al.*, 2006]	**Health:** No data on human cancerogenicity, inadequate data in animal. Negative results in most of DNA damage /mutation tests [EPA, 2012d] **Disposal**: controlled incineration
4	Benz(a)-	It is not produced **commercially**, but is **used** in research laboratories. It is also	**Health:** Carcinogen to laboratory mice. Cause liver

	Anthracene BaA $C_{20}H_{10}$	**found** in Coal Tar, roasted coffee, smoked foods, and automobile exhaust, and is formed as an intermediate during chemical manufacturing [NJDH, 2008]	cancer and lung tumors [NTP, 2001] Probably carcinogen in humans [NJDH, 2008] **Disposal**: rotary kiln incineration at t = 820-1.600^{0}C; fluidized-bed incineration at t = 450-980 ^{0}C; liquid injection incineration at t=650-1.600 ^{0}C; can be oxidized
5	Benzo(b)- Fluoranthene BbF $C_{20}H_{12}$	**Can be** extracted from coal tar pitch [NJDH, 2001] **Produced** by incomplete combustion or pyrolysis of organic matters, especially fossil fuels and tobacco [IPCS, 1999]	**Health:** Is probable carcinogen in humans. Couse lung, liver and skin cancer in animals [NJDH, 2001] **Disposal**: rotary kiln incineration at t = 820-1.600^{0}C
6	Benzo(a)- Pyrene BaP $C_{20}H_{12}$	**Main source** of atmospheric BaP is residential wood burning [Soehl and Yi Wu, 2012]; also found in coal tar, in automobile exhaust fumes(especially from diesel engines), in all smoke resulting from the combustion of organic material (including cigarette smoke), and in charbroiled food. Cooked meat products, have been shown to contain up to 4 ng/g of baP [Kazerouni *et al.*, 2002] and up to 5.5 ng/g in fried chicken [Lee and Shim, 2007] and 62.6 ng/g in overcooked charcoal barbecued beef [Aygun and Kabadayi, 2005]	**Health:** Birth defects on mice, decrease of body weight, damage of skin, body fluids and immune system [ATSDR, 1990; HSDB, 2001]. Probable cancer-causing agent in humans. There is some evidence that it causes skin, lung, and bladder cancer in humans and in animals [DPH, 2009] **Disposal**: rotary kiln incineration at t = 820-1.600^{0}C; fluidized-bed incineration at t = 450-980 ^{0}C; can be oxidized
7	Benzo(g,h,i)-perylene BgP $C_{22}H_{12}$	Small amounts are intentionally **manufactured**. It is extracted from coal tar to be used in dyes. It can be found in creosote, tar paints, waterproof membranes and other products. Is **released** to the environment when combustion is (from vehicle exhausts and domestic wood and coal fires) incomplete,	**Health:** No data are available in humans. Inadequate evidence of carcinogenicity in animals [TDN, 1998; Faust, 1994] **Disposal**: can be decontaminated by carbon adsorption

		from industrial effluents, municipal wastewater treatment facilities, waste incinerators and aluminium smelting. Trace amounts are found in cigarette smoke. **Naturally** from volcanoes and forest fires, but the amounts are very small [SEPA]	
8	Benzo(k)- Fluoranthene BkF $C_{20}H_{12}$	**Not commercially** used or produced. content in the environment usually resulting from the incomplete combustion or pyrolysis of organic matters, especially fossil fuels and tobacco[EPA, 2012e]	**Health:** Probably human carcinogen. Animal cancerogen. Mutagen for prokaryotic cells [EPA, 2012e] **Disposal**: can be oxidized
9	Chrysene Chr $C_{18}H_{10}$	**Formed** in small amounts during the burning or distillation of coal, crude oil, and plant material	**Health:** Chrysene causes cancer in laboratory animals [ECO-USA, 1990; GSI, 2010] **Disposal**: rotary kiln incineration at t = 820-1.600^{0}C; fluidized-bed incineration at t = 450-980 ^{0}C; can be oxidized
10	Fluoranthene Fla $C_{16}H_{10}$	**Commercially**: from coal tar pitch	**Health:** No data on human toxicity. Positive data on animal sub chronic toxicity and reproduction functions. **Target organs**: kidney, liver [Faust, 1993] **Disposal**: rotary kiln incineration at t = 820-1.600^{0}C; fluidized-bed incineration at t = 450-980 ^{0}C
11	Fluorene Flu $C_{13}H_{10}$	**Commercially**: from coal tar **In laboratory**: by dehydrogenation of diphenylmethane [Griesbaum *et al.*, 2002] **Used** to make dies, plastic, pesticides [EPA, 1990]	**Health:** No data on human cancerogenicity, inadequate data in animal cancerogenicity. produced positive results in a DNA damage assay (strand-break assay) in L5178Y/mouse lymphoma cells [EPA, 2012c]

12	Naphthalene Nap $C_{10}H_8$	**Commercially:** Most naphthalene is derived from coal tar. During 1960-1990 produced from heavy petroleum fractions. Approximately 1M tons are produced annually [Collin *et al.*, 2003] **Naturally:** by endophytic fungus *Muscodor albus, Muscodor vitigenus* [Daisy *et al.v*, 2002] **Has been found** in meteorites.	**Health:** May damage or destroy red blood cells. Classifies by IARC [WHO, 2002] as possibly carcinogenic to humans and animals (Group 2B). Can causes cataracts and hemolytic anemia
13	Phenanthrene Phe $C_{14}H_{10}$	**Naturally**: Ravatite is a natural mineral consisting of phenanthrene [RMD]	**Health:** Irritation-Eyes, Nose, Throat, Skin---Mild (HE16) **Affected Organs:** Skin; multiple tumor sites in animals (e.g., mammary, stomach, lung, skin) [OSHA, 2007]
14	Pyrene Pyr $C_{16}H_{10}$	**Commercially**: from coal tar Can be produced in a wide range of combustion conditions. For example, automobiles produce about 1 µg/km [Senkan and Castaldi, 2003]. **Used** commercially to make dyes and dye precursors Found in space [Mulas, 2006]	**Health:** Irritation-Eyes, Skin---Mild (HE-16) OSHA, 2012] **Disposal**: should be atomized in incinerator
15	Biphenyl Bip $(C_6H_5)_2$	**Commercially**: coal tar, crude oil, and natural gas **Sources in the environment**: production and processing plants, citrus fruits or wood preserving facilities, municipal waste disposal [Boehncke *et al.*, 1999]	**Health:** Irritant (Xi); Dangerous for environment (N); Mildly toxic. **Disposal**: can be biodegraded: main pathway in troposphere is the reaction with hydroxyl radicals. [Boehncke *et al.*, 1999]

Appendix II

All experimental tasks for JCR Arctic cruise

Experimental conditions:

Laser Power: 18 mW (275 mA, t = 25^0 C), Flow rate Nr 1 = 0.05 ml/s

Integration Time: average from 10 spectra x 0.3 s, 0.5 s, 1 s, 5 s, 10 s, 25 s, 35 s, 50 s.

Techniques applied:

- Conventional Raman
- SERS
- 25 from 40 of Ag,DMCX:MTEOS substrates

Experiments:

- Substrate stability test
  - 5 substrates were stored in a fridge in real sea water/sweet water for time period of around 2 weeks. Measurements done before and after storage.
  - Substrate was exposed to real sea water for 24 hours (without taking it out of flow cell). The measurements done in 1^{st} hour, in 10 h and after 24 h.
- Laser power dependence for RAMAN measurements
  - 12 mW (265 mA)
  - 18 mW (275 mA)
  - 24 mW (285 mA)
  - 30 mW (295 mA)
  - 36 mW (305 mA)
  - 42 mW (315 mA)
- Water turbulence dependence (flow rate change)
  - flow rate Nr 1 = 0.05 ml/s, Nr 5 = 2.5 ml/s

Surface water samples:

1: Location: from $78^0$38.74443 N; $009^0$17.2733 E to $78^0$33.3059N; $009^0$28.6100 E
Temperature: 5^0C, Salinity: 35 ‰
2: Location: $78^0$33.9485 N; $009^0$34.0791 E; (T = 3.8 ^{0}C, Sal. = 35 ‰)

3: Location: $78^0$32.6458 N; $009^0$11.8842 E; (T = 5.37 ^{0}C, Sal. = 35 ‰)
4: Location: 78^0 33.6100 N; 009^0 33.1100 E; (T = 5.57 ^{0}C, Sal. = 35 ‰)
5: Location: $78^0$29.1230 N, $010^0$14.562 E; (T = 3^0C, Sal. = 35 ‰)
6: Location: $78^0$34.3301 N, $010^0$13.4279 E; (T = 3^0C, Sal. = 35 ‰)
7: Location: $78^0$33.7700 N, $010^0$10.4700 E; (T = 3^0C, Sal. = 35‰)
8: Location: $78^0$33.6399 N, $009^0$59.1944 E; (T = 3^0C, Sal. = 35‰)
9: Location: 78^o33.4527 N; $010^0$03.9969 E; (T = 4.5^0C, Sal.=35‰)
10: Location: 78^o33.4527 N; $010^0$03.9969 E; (Sal. = 35‰)
11: Location: $78^0$34.5101N; $010^0$10.8581 E; (T = 4.5^0C, Sal = 35‰)
12: Location: $78^0$34.4800 N; $101^0$10.5500E (Sal. = 35‰)
13: Location: $78^0$35.0605 N; $010^0$10.3946 E (Sal. = 35‰)

Mud Samples:

1. Sediment name: **JR 253-26-BC04**
Location of mad 1: **$78^0$55.899 Latitude; $009^0$53.483 Longitude; 339,61 m Depth**
Location of surface water: $78^0$36.2730 N; $009^0$31.7442 E

2. Name: **JR 253 – 43 – BC06**
Location mad 2: **$78^0$59167 N; $9^0$38312 E; depth: 407.3 m**
Surface water Location: $78^0$37.1333 N, $009^0$19.1777 E

3. Name: **JR 253-49-BL08**
Location mad 3**: $78^0$59874 N; $9^0$44384 E; depth: 375.45 m**

4. Name: **JR 253 -64 - BC10**
Location of mad 4: **$78^0$61773 N; $9^0$42273 E; depth: 307.7 m**
Real Water location: $78^0$37.0617 N, $009^0$18.1350 E

5. Name: **JR 253 - 69 – BC11**
Location of mad 5**: $78^0$59167 N; $9^0$38312 E; depth: 407.3**

6. Name: **JR – 253 – 73 – BC12**
Location of mad 6: **$78^0$61767 N; $009^0$3027 E, depth: 439.74 m**
Real Water location: $78^0$34.2900 N; $010^0$11.5000 E

Real sea water spiked with PAHs samples:

<u>Spiking PYRENE</u>

Water Location: 78^0 33.6100 N; 009^0 33.1100 E

Pyrene concentrations: 0.25 nM, 0.5 nM, 1 nM, 2 nM, 4 nM, 8 nM, 12 nM, 20 nM, 100 nM, 200 nM, 400 nM.

Spiking ANTHRACENE

Water Location: $78^0$34.2556N, $009^0$38.3196 E

Concentrations: 0.3 nM, 0.75 nM, 1.5 nM, 3 nM, 7.5 nM, 15 nM, 30 nM, 75 nM, 150 nM

Spiking FLUORENTHENE

Water Location: $78^0$34.2319 N, $9^0$25.5464 E

Concentrations: 1 nM, 2 nM, 4 nM, 8 nM, 12 nM, 20 nM, 100 nM, 200 nM, 600 nM

PAH solution mixes:

Water location: $78^0$38.2371 N; $009^0$18.1350 E

- PYR 400 nM (50) : ANT 150 (50) nM
- PYR 0,25 nM (50) : ANT 0,3 nM (50)
- PYR 8 nM (50) : ANT 7,5 nM (50)
- PYR 400 nM (50) : FLO 600 nM (50)
- PYR 0,25 nM (50) : FLO 1 nM (50)
- PYR 8 nM (50) : FLO 8 nM (50)
- FLO 600 nM (50) : ANT150 nM (50)
- FLO 1 nM (50) : ANT 0,3 nM (50)
- FLO 8 nM (50) : ANT 7,5 nM (50)
- PYR 400 nM (33) : FLO 600 nM (33) : ANT 150 nM (33)
- PYR 0,25 nM (33) : FLO 1 nM (33) : ANT 0,3 nM (33)
- PYR 8 nM (33) : FLO 8 nM (33) : ANT 7,5 nM (33)

Appendix III

Sensor housing (manufactured by “Develogic” GmbH)

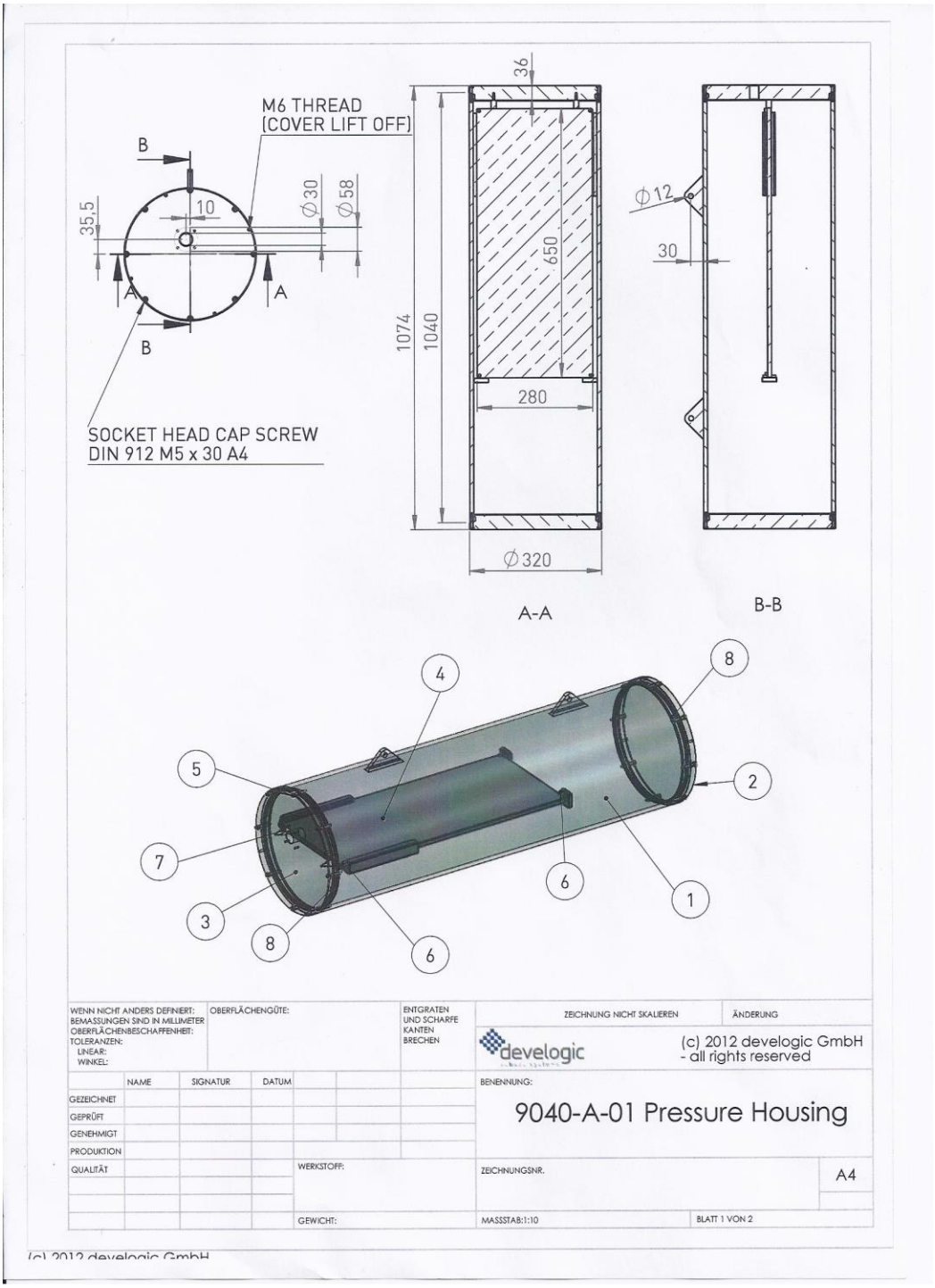

POS.-NR.	NAME	DESCRIPTION	AMOUNT
1	Pressure Housing	Material EN AW 6082	1
2	Cover Plate Rear	Material EN AW 6082	1
3	Cover Plate Front	Material EN AW 6082	1
4	Plate	Material EN AW 6082	1
5	DIN 912 M5 x 30 A4	Socket Head Cap Screw Cover Fastening	16
6	DIN 912 M6 x 10 A2	Socket Head Cap Screw Plate Stopper	8
7	Rubber Dampers		2
8	O-Ring	70 NBR 278,77 x 6,99	2
9	Shackle	WLL 3/4T	2
10	DIN 912 M6 x 30 A2	Socket Head Cap Screw Cover Lift Off	4

WENN NICHT ANDERS DEFINIERT:
BEMASSUNGEN SIND IN MILLIMETER
OBERFLÄCHENBESCHAFFENHEIT:
TOLERANZEN:
LINEAR:
WINKEL:

OBERFLÄCHENGÜTE:

ENTGRATEN UND SCHARFE KANTEN BRECHEN

ZEICHNUNG NICHT SKALIEREN

ÄNDERUNG A-01

develogic

	NAME	SIGNATUR	DATUM
GEZEICHNET			
GEPRÜFT			
GENEHMIGT			
PRODUKTION			
QUALITÄT			

BENENNUNG:

INCLUDED IN DELIVERY

WERKSTOFF:

ZEICHNUNGSNR.

A4

GEWICHT:

MASSSTAB:1:5

BLATT 2 VON 2

Appendix IV

Circuit diagram (designed by Alex Strange)

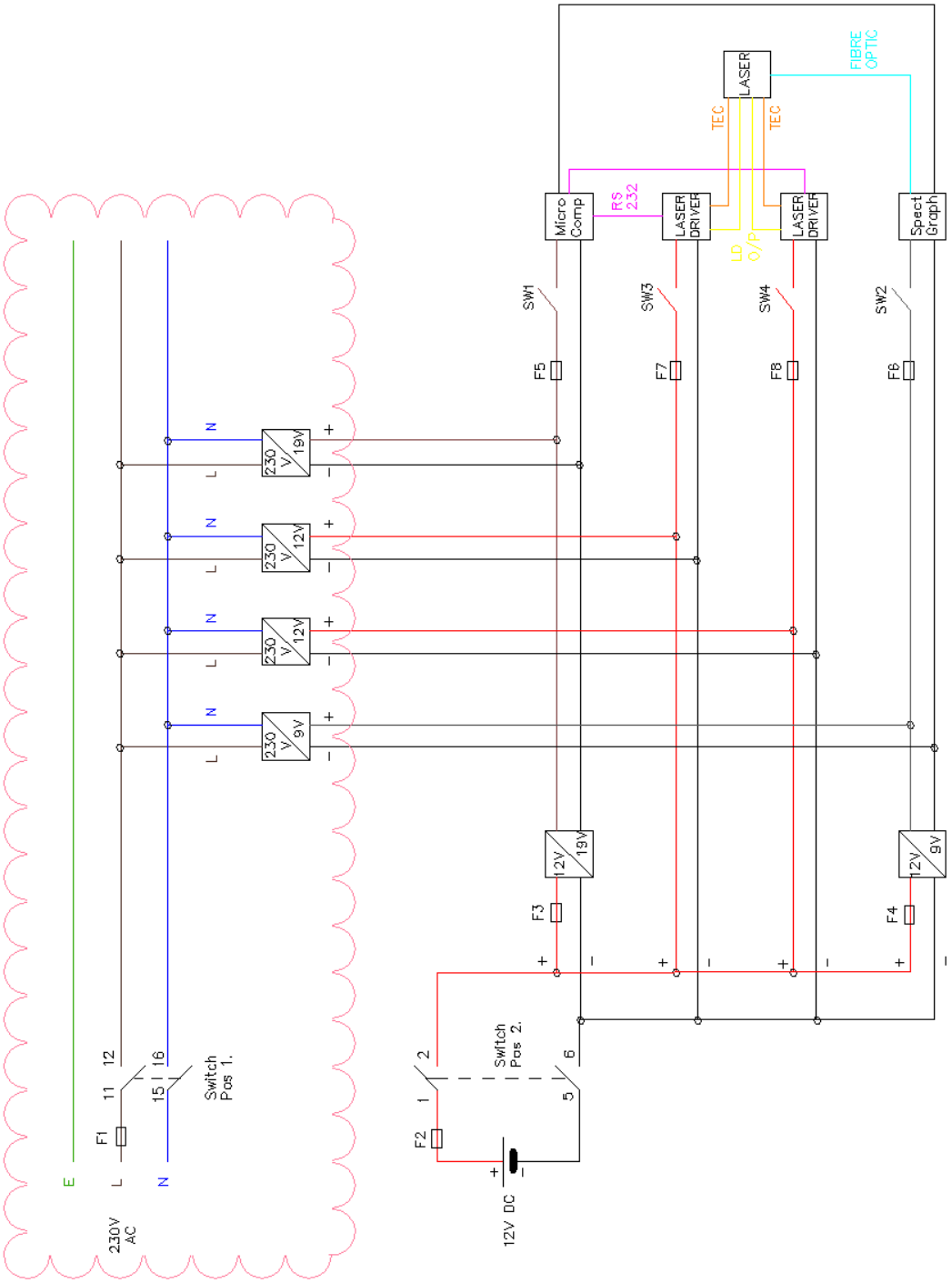

Appendix V

Wiring diagram (designed by Alex Strange)

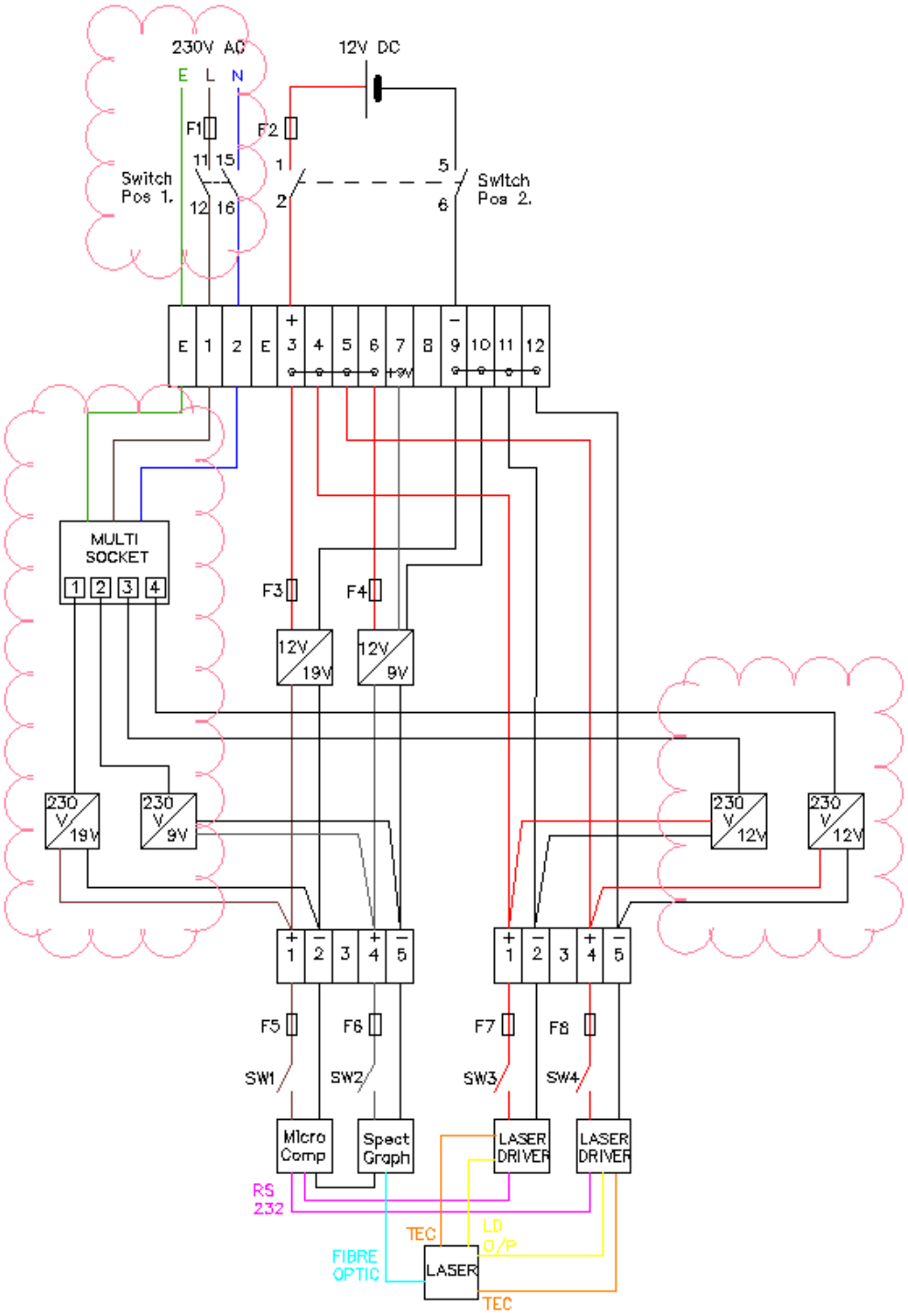

Appendix VI

Water samples

The pacific Ocean, West coast: Hawaii; the coast of CA, USA								
Sample, Nr	date	Temperature, ^{o}C	Salinity, ‰	GPS, N	GPS, W	Remarks/ Nearest address	Vibrations detected, cm^{-1}	Possible PAHs or biphenyl (± 11 cm^{-1})
1	26.06.11	26.50	35	20.9100	156.6890	Hawaii	491	Bip
2	27.06.11	16.81	35	37.8198	122.3639	SF	n/d[1]	
3	29.06.11	16.11	35	36. 4836	121.4735	7400 Sandholdt Rd; Moss Landing, CA 95039	**457** 491	Acenap; Acetylene Bip
4	30.06.11	13.15	35	35.5900	121.2953	65199 HWY 1; Big Sur, CA 93920	**461** 491	Acnap Bip
5	30.06.11	14.64	35	35.4133	121.1734	16422 HWY 1; San Simeon, CA 93452	453 1119	Aceylene n/a[2]
6	01.07.11		35	35.27.47	120.5793	5378 HWY 1; Cayucos, CA 93430	**459** **936** **1175** 1284 1463 1477 1518 1637 **1755**	Acenap n/a n/a n/a n/a n/a n/a n/a n/a
7	01.07.11		35	35.2189	120.5120	711 Embarcadero Rd; Morro Bay CA 93442	451 565 718 **1753**	n/a n/a n/a n/a
8			35	34.2472	119.4131	9 E Cabrillo Blvd; Santa Barbara, CA 93101	n/d	
9			35	34.0236	118.3581	19328 Pacific Coast Hwy; Malibu, CA 90265	n/d	
10			35	33.1246	117.2362	1399 Harbor Dr; N Oceanside, CA 92054	n/d	
11			35	32.5066	117.1674	622 Coast Blvd S, La Jolla, CA 92037	n/d	

[1] n/d – not detected
[2] n/a – not applicable

The Atlantic Ocean, East coast and Great Lakes, NY, USA								
Nr	*Date*	***Temperature***	***Salinity***	***N***	***W***	*remarks*		
1	15.04.11	15.92	5.5	39.6938	74.1443	Long Branch Beach, NJ	442 564 711 1113 1138 1257 1323 1409 1475 1518 1750	n/a n/a n/a n/a Bip n/a Acetylene, Acenap Acetylene, Acenap n/a n/a n/a
2	15.04.11	8.99	5.9	39.3474	74.45.29	Atlantic City, NJ	**458 !** 493 1756	Acetylene, acenap Bip n/a
3	16.04.11	12.48	0	39.9623	75.1810	Philadelphia, PA	1561 1755	n/a n/a
4	17.04.11	8.11	4.5	41.0012	73.6465	Port Chester, CT	641 1091 1384 1529 1566 1658 1751	n/a Fla n/a n/a n/a n/a n/a
5	17.04.11	8.46	5.5	41.0521	73.4689	Noroton, CT	459 525 574 612 818 1259 1296 1529 1574 1752	Acetylene, Acenap n/a n/a n/a Phe n/a n/a n/a n/a n/a
6	17.04.11	8.44	5.0	41.2235	72.9950	Woodmond, CT	450 662 682 1248 1280 1358	Acetylene Acetylene n/a n/a n/a Acenap, Bip

							1432 1458 1505 1574 **1753** 1796	n/a n/a n/a n/a n/a n/a
7	17.04.11	11.64	0	41.4987	71.5649	Barbers Pond, RI	**1755**	n/a
8	17.04.11	12.08	4.8	41.6581	70.8084	Matforpoisett, MA	**457** 489	Acetylene, Acenap Bip
9	19.04.11	7.88	6.8	41.5268	70.6757	WHOI, MA	670 1149	n/a n/a
10	19.04.11	7.85	7.3	42.3340	71.0224	Boston, MA	**457**	Acetylene, Acenap
11	21.04.11	4.87	0	42.8411	78.8593	Buffalo NY **Lake Erie**. Second last (before the North Atlancic ocean) one of the five great leaks. Splits to Welland Canal and Niagara river-both go to Lake Ontario	n/d	
12	22.04.11	4.49	0	43.0774	79.0661	Niagara Falls, NY;**Upper Niagara River** connecting Lake Erie with lake Ontario	1252 1475 1556	n/a n/a Nap
13	22.04.11	4.03	0	43.1602	79.0447	Art Park, Lewiston, NY **Bottom Niagara River**	n/d	
14	22.04.11	5.13	0	43.2646	79.0589	Old Fort Niagara, Youngstown, NY; **Lake Ontario**. Last one from five great lakes connected with St. Lawrence seaway go to the North Atlantic Ocean	n/d	
15	23.04.11	9.09	0	43.1719	78.6921	Lockport Cave, NY Water from the **cave** (comes from Erie canal) but must be filtered (?)	664 774 796 832 920 974 1202 1236 1373 1531	Fla n/a Acetylene, Acenap; Fla Acenap n/a n/a n/a n/a Nap;Fla n/a
16	23.04.11	8.35	0	43.1724	78.6912	Lockport, NY **Erie**	n/d	

						canal		
17	02.05.11	11.73	4.2	40.7392	74.0108	NYC (mid. Manhattan); **Hudson river**	786 1113 1149 1278 1382 1412 1434 1480 1503 **1582** 1615 1655	Fla n/a Pyr Bip n/a Acetylene, Acenap; Fla Fla n/a n/a Fla , Bip n/a n/a
18	02.05.11	11.79	5.6	40.715	74.0161	NYC (downtown Manh.)**Upper NY Bay**	406 719 752 786 932 1093 1124 1199 1534 **1744** 1772	n/a n/a Nap n/a n/a Fla n/a Phe; Bip n/a Flu n/a
The Norwegian Sea, Svalbard Island, Norway								
Nr	*Date*	***Temperature***	***Salinity***	***N***	***E***	*Water type/remarks*		
1	27.07.11	3.22	0	78.1989	15.5783		1300	Flu
2	27.07.11	2.03	0	78.2015	15.8972	Svalbard, Water stock	666 692 758 842 932 1122 1150 1175 1230 1254 1353 1380 1412 1434 1474 1531	Fla n/a n/a n/a n/a n/a n/a n/a Pyr Fla Acenap; Phe n/a Fla; Phe Fla n/a n/a

							1590	Acetylene; Fla
3	02.08.11	4.93	2.0	78.2254	15.6332	Svalbard, power plant	587 616 643 1051 1211 1540	Pyr n/a n/a Acetylene; Pyr n/a Flu
4	05.08.11	5.11	35	78.3874	9.1727	Cruise: Raman real water	540 586 752 1584 1968	Phe; Acetylene, Acenap Pyr n/a n/a n/a
4'	05.08.11	4.19	35	78.3330	9.2861	Cruise: Raman real water	n/d	
5	06.08.11	3.79	35	78.3394	9.3407	Cruise: SERS real water	383 540 580 645 738 885 967 1199 1263 1324 1416 1506	n/a Phe; Acetylene, Acenap Pyr Acenap Bip n/a Acenap Phe; Bip Bip; Fla Acetylene, Acenap Acetylene, Acenap; Phe; Fla n/a
6	06.08.11	5.79	35	78.3264	9.1188	Cruise: SERS real water	489 1164 1968	Bip n/a n/a
7	07.08.11	27.41	35	78.3627	9.3174	Cruise: Raman real water	n/d	
8	08.08.11	19.30	35	78.3627	9.3174	Cruise: SERS sediment water	612 1370 1742	n/a Nap; Fla Flu
9	08.08.11	5.49	35	78.3361	9. 3311	Cruise: SERS real water	662 782 1373 1417	Fla Fla Nap; Fla Fla;Phe;

								Aceylene
10	09.08.11	4.06	35	78.5916	9.3831	Sediment	**459**	Acetylene, Acenap;
10	09.08.11		35	78.3713	9.1917	Sediment/filtred	n/d	
10'	09.08.11		35	78.3713	9.1917	Cruise: SERS real water	n/d	
11	10.08.11		35	78.5987	9.4438	Sediment 3	566 597 912 1128 1238 1312 1392 1431 1608	n/a Pyr n/a n/a Pyr n/a Pyr n/a Phe; Pyr
12	10.08.11	2.50	35	78.2912	10.1456		n/d	
13	12.08.11	3.08	35	78.3433	10.1342		n/d	
14	1308.11		35	78.3706	9.1813	Sediment 4	440 566 597 800 912 1124 1154 1172 1236 1296 1312 1390 1431 1610	n/a n/a Pyr n/a n/a n/a n/a n/a Pyr n/a n/a Pyr n/a Pyr
14	13.08.11		35	78.6177	9.4227	Sediment 4	442 816 1155 1197	n/a Phe n/a Phe; Bip
15	14.08.11	4.52	35	78.3345	10.0399		n/d	
16	17.08.11	4.49	35	78.5916	9.3831	Sediment 5	**457 !**	Acetylene, Acenap
16			35	78.3451	10.1085	Sediment 4, filtred	666 904 1083 1159 1446 1606	Fla n/a Fla n/a Fla Phe; Pyr; Fla
16	17.08.11	4.49	35			(17.08)	n/d	
17	17.08.12		35	78.61767	9.3027	Sediment 6	597 1124	n/a n/a

							1172 1238 1297 1654 1745	n/a n/a n/a n/a Flu
17	17.08.12		35	78.34.2900	10.1150	Sediment 6, filtred	n/d	
18	17.08.12		35	78.34.4800	10.1055		n/d	
19	18.08.12		35	78.35.0605	10.1039		562 597 1084 1286 1523 1533	n/a n/a n/a n/a n/a n/a
Mine 7	22.08.11		0	78.1720	15.9791	Svalbard	595 1050	Pyr Pyr
Drinking Water	22.08.11		0	78.2063	15.7947	Svalbard	530 658 788 924 1355 1384 1433 1497	n/a Acetylene, acenap Acenap; Fla n/a Acenap; Bip; Phe n/a n/a n/a
last	22.08.11	7.84	1.9	78.2306	15.5803	Svalbard	433 459 524 609 947 1113 1486	n/a Acetylene, Acenap n/a n/a n/a n/a n/a
The Mediterranean Sea, Barcelona, Spain; Banyuls-Sur-Mer, France								
Nr	*Date*	***Temperature***	***Salinity***	***N***	***E***	*remarks*		
1	29.02.12	9.96	35	42.5256	3.0857	Collioure	n/d	
2	01.03.12	10 (±1)	35	42.4803	3.1336	Banyuls	n/d	
3	01.03.12	10 (±1)	35	42.48172	3.1332	Banyuls	n/d	
4	01.03.12	10 (±1)	35	42.5273	3.0857	Collioure	926 965 1023	n/a Acenap Acenap; Acetylene; Phe; Fla

							1272 1289	Bip; Fla n/a
5	01.03.12	10 (±1)	35	42.5408	3.0519	Argeles-sur-mer	n/d	
6	01.03.12	10 (±1)	35	42.5420	3.0541	Argeles-sur-mer	n/d	
7	04.03.12	10 (±1)	35	41.3951	2.2107	Barcelona	**536** 662 758 914 1458	Phe Fla Nap n/a n/a
8	04.03.12	10 (±1)	35	41.3910	2.2052	Barcelona	715	n/a
The Chesapeake Bay, MD, USA								
Nr	*Date*	***Temperature***	***Salinity***	***N***	***W***	*remarks*		
1	29.04.12	14.41	35	39.2817	76.6069		**457**	Acetylene, acenap
1'	29.04.12	14.41	35	39.2817	76.6069		n/d	
2	29.04.12	14.57	35	39.2818	76.6117		719 871 955 1431 1464 1550	n/a n/a Acenap n/a n/a Nap
3	29.04.12	14.57	35	39.2859	76.6115	Constualtion	**457** **491**	Acetylene, Acenap; Bip
4	29.04.12	14.85	35	39.2839	76.6052	Fisheries	**457**	Acetylene, Acenap;
4'	29.04.12	14.85	35	39.2839	76.6052		491 584 725 1402 1641 1584 1778	Bip Pyr Bip n/a n/a n/a n/a
W.DC	30.04.12					Potomac River	756 1383	Nap Nap
The East China Sea Qingdao, China								
Nr	*Date*	***Temperature***	***Salinity***	***N***	***E***	*remarks*		
1	04.06.12	22.48	35	36.0867	120.4597	Input/beach water	**489** 587 659	Bip Pyr Acetylene,

							735 881 1078 1113 1401 1437 1465 1527 1591	Acenap; Fla Bip n/a n/a n/a Fla n/a n/a Fla
1'	04.06.12	20.0	35			sea	538 727 1049 1414 1280	Phe; Acetylene, Acenap Bip Acetylene; pyr Phe; Acetylene, Acenap
2	04.06.12	17.52	35	36.0513	120.3891	Olympic sailing	784 838 1523	n/a n/a n/a
3	04.06.12	17.40	35	36.0533	120.3882	bay	n/d	
The pacific Ocean, West coast, USA								
Nr	*Date*	***Temperature***	***Salinity***	***N***	***W***	*remarks*		
1	21.4.11	26.51	35	25.7964	80.1278	Miami Beach	1261	Bip
2	19.4.11	27.14	35	27.5900	82.6272	Sunshine Bridge	597 1745	Flu Flu
3	19.4.11	27.89	35	27.2852	80.2116	Lucian Roads Beach	n/d	
4	20.4.11	28.50	35	26.4158	81.9019	Holiday inn	**449**	n/a
5	22.4.11	29.94	35	24.8933	80.6690	Keys	n/d	
6	23.4.11	25.13	35	24.5476	81.7912	Key west end I	**459** 672 741 1137 1232 1317 1370 1485 1571	Acetylene, Acenap n/a Nap Bip Pyr n/a Nap; Fla n/a n/a
7	20.04.11	32.98	35	25.8927	81.3263	Ever glades	1446 1498	Fla Bip
8	28.4.11	34.59	35	28.6781	80.7719	Kennedy Space	**457**	Acetylene,

						Centre		Acenap
The Aegean Sea, Rhodes, Greece								
Nr	*Date*	***Temperature***	***Salinity***	***N***	***E***	*remarks*		
1	06.12	23.8	35	35.8770	27.7494	South edge	**564** 1069	Fla Pyr
2	06.12	23.5	35	36.2720	27.8131	Factory	**563** 676 **1067** 1119 1232	Fla Fla Pyr n/a Pyr
3	06.12	23.3	35	36.4133	28.1947	Hotels	560 670 779 922 1231 1444 **1588** 1523	Fla Fla n/a n/a Pyr Fla Fla n/a
The Mediterranean Sea, Riviera, France								
Nr	*Date*	***Temperature***	***Salinity***	***N***	***W***	*remarks*		
1	15.11.12	16.09	35	43.2957	5.3695	Marseille, city harbour	**1071** **1172** 1272 1595	n/a n/a Bip Fla
2	17.11.12	18.07	35	43.5488	7.0266	Canes	n/d	
3	18.11.12	12.99/14.78	0/35	43.6945	7.2686	Nice x 2 (stock water/ sea water)	638 1347 1376	Acenap Acenap, Aceylene, Phe,Flu Fla, Nap
4	19.12.12	12.77	35	43.1054	5.8856	IFREMER	534 787 1159 1293	Phe Acenap, Aceylene Acenap, Aceylene, Fla n/a n/a
5	25.12.12	14.67	35	43.2719	6.6391	St. Tropez	n/d	
6	01.01.13	13.51	35	43.0971	5.8119	Six fours bay	443	n/a
7	01.01.13	13.75	35	43.1061	5.8131	Six Fours parking	451 490	Acenap, Aceylene Bip

							659 917 1079	Acenap, Aceylene, Fla n/a n/a
8		12.81	35	43.1166	5.8027	Six Fours town	n/d	
9	7.01.13	12.89	35	43.0053	5.0544	Sea trial II	445 660 775 795 942 1145 1185 1490 1605 1740	Acenap, Aceylene n/a Acenap, Aceylene, Fla n/a Bip Bip Bip Phe, Pyr Flu
10	07.01.13	12.80	35	43.0052	5.0571	Sea trial I	566 651 884 1285 1316 1400	n/a Acenap, Aceylene n/a n/a Aceylene Pyr, acenap
11	01.01.13	13.54	35	43.1010	5.8067	Six fours rock	600 709 749 990 1018 1266 1501	Acenap, flu Phe Nap Bip Acenap, Aceylene, Fla, Phe Bip, Fla Bip
The Mississippi River, LA, USA								
Nr	*Date*	***Temperature***	***Salinity***	***N***	***W***	*remarks*		
1	23.02.13	9.61	0	29.9541	90.0628	New Orleans city harbour	436 464 532 566 657 755	n/a Acenap, Aceylene n/a n/a Acenap, Aceylene Nap

							785 1152 1391	Fla, Aceylene n/a Pyr
2	23.02.13	9.33	0	29.9565	90.0615	New Orleans city harbour	397 457 509 **612** 640 686 775 919 1455 1630	n/a Acenap, Aceylene n/a n/a n/a n/a n/a n/a n/a Flu
The Baltic Sea, Warnemunde, Germany								
Nr	*Date*	***Temperature***	***Salinity***	***N***	***W***	*remarks*		
1	04.05.13	9.5	35	54.1666	12.0833	harbor	**564** 713 857 1067 1119 1231 1258 1358 1428 1512 1551 1599	n/a n/a n/a n/a n/a Pyr Fla Acenap, Bip, Phe n/a n/a Nap, Flu Fla, aceylene

Appendix VII

Raman bands of selected PAHs and biphenyl

Nr.	PAH	Substrate	Peak position/cm^{-1}													
			400	**500**	**600**	**700**	**800**	**900**	**1000**	**1100**	**1200**	**1300**	**1400**	**1500**	**1600**	**1700**
1	**Acenap**	n/a*	n/m†													
		Gold island	485	545	656 **633** 600	793	825	960	1026			1356 1324	**1411**			
		Ag, DMCX: MTEOS	n/m													
2	**Aceylene**	n/a	n/m													
		Gold island	456	**545**	**654**	795			1051 1022			1346 **1325**	**1414**	1592		
		Ag, DMCX: MTEOS	n/m													

* Most Raman measurements (without substrate) of PAHs in pure state are provided by Dr. Heinar Schmidt, Universität Bayreuth. Private communication.

† not measured

3	**Ant**	n/a				754			1008	1163 1186	1259		**1402** 1479	1555		
		Gold island	-‡	-	-	-	-	-	-	-	-	-	-	-	-	-
		Ag, DMCX: MTEOS				752			1002	1157 1183		1395	1480		1615	
4	**BaA**	n/a				723 793	879		1008 1042	1166	1265	1321 1340 1392	1428	1559	1606	
		Gold island	-	-	-	-	-	-	-	-	-	-	-	-	-	-
		Ag, DMCX: MTEOS	n/m													
5	**BbF**	n/a	n/m													
		Gold island												1533		1749
		Ag, DMCX: MTEOS	n/m													
6	**BaP**	n/a								1196	1212 **1234**	1343 **1384**		1581	1628	

‡ - substrate is not sensitive

		Gold island													1744
		Ag, DMCX: MTEOS	n/m												
7	**BgP**	n/a	454 482	543				988	1083	1153	1222 **1259**	**1304** **1389**			**1606**	
		Gold island	-	-	-	-	-	-	-	-	-	-	-	-	-	-
		Ag, DMCX: MTEOS	n/m													
8	**BkF**	n/a	450 493	554	667	761	803	920	1025 1093		1272	1357	**1447** 1498		**1609**	
		Gold island	-	-	-	-	-	-	-	-	-	-	-	-	-	-
		Ag, DMCX: MTEOS	n/m													
9	**Chr**	n/a		598	677	772			1019			**1383**	1431	1571		
		Gold island	-	-	-	-	-	-	-	-	-	-	-	-	-	1743
		Ag, DMCX: MTEOS	n/m													
10	**Fla**	n/a	486	564	**674**		803		1022	**1103**	1272	1370	**1421**		1609	

							827			1136			1457			
		Gold island	416	**553**	**662**	793			**1092** 1024		1269	1370	**1441** 1412	**1592**		
		Ag, DMCX: MTEOS	457	560	671		800 830		1015	1102 1136	1267		1421 1450		1606	
11	**Flu**	n/a	418			**744**	844		**1022**	1149	1236 1291	1340 1392	1473		1609	
		Gold island			600							1336 1304		1544	1627	**1743**
		Ag, DMCX: MTEOS	n/m													
12	**Nap**	n/a		515		**765**			1022			**1385**	1460	1571		
		Gold island				**750**						**1372**		1557		
		Ag, DMCX: MTEOS		511		762			1018			1379	1461			
13	**Phe**	n/a				**712**	834		1039	1169	1245	**1350**	1437			
		Gold island		541		**701**	819		1028	1198		**1349**	1419		1602	
		Ag, DMCX: MTEOS	n/m													

14	**Pyr**	n/a		596					1066	1143	**1242**		**1405**	1593	1625	
		Gold island		**587**					1053		1227	1392			1603	
		Ag, DMCX: MTEOS	406	589					1062	1139	1234		1401	1589	1622	
15	**Bip**	n/a				734			**998** 1034		**1273**			**1584**	1603	
		Gold island	**488**			732		**992**		1194 1136	1269	1360	1492			
		Ag, DMCX: MTEOS	n/m													

Abbreviation of some organic compounds

Acenap: Acenahpthene

Aceylene: Acenaphthylene

Ant: Anthracene

BaA: Benz(a)Anthracene

BaP: Benzo(a)Pyrene

BbF: Benzo(b)Fluoranthene

BgP: Benzo(g,h,i)- perylene

Bip : Biphenyl

BkF: Benzo(k)Fluoranthene

Chr: Chrysene

DDT: dichloro**d**iphenyl**t**richloroethane

DMCX: 25,27-dimercaptoacetic acid-26,28-dihydroxyl 4-terbutylcalix[4]arene

Fla: Fluoranthene

Flu: Fluorene

MTEOS: Methyltriethoxysilane

Nap: Naphthalene

PAH: Poly **A**romatic **H**ydrocarbons

PCB: Poly **C**hlorinated **B**iphenyls

Phe: Phenanthrene

Pyr: Pyrene

Other abbreviations

SGI: Sea **G**oing **I**nstrument

ROV: Remotely **O**perated **V**ehicle

AOV: Autonomously **O**perated **V**ehicle

LOD: Limit **O**f **D**etection